

UNIVERSITY OF CANTERBURY

Department of Chemical and Process Engineering

Yan Li

**The Current Response of a Mediated
Biological Fuel Cell with *Acinetobacter
calcoaceticus*: The Role of Mediator
Adsorption and Reduction Kinetics**

Thesis presented to the University of Canterbury in fulfillment
of the requirements for the Degree of

Master of Engineering

in Chemical and Process Engineering

Thesis supervisor: Associate Professor Peter Gostomski

Thesis co-supervisor: Dr. Aaron Marshall

Christchurch, New Zealand, 29 April 2013

To my farther

Abstract

Microbial fuel cells (MFC) are an emerging renewable technology which converts complex organic matter to electrical power using microorganisms as the biocatalyst. A variety of biological relevant organic matters such as glucose, acetate and ethanol have been utilized for the successful operation of a MFC. In this regard, the investigation of a MFC inoculated with ethanol oxidizing bacteria is of particular interest for this research due to its ability to simultaneously produce electricity while reducing ethanol pollution (a type of volatile organic carbon (VOC) pollutant) with potential use in modified biological air pollution control technology such as biofiltration.

In this research, ethanol-oxidizing microbial species isolated from soil and compost samples were identified, with *Acinetobacter calcoaceticus* being the dominant strain. In order to understand the metabolism of the anode microbial cells, which is considered to be the key dictating the performance of a MFC, a systematic analysis/optimization of the growth rate and biomass production for *A. calcoaceticus* were carried out. A maximum specific growth rate with a final biomass concentration of 1.68 g/l was derived when aerated at a rate of 0.68 vvm.

It has been recognized that one of the principle constraints in increasing the current density of MFCs is the electron transfer from the bacteria to the anode. In this sense, the addition of a redox mediator, which facilitates the process of the electron transfer, is desired for the efficient operation of a MFC. Thionine, methylene blue (MB), resorufin and potassium ferricyanide that have been profusely utilized as effective mediator compounds in many MFC studies, however, specific information on the biomass sorption of these compounds was lacking and therefore were selected for this research. All mediators tested were reduced biologically in *A. calcoaceticus* inoculated samples as indicated by the color transition from the pigmented oxidized form to the colorless reduced form. Subsequent tests on mediator color removal revealed that physical adsorption by the biomass, aggregation as well as precipitation accounted for a significant portion of the color loss for thionine and MB. It was speculated that the fraction of the initial mediator concentration sequestered, aggregated and/or precipitated no longer contributed to the electron transfer process, resulting in a current production which was proportional to the measurable mediator concentration remained in

anode solution. To verify this hypothesis, chronoamperometric measurements were conducted for various mediator systems at known initial and measurable concentrations. The data obtained on the current produced were in good agreement with the theoretical predictions calculated from the actual mediator concentration, suggesting that the current produced depended on the concentration of mediator remaining in solution.

Finally, the microbial reduction kinetics and the cytotoxicity of potassium ferricyanide were analyzed. The reduction of potassium ferricyanide followed zero order kinetics with the specific reduction rate increased as the initial mediator concentration increased from 1 mM to 200 mM. Inhibitory effects on cell growth were observed at initial potassium ferricyanide concentration of 50 mM.

Acknowledgements

I would hereby like to express my immense gratitude and appreciation to my supervisor, Associate Professor Peter Gostomski, for providing me the opportunity to partake in his research group. I feel very fortunate to have had him as my advisor, whose broad expertise in the field of biotechnology and chemical engineering has been an inspiration for me. His continuous guidance, encouragement and patience throughout my Masters work have made the journey very pleasant, and for that, I am deeply thankful.

An overwhelming thank you goes to my other supervisor, Dr. Aaron Marshall. His exceptional knowledge and expertise in the field of electrochemistry have provided me additional insights into the understanding of this research project. Through all the meetings I have had with him, I have always left his office more encouraged and motivated and I am very grateful for that.

A special note of appreciation goes to all the technical staff of the Chemical and Process Engineering department for their brilliant work on fabricating my experimental apparatus, providing practical advices and ordering experimental materials. Without the generous support of all these people, the work presented in this thesis could not have been made possible.

All of the members past and present of our research group under the supervision of Dr. Peter Gostomski deserve a big thank you to support and assist my research work.

Last and most importantly, my love and gratitude go to my parents, Hongchun Li and Yirong Zhang, to value my education, for being my inspiration and putting my success and happiness before their own. Their love and encouragement have always been a constant source of comfort to me wherever I was when times were difficult. Specially, in loving memory of my farther, I would like him to know how blessed and proud I am to be his daughter.

Table of Contents

Chapters

1: Introduction	1
1.1 LIFE AND ELECTRICITY	1
1.2 SHORT HISTORY OF MFC	2
1.3 ETHANOL POLLUTION.....	2
1.4 PROBLEM STATEMENT.....	5
1.5 OBJECTIVES AND ORGANIZATION OF THIS THESIS	6
2: Technical review of MFC.....	8
2.1 BASIC PRINCIPLES.....	8
2.2 FUNDAMENTALS OF THERMODYNAMIC PRINCIPLES OF MFC.....	10
2.3 MICROBIOLOGICAL ASPECTS OF MFC.....	11
2.3.1 Microbes in the anodic chamber	11
2.3.2 Bacteria metabolism and Electron transfer chain.....	13
2.3.3 Electron transfer mechanisms	16
2.4 ELECTROCHEMICAL ASPECTS	23
2.4.1 Architecture	23
2.4.2 Analysis techniques.....	27
3: Experimental	29
3.1 MICROORGANISM ISOLATION AND GROWTH MEDIUM.....	29
3.1.1 Bacteria from soil and compost samples	29
3.1.2 Preparation of growth medium and nutrient agar	30
3.1.3 Cultivation procedures	31
3.2 BIOMASS CONCENTRATION ANALYSIS	33
3.2.1 Optical density test.....	33
3.2.2 Colony forming unit	34
3.2.3 Dry biomass weight.....	34
3.2.4 Contamination test	35
3.2.5 Carbon source utilization.....	35
3.2.6 Calculation of specific growth rate	36

3.3	OPTIMIZATION OF GROWTH RATE.....	36
3.4	CHEMICAL COMPONENTS.....	37
3.4.1	Biotic reduction of mediators	38
3.4.2	Intracellular partitioning analysis.....	39
3.5	REACTOR DESIGN.....	39
3.5.1	MFC configuration.....	40
3.5.2	Anode and Cathode feed solutions.....	41
3.6	ELECTROCHEMICAL ANALYSIS	41
3.6.1	Electrochemical cell preparation.....	41
3.6.2	Chronoamperometric analysis	42
3.7	MEDIATOR CASE STUDY – POTASSIUM FERRICYANIDE	42
3.7.1	Sample preparation	43
3.7.2	Kinetic of ferricyanide reduction	44
4:	Microbe Growth analysis	45
4.1	ENRICHMENT OF ETHANOL OXIDIZERS	45
4.2	AGAR ISOLATION AND STRAIN IDENTIFICATION	45
4.3	GROWTH CURVES AT VARIOUS ETHANOL CONCENTRATIONS	49
4.4	ALTERNATION OF CULTURE CONDITIONS TO OPTIMIZE GROWTH.....	51
4.4.1	Nitrogen sources.....	52
4.4.2	Oxygen level	57
4.4.3	Antifoaming agent.....	60
4.5	CONCLUDING REMARKS	63
5:	Microbe-mediator interactions and the effect on current responses	65
5.1	BIOTIC REDUCTION OF MEDIATOR	66
5.1.1	Thionine	66
5.1.2	Methylene Blue.....	68
5.1.3	Potassium Ferricyanide	70
5.1.4	Resorufin reduction.....	71
5.1.5	Comparison of biotic reduction rate.....	73
5.2	BIOMASS MEDIATOR ADSORPTION ANALYSIS.....	77
5.2.1	Quantification of mediator adsorption	77
5.2.2	Effect of initial mediator concentration on adsorption.....	78
5.2.3	Adsorption of various mediators.....	80
5.2.4	Explanations on the adsorption discrepancies	82

5.3	THE EFFECT OF MEDIATOR ADSORPTION ON CURRENT RESPONSE.....	85
5.3.1	Current response analysis	86
5.3.2	Free mediator concentration and current response.....	89
5.4	CONCLUDING REMARKS	92
6:	Case study- potassium ferricyanide.....	94
6.1	KINETIC ANALYSIS OF POTASSIUM FERRICYANIDE REDUCTION	95
6.2	EFFECT OF OXYGEN ON THE KINETICS OF FERRICYANIDE REDUCTION.....	99
6.3	TOXICITY OF FERRICYANIDE TO ACINETOBACTER CALCOACETICUS.....	100
6.4	CONCLUDING REMARKS.....	102
7:	Conclusion and future work	103
7.1	SUMMARY OF THIS RESEARCH	103
7.2	RECOMMENDATIONS FOR FUTURE RESEARCH.....	105
	References	106
	Appendices	119
	APPENDIX I: EFFECT OF TEMPERATURE ON THE GROWTH OF <i>A. CALCOACETICUS</i>	119
	APPENDIX II: OPTICAL DENSITY VS. DRY WEIGHT MASS	120
	APPENDIX III: ETHANOL CONSUMPTION OF <i>A. CALCOACETICUS</i> DURING BATCH CULTURE.	121

List of Figures

Figure 2.1:	Simplified overview of a typical dual chamber microbial fuel cell.	8
Figure 2.2:	A typical electron transfer chain (top) and the standard reduction potential of the key enzymes (right).	15
Figure 2.3:	Schematic of proposed direct electron transfer upon contact via cytochrome C	18
Figure 2.4:	SEM image of the pili structure in <i>Shewanella oneidensis</i> MR-1.....	19
Figure 2.5:	Simplified diagrams for various MFC architectures.....	25
Figure 3.1:	Schematic of the bacterial cultivation apparatus.	32
Figure 3.2:	Schematic of the MFC design fabricated for this research.	40
Figure 4.1:	A comparison of the optical density versus incubation time plots at various initial ethanol concentrations (in medium 1).....	50
Figure 4.2:	Optical density growth data of <i>A. calcoaceticus</i> with ammonium chloride or sodium nitrate as the N source (in medium 2)	53
Figure 4.3:	Semilogarithmic plot of <i>A. calcoaceticus</i> growth data obtained from three growth detection methods: the turbidity reading, the dry biomass and the colony forming unit count (CFU).	55
Figure 4.4	<i>A. calcoaceticus</i> growth curves showing the exponential relationship between optical density data and CFU count data in the suspected exponential phases.	56
Figure 4.5:	Effect of increased aeration rate (from 0.2-0.4 vvm to 0.64 vvm) on bacterial growth.	59
Figure 4.6:	Growth behaviour of Antifoam A added culture.....	62
Figure 5.1:	The reversible redox reaction of thionine	67
Figure 5.2:	The color changes of thionine before and after reduction, the concentrations are control, 100, 200, 300, 500 and 600 μ M from left to right.	68
Figure 5.3:	The redox reaction of methylene blue.....	68
Figure 5.4:	The color changes of methylene blue by bacterial suspensions before and after reduction	70
Figure 5.5:	The reversible redox reaction of ferricyanide.....	70
Figure 5.6:	The redox reaction of resorufin.	72

Figure 5.7:	The color removal of resorufin at various concentrations by <i>Acinetobacter</i> suspensions, the concentrations are control, 25, 50, 100, 150 and 200 μM from left to right.	73
Figure 5.8:	The adsorption behavior of thionine, MB and resorufin at a fixed amount of biomass in terms of percentage of mediator adsorbed with respect to the initial mediator concentration.	79
Figure 5.9:	Adsorption capacity of different mediators.	80
Figure 5.10:	Freundlich isotherm of two mediators.	82
Figure 5.11:	The adsorption spectra shift of thionine and MB at different concentrations	84
Figure 5.12:	Detection of green precipitation	84
Figure 5.13:	The chronoamperometric responses of various mediators at 100 μM initial concentration.	87
Figure 5.14:	The current responses of samples containing 300 μM of thionine, MB and ferricyanide.	88
Figure 5.15:	The mean current responses as a function of initial mediator concentration	89
Figure 6.1:	Ferricyanide reduction over time by <i>Acinetobacter</i>	96
Figure 6.2:	Specific reduction rate during the linear region by <i>Acinetobacter</i> cultures as a function of initial ferricyanide concentration.	97
Figure 6.3:	Comparison of specific reduction rates of ferricyanide under aerobic and anaerobic conditions.	100
Figure 6.4:	Optical density changes over 6 hours in samples containing various ferricyanide concentrations.	101

List of Tables

Table 1.1:	Common VOC species and their structures.....	3
Table 2.1:	Half-cell reactions of a MFC using acetate as substrate	11
Table 2.2:	Examples of commonly used mediators.....	22
Table 2.3:	List of commonly used MFC building materials	26
Table 3.1:	Mineral recipe for the nutrient solution (medium 1)	31
Table 3.2:	Strain-specific mineral recipe for the nutrient solution (medium 2).....	31
Table 5.1:	Selected properties of tested mediators and the rate of reduction	74
Table 5.2:	The Freundlich isotherm constants for MB and resorufin	82
Table 5.3:	The theoretical current of different mediators.....	91
Table 6.1:	pH decrease at various initial ferricyanide concentrations.....	98

Chapter 1: Introduction

1.1 LIFE AND ELECTRICITY

22nd February 2011, 9pm, southeast of Christchurch, a group of six friends gathered around to play a board game hoping to keep each other calm and safe while the darkness slowly crept in. The feeble light of candles flickered throughout the house; the battery operated radio was the only source of communication with the outside world while computers and televisions became worthless. Cell phones had to be switched off as when the batteries could be recharged again remained unknown. A deadly earthquake which claimed more than 180 lives eight hours ago left most parts of the city grieving in the dark.

Many of us who have experienced a series of devastating earthquakes in Christchurch over the last year know exactly how life is like without electricity. Reliable power supply lies at the heart of the modern, increasingly digital lifestyle we have adapted to. It is no exaggeration to regard electricity as society's "central nervous system". When a disaster like an earthquake strikes, our vital system is hopelessly impaired, leaving the entire community paralyzed in many ways. From simply fuelling household appliances, providing ways of entertainment and communications; to controlling the mass scale traffic, transportation and water distribution systems, electricity is terribly missed when absent.

At any given moment, the maximum worldwide electricity consumption is around 12.5 terawatts (TW) and this value is projected to reach 16.9 TW in 2030, as predicted by the U.S. Energy Information Administration (Eccleston et al. 2012). In 2005, 66% of that electricity was generated from coal, petroleum and natural gas and was responsible for 10.9 Gt (41%) of world energy- related CO₂ emission (Taylor et al. 2008). Depending on the region, your electricity could come from the dirtiest coal burning plant, a high risk nuclear facility, or a hydro electrical dam, which, although pollution free, still deteriorates the local geological and ecological systems.

The human-induced greenhouse effect as a result of fossil fuel reliance has become an increasingly controversial issue in many countries since the 1960s. The

fast depletion of fossil fuel due to intensive extraction and usage is widely believed to be associated with the atmospheric CO₂ concentration increase from 275 ppm to 397 ppm in the last two centuries (Observatory 2013). As a result, development of sustainable energy technologies which can continue providing society with energy-derived benefits without further environmental destructions is highly desirable. A series of green energy solutions, such as solar, wind and biomass energy, have been introduced in the hope of preventing the impending global environmental crisis.

Electricity is an essential element in our daily life, something we cannot live without literally, we would die without it. From the simplest form of living organism to the complicated human body, electrical force governs every single physiological process. Bio-electricity is vital in storing metabolic energy and providing signals to other cells which influence growth, regeneration and communication (Levin and Stevenson 2012). The body's central nervous system relies on the flow of electrical charges to send signals which in turn allow brain functions, body movements and making sense of the surroundings. In the light of this concept, it makes one wonder if it is possible to extract electricity from the diverse and vast existing bacterial cells. Fortunately, the answer is confirmative.

1.2 SHORT HISTORY OF MICROBIAL FUEL CELL

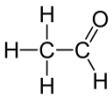
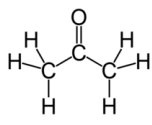
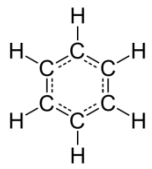
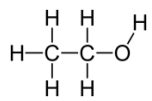
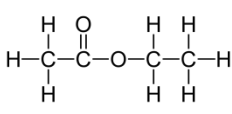
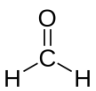
The idea of extracting electricity directly from organic matter through the catalytic reactions of microorganisms emerged a century ago, credited to Michael Cresse Potter (Logan 2007). Although it was popular in the 1960s, research interest in MFCs diminished due to their low power density and lack of durability. Recently, significant advances in elevated power density and improved understanding of underlying microbiological concepts have provided us new and valuable insights into improved MFC designs with potential practical applications.

1.3 ETHANOL POLLUTION

While the aroma from freshly baked bread is satisfying to the appetite, harmful substances emitted from bakeries are not helpful to the environment. Despite many contaminants being released from various processes in a bakery, volatile organic compounds (VOCs) are of paramount concern to emission control agencies (Govind et al.).

VOCs, as defined by the European Community, are any organic compound with a high enough vapour pressure to evaporate into the air at 293.15⁰ K (20⁰C or 68⁰F) under standard atmospheric pressure of 101.3kPa (Passant et al. 1993). The variety of compounds that fit the above criteria differs significantly in their chemical composition, structure and toxicity. Some commonly encountered VOC species are listed in Table 1 (Atkinson and Arey 2003; Risholm-Sundman et al. 1998).

Table 1.1: Common VOC species and their structures.

Name	Structure
Acetaldehyde	
Acetone	
Benzene	
Carbon disulfide	S=C=S
Ethanol	
Ethyl acetate	
Formaldehyde	

The potential adverse health and environmental impact of VOCs vary significantly according to the nature and level of exposure to the compound. Benzene, for example, is a well-recognized carcinogenic substance, documented in the Twelfth Report on Carcinogens published by the U.S Department of Health and Human

Services (Maltoni et al. 1989). Long term inhalation of vaporized benzene originating from tobacco smoke, automobile exhaust and petroleum products is directly associated with acute leukaemia and bone marrow abnormalities (2011).

VOCs, in addition to their direct toxicity, are also responsible for the formation of secondary pollutants. When in contact with nitrogen oxides in the atmosphere, VOCs undergo series of photochemical reactions catalysed by sunlight to form tropospheric ozone (Atkinson 2000). The by-products of this reaction are visible as smog. Ground level ozone accumulation is proved to have detrimental effects on human health, crop production and building materials. Clinical studies have proved that elevated ozone inhalation can lead to asthma, respiratory related illness, premature death and cancer (Hafner et al. 2010; Jacobson 2007). As a consequence of their hazardous nature, environmental protection agencies around the globe introduced stringent legislations to control ambient ozone concentration and its precursor emissions (B.Ozturk and D.Yilmaz 2006).

The sources of anthropogenic volatile organic compounds are dispersed, diverse and numerous. Typical emissions stem from the organic solvents used in the cleaning and painting industries and the production, transport and storage of these products (Guenther et al. 1995). Combustion of fossil fuels, commercial bakeries, breweries, agricultural activities and petro-chemical industries are the major remaining contributors of emissions.

Among the different VOCs emitted, the amount of ethanol released is abundant and noteworthy. Although ethanol itself at a low level poses limited threat to the environment and human health, its photochemical reactivity is undeniably dangerous at elevated levels. In the year 2006 to 2007, ethanol alone accounted for approximately 6% of total industrial VOCs produced in Australia (Kirstine and Galbally 2004). As a result, a series of ethanol emission control guidelines and enforcement actions were incorporated into the environmental laws there, and also in Canada and the United States (Ramirez et al. 2007). However, in 2011, the Australian figure still increased by 3%, with a total volume of 8.6 kt ethanol detected in the atmosphere (2012).

Despite its harmful effects, ethanol is an important chemical compound that has served a wide range of purposes since ancient history. Besides the well-known

psychoactive effect of alcoholic beverages, ethanol is also a useful solvent in the synthesis of other chemicals and, more recently, a substitute for high octane automotive fuels. Ethanol production through anaerobic fermentation, when certain microorganisms break down sugar molecules, is one of the oldest biotechnologies known to humanity (Zverlov et al. 2006). This process is a crucial step in the rising of yeast-leavened dough in bread making industries and the manufacture of alcoholic beverages. According to the Australian National Pollutant Inventory data, the commercial beverage manufacturing and baking plants accounted for 41% and 11.6% of entire industrial ethanol emissions respectively in 2010 (2012). With ethanol being a principle pollutant, the attempt to bring its emission into compliance is at the forefront of concerns in the emission control schemes from these facilities.

A wide range of competitive abatement approaches have been employed to reduce ethanol emission which include: biofilter, biotrickling filter, adsorption, catalytic combustion, etc. (A.Silvestre-Albero et al. 2009). Biotrickling filtration is a widely adopted resolution with reported removal efficiency higher than 95% (Chung et al. 2005). The underlying principle of a biotrickling filter relies on the microorganism's ability to transform toxic substances into eco-friendly compounds (Gavrilescu 2009). The general structure of a biotrickling filter consists a porous packed bed sustaining a large quantity of immobilized microbial consortium (Ralebitso-Senior et al. 2012). The filter is suspended in continuously recycled liquid nutrients. When the contaminated gas passes through the bio-layer, the thriving population of microorganisms will convert the organic pollutants into water, carbon dioxide and biomass under aerobic conditions. In spite of the many advantages that the biotrickling technique has offered ethanol emission control, newer developments offer further improvements.

1.4 PROBLEM STATEMENT

Taking of all the above into consideration, two potentially relevant issues and the following questions are raised:

- ❖ What energy alternatives can be implemented that can reconcile the increasing electricity demand with least environmental impacts?
- ❖ What methods are available, or can be refined, to not only reduce toxic pollutants but recycle them in a way useful to the economical production of electricity?

Microbial Fuel Cells (MFCs), which are capable of harvesting electricity from renewable biomass and organic wastes, arise as a promising yet challenging candidate to expand the existing sustainable energy portfolio (Piciooreanu, et al. 2010). Ethanol has been used previously in enzyme-catalyzed fuel cells employing alcohol dehydrogenase isolated from yeast cells. However, the lack of long-term stability, as a result of denaturation of the enzyme under *in vitro* conditions, poses a major challenge in enzyme biofuel cells (Kim et al. 2007b). As an alternative, the use of intact bacterial cells which are capable of degrading ethanol and generating electricity simultaneously in a fuel cell provides a new approach for ethanol removal.

1.5 OBJECTIVES AND ORGANIZATION OF THIS THESIS

In order to facilitate the electron transfer process which in turn enhances the performance of a MFC, redox mediators have been incorporated in many MFC studies (Sund et al. 2007). This research is designed to investigate the feasibility in utilizing ethanol oxidizing bacteria as the biocatalyst and the performance of a MFC using various redox mediators.

The specific objectives of this research are outlined as follows:

- i) Isolate and identify ethanol oxidizing microorganisms from environmental samples such as soil and compost.
- ii) Determine the suitable growth conditions for the chosen ethanol oxidizers.
- iii) Investigate the feasibility of generating electricity in an MFC with ethanol oxidizing bacteria as the biocatalysts.
- iv) Analyze the interaction between the ethanol oxidizing microorganisms and various redox mediators selected for the purpose of enhancing MFC current production.
- v) Assess the influence of mediator adsorption by biomass on current production.
- vi) Characterize the reduction kinetics of the most suitable mediator that has produced the highest current.

This thesis is organized into seven chapters. Chapter 1 includes a brief introduction to the subject and the research objectives. Chapter 2 reviews the basic principles of MFC technologies with a special focus on the microbiological aspects

including the biocatalysts and the electron transfer mechanisms between bacteria and electrode. Chapter 3 describes the experimental materials and methods used for this work. The fourth chapter provides the results obtained with discussion on harvesting the ethanol oxidizing microorganisms at various conditions. Chapter 5 is a discussion of the results on microbe-mediator interactions and their potential effect on current production. The results derived from the electrochemical analysis on the performance of the MFC with different mediators were compared and interpreted. In Chapter 6, detailed knowledge towards the reduction kinetics of the most suitable mediator for this study, selected based on the result of current production in the last chapter, was illustrated. Finally, conclusions are derived from the results and recommendations are included for further improvements in Chapter 7.

Chapter 2: Technical review of MFC

2.1 BASIC PRINCIPLES

The Microbial fuel cell (MFC) is a bio-electrochemical device which, through microbial-catalyzed redox reactions, converts the energy stored within bio-convertible substrates to electricity. The fundamental physical components of a typical dual-chamber MFC includes the electrolytes, an anode and a cathode partitioned by a proton exchange membrane (Fig. 2.1).

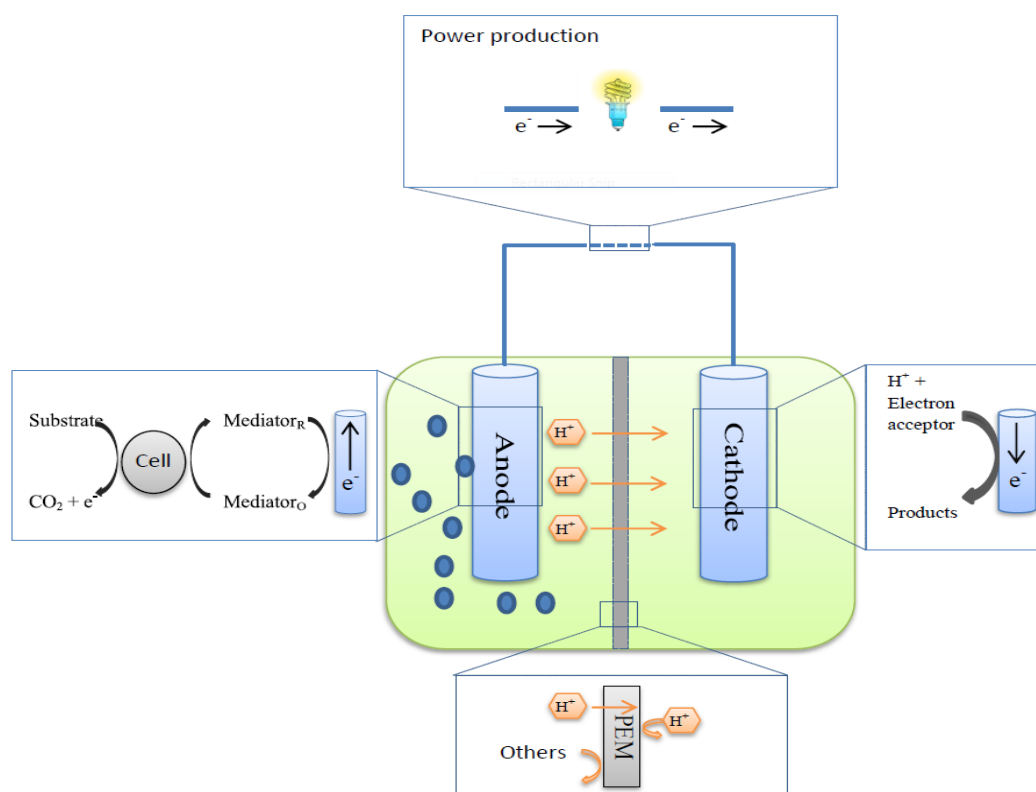


Figure 2.1: Simplified overview of a typical dual chamber microbial fuel cell. On the anode, bacteria oxidize organic substrates to carbon dioxide and electrons. Dissolved artificial electron mediators assist the electron transfer from bacterial cells to the electrode and further routed through an external circuit to the cathode to deliver electrical energy. Mediator_R= Reduced mediator; Mediator_O = Oxidized mediator; PEM = Proton exchange membrane.

In the anode chamber, microbial respiration oxidizes available substrates to carbon dioxide that results in the liberation of electrons and protons. These electrons are diverted out of the cell membrane onto the anode via either direct contact with the membrane-associated electron transfer enzyme or electrochemically active carriers,

also known as electron mediators, and further to the cathode through an integrated external circuit (Kim et al. 2008) . At the same time, for each electron that is transferred, the corresponding proton must migrate across a proton permeable membrane to the cathodic chamber to sustain charge neutrality. A diverse range of microorganisms have been used in the successful operation of MFCs. Metal-reducing bacteria such as *Geobacteraceae* family and *Shewanella* genus are capable of extracellular electron transfer in a self-mediated manner whereas *Escherichia coli* and other fermentative bacteria, e.g. *Clostridium* and *Proteus*, require the incorporation of artificial electron mediators to transfer electrons externally (Franks and Nevin 2010). In the cathode, a terminal electron acceptor such as oxygen becomes reduced by accepting the electrons and protons (Logan 2007). The two compartments are connected externally through an electrical wire which typically includes a resistor and separated internally by the proton exchange membrane (PEM) in a laboratory setup. The membrane acts as a barrier which restricts the oxygen diffusion from the cathode to the anode while permeable to proton migration from the anode to the cathode (Logan 2007).

The research of microbial fuel cells around the globe is rapidly increasing with potential niche applications in a number of fields. Owing to its voltage generation capacity, MFCs are proposed for implementation in sustainable wastewater treatment, and biosensors etc.

- ❖ The first MFC powered monitoring device in benthic marine environment has been demonstrated at practical scale (Tender et al. 2008). This specific MFC system, capable of oxidizing organic substrates residing in marine sediments, was estimated to operate indefinitely in a self-sustained manner.
- ❖ Another envisioned feasible application for MFCs is in wastewater treatment. It has several advantages over the conventional method. The replacement of currently energy-demanding, wastewater-treatment bioreactor (e.g. activated sludge system) by an energy-producing MFC not only results in a net reduction of energy consumption but reduction of excess sludge formation (Kim et al. 2007a).
- ❖ A MFC-integrated biochemical oxygen demand (BOD) sensor using *Shewanella putrefaciens* as the anode consortia demonstrated remarkable stability over 5 years of operation (Du et al. 2007).

- ❖ Modification to a MFC for bio-hydrogen production from biodegradable substrates has been proposed. Although the process is thermodynamically unfavorable, it is achievable by applying a small electrical current to the cathode via the bio-electrochemically assisted microbial reactor (BEAMR) in an oxygen-free environment (Du et al. 2007). A theoretical power input of 0.11 V was estimated to emit as high as 8-9 mole of H₂ per mole of glucose consumed, compared to only 4 mol H₂ per mol of glucose using current fermentation methods (Logan and Regan 2006).

2.2 FUNDAMENTALS OF THERMODYNAMIC PRINCIPLES OF MFC

The theoretical maximum voltage, termed as electric potential (E_{emf}), that can be attained from a MFC system is determined by the potential difference between the anode and cathode half cells, when the overall reaction is thermodynamically favorable (Rozendal et al. 2008). According to Eq. 2.1, the electromotive potential can be derived from the Gibbs energy expressing the maximal useful work extractable from a reaction, where E_{emf} stands for the electric potential (V), ΔG is the Gibbs energy (J/mol), n is the amount of electrons transferred in the reaction (mol) and F is the Faraday's constant.

$$E_{emf} = - \frac{\Delta G}{nF} \quad [2.1]$$

A positive E_{emf} value, while defining the upper limit of the cell potential, implies that electricity generation is possible. The following example is the simplified stoichiometric reactions involved in an acetate-fed MFC in the anode and oxygen as the terminal electron acceptor in the cathode (Table 2.1). It should be noted that when an artificial mediator is involved, the difference between the redox potential of the mediator and the final electron acceptor determines the maximum fuel cell potential (Sund et al. 2007).

Table 2.1: Half-cell reactions of a MFC using acetate as the substrate (Rozendal et al. 2008).

Anodic Oxidation Reaction:	E_{emf} (V vs NHE*)
$CH_3COO^- + 4H_2O \rightarrow 2HCO_3^- + 9H^+ + 8e^-$	-0.289
Cathodic Reduction Reaction:	E_{emf} (V vs NHE)
$2O_2 + 8H^+ + 8e^- \rightarrow 4H_2O$	0.805
Overall:	$E_{emf} = 1.094$ V
	$\Delta G = -847.6$ kJ/mol

* NHE = Normal hydrogen electrode

2.3 MICROBIOLOGICAL ASPECTS OF MFC

2.3.1 Microbes in the anodic chamber

The key character which differentiates a microbial fuel cell from any other form of biological fuel cell (e.g. enzymatic fuel cell) is the incorporation of intact bacterial cells in the anode chamber. It is their ability to mineralize the energy-bearing substrates into accessible, electrochemically-active substances that makes the electricity production a reality.

Virtually any dynamic bacterial cells fed with appropriate substrates can be employed to catalyze power generation. However, the choice of microorganisms, depending on their metabolic characteristics, could compromise the power output of a MFC to a certain degree. It is because microorganisms have evolved to adjust among various metabolic pathways based on feedstock availability, which could potentially lead to the incomplete oxidization of less preferable substrates. In MFC research, coulombic efficiency is an important evaluation criterion (Franks and Nevin 2010). It is expressed as the ratio of actual electrical current flux measured to the theoretical maximum coulombic energy stored in a substrate as a result of the microbial respiration. It, in part, depends on the property of that organic substrate where electrons are derived and the microorganisms delivering them.

In earlier MFC research, a number of fermentative bacterial species were examined as the active agent in the anode compartment. *Escherichia coli*, the most intensively studied prokaryote microbe, has been the choice for many MFC studies. In fact, the pioneering study conducted on a living *E. coli* culture by Potter (1911) was the first successful practical proof of the MFC principle. The microbial fuel cell potential of other fermentative bacterial species like *Clostridium*, *Actinobacillus* and *Proteus* have been explored over the years (Park and Zeikus 2000; Rabaey and Verstraete 2005). As these microorganisms do not normally transfer electrons across the cell membrane (oxygen reduction occurs within the cell), an exogenous redox mediator must intervene so that the electrons inside the cell can reach the electrode.

The addition of mediators into the anode solution enables the production of electrical current from bacteria that have no inherent mechanism of direct electron transfer to electrodes (Sund et al. 2007). Thurston *et al.* (1985) demonstrated a thionine-mediated MFC, which delivered a coulombic efficiency of about 50% from glucose metabolism by *Proteus vulgaris*. With an anode surface area of 800 cm², the current drawn from this setup was close to 0.025 mA/cm². MFC performance is constantly improving with more information on the effects of electrode material along with physiological interaction between the electron mediator and the microorganism. Instead of dissolving the mediators in the anode solution, it is feasible to fix mediators on to the anode electrode. Glucose, molasses and starch were injected to fuel a conductive polymer coated platinum electrode fuel cell (Davis and Higson 2007). Current densities between 1.0 and 1.3 mA/cm² were recorded from *Clostridium sp.* respiration (Niessen et al. 2004). Although the utilization of artificial electron mediators can greatly enhance the power generation of MFCs, their applications are usually constrained by increased operational cost, difficulty in recycling if not immobilized and potential cytotoxicity to certain bacterial strains.

The recent discovery of dissimilatory metal respiring bacteria capable of extracellular electron transfer in a self-mediated manner has sparked considerable interests among MFC researchers. This exo-electrogenic ability was first revealed in the study of *Shewanella putrefaciens* in pure cultures (Kim et al. 2002). As the search expands, more species of this kind such as *Geobacteraceae* and *Desulfuromonaceae* have emerged. These microbes naturally inhabit in marine sediments where Fe (III) or Mn (IV) are readily available as electron acceptors rather than oxygen. *Rhodospirillum rubrum*

species can also actively exchange electrons with artificial electrolytes and donate energy from glucose consumption into electricity generation (Chaudhuri and Lovley 2003). A coulombic efficiency of 96.8% was achieved by *Geobacter sulfurreducens* (Logan 2009).

Although the use of pure culture provides benefits in sample preparation, performance analysis and data interpretation, it implies a continuous risk of contamination. From a practical point of view, mixed culture inoculum enriched from either sediments or activated sludge supplied with diverse substrates is more resilient to operational disturbances and high in power output. An anaerobic sludge activated MFC was reported to recover up to 86% of the electrons engaged in electricity production. The system produced 360 $\mu\text{W}/\text{cm}^2$ power upon glucose degradation, (Rabaey et al. 2003).

2.3.2 Bacteria metabolism and Electron transfer chain

The energy conversion of substrates through microbial metabolism is important to the MFC system. Before going into details of the other aspects of MFC operation, a brief understanding of the relevant bacterial metabolic pathways is beneficial. During the process of glycolysis, heterotrophic microorganisms attain the energy required for their survival by breaking down complex organic compounds including lipids, proteins and carbohydrates. These organic molecules are the original energy source for the subsequent redox processes that enable the biosynthesis of adenosine triphosphate (ATP). ATP secures the energy emitted from catabolic reactions in its phosphate bonds and serves as the universal energy currency within living organisms. The resulting metabolites from glycolysis are diverted into either respiration or fermentation pathways according to the availability of terminal electron acceptors such as oxygen in the surrounding environment (Schroder 2007).

Under aerobic condition, the respiration process proceeds via the tricarboxylic acid (TCA) cycle through which nicotinamide adenine dinucleotide (NAD^+) and flavin adenine dinucleotide (FAD) are reduced to (NADH and FADH_2) (Schaetzle et al. 2008). The electrons freed after NADH and FADH_2 re-oxidation are finally accepted by the external terminal electron acceptor, oxygen, in this case (Fig. 2.2). Before released to the exogenous environment, electrons are transmitted sequentially

through a membrane-embedded protein relay often referred to as the electron transport chain (ETC). The exact enzymatic organization varies accordingly to the type of species, but broadly consists of mobile electron carriers and membrane bound proton pumps. Electrons are removed from NADH by the first molecule of the ETC, a flavin mononucleotide (FMN) containing protein, while passing protons out of the membrane. These electrons then shuffle between electron-binding sites that are conjugated to the iron-sulfur protein backbone before being transferred to coenzyme Q. The coenzyme Q delivers the electrons on to cytochrome bc_1 and eventually cytochrome aa_3 via an intermediate protein named cytochromes c. Cytochrome bc_1 and cytochrome aa_3 also act as proton pumps and the latter is responsible for the release of electrons onto a waiting oxygen molecule (Campbell and Reece 2002). Figure 2.2 illustrates the sequence of fundamental features of the electron transport machinery and redox potentials of each component. As electrons pass, protons are simultaneously translocated to the periplasmic space creating a proton gradient. The energy of the proton gradient drives the migration of protons back into the cell to restore charge equilibrium which in turn initiates the phosphorylation of ADP to ATP.

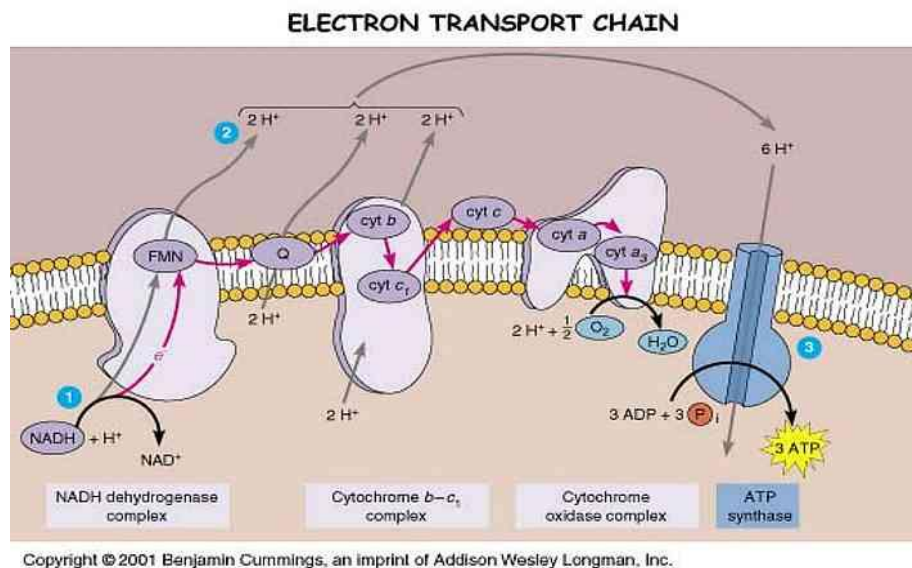
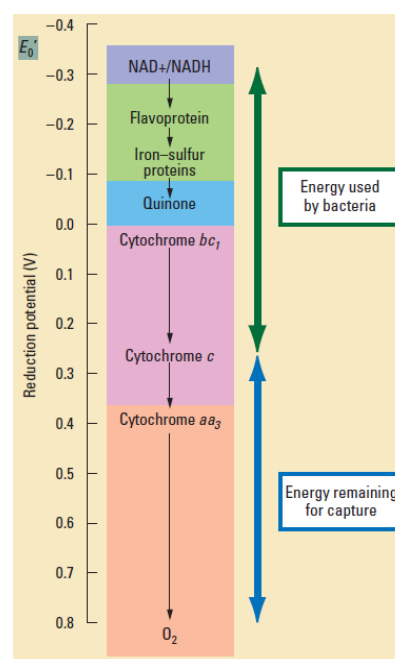


Figure 2.2: A typical electron transfer chain (top) and the standard reduction potential of the key enzymes (right). Energy recovered from potential difference between each component in the green arrow zone is used for bacterial activity. The energy extractable for MFC electricity production is derived from the potential difference between cytochrome c and O₂ (Logan and Regan 2006).



In anaerobic operation, facultative aerobes and obligate anaerobes undergo fermentation by donating electrons derived from substrate mineralization to other organic or inorganic compounds other than oxygen. In addition to the frequently encountered nitrate, sulphate and metal ions (e.g. Fe³⁺) acting as the terminal electron acceptors, bacteria can partially reduce their organic substrates in order to survive. The spare electrons are transferred to the available organic substrates leading to the subsequent dehydrogenation, decarboxylation and methanogenesis reactions (Mohan et al. 2008). Although it is thermodynamically viable, this will result in incomplete utilization of a large part of the energy content within the substrate. The energy gain

is inextricably much lower in this case than that of aerobic respiration due to less positive redox potentials of the final electron acceptor.

This electron flow from reduced organic substrates to the final electron acceptors will release a certain amount of energy, in the form of the Gibbs energy, due to the difference in their redox potential. By promoting this movement, bacteria become the primary beneficiary entitled to capture and conserve this energy for the maintenance of biological vitality. The amount of energy that can be obtained from this process is proportional to the magnitude of the redox potential difference. When suitable exogenous electron acceptors are not available, and an electrode with the appropriate potential is available, microorganisms can be induced to donate electrons directly or indirectly to the anode electrode. The requirements to accomplish such a task will be explored in the next section.

2.3.3 Electron transfer mechanisms

Using microbes as the active ingredient in the fuel cell offers several advantages compared to enzymatic fuel cells including degradation of hazardous organic compounds and an extended operation period (Rabaey and Verstraete 2005). One major drawback, however, is the electrons liberated though enzymatic pathways are shielded from the external environment by the cell membrane. Thus, an effective transfer mechanism between the interior of the bacteria and the anode must be established. An understanding of how these electrons are shuttled between the inner cell and the electrode surface would provide an additional tool for the optimization of the MFC performance. By means of bacterial origin and the nature of their metabolic mechanism, different route of the electron transport process is observed.

Four likely mechanisms of electron transfer processes to the anode in a MFC have been proposed which include:

- ❖ direct transfer via membrane associated protein relay,
- ❖ direct physical communication via electrical conductive bacterial nanowires or pili,
- ❖ self-excretion of natural mediators,
- ❖ addition of artificial electron shuttles.

The concept of direct electron transfer (DET) originated from investigations of sediment-inhabiting, mineral-oxidising strains like *Geobacter* and *Shewanella* (Lovley 2006). A physical gateway between the inner metabolic site and the solid electrode entity *via* cell membrane organelles was detected in these species based on biochemical and sequencing analysis. The primary obstacle encountered when utilizing sediment minerals like Fe (III) as the terminal electron acceptor is their insolubility at a cell-sustainable pH. As a result, in an anoxic environment, oligotrophic *Geobacter* spp. and *Shewanella* spp. thrive at solid mineral surfaces and rely on their membrane associated proteins to move redox materials to the external site of reduction in exchange for metabolic activities. Membrane-bound, multi-heme cytochrome c complexes are at the center of the focus as it is evidently the key component coordinating this DET process (Logan 2009).

In the model for a *Geobacter*-enriched MFC, electrons are transferred via an outer-membrane bound NADH dehydrogenase associated with a cytochrome c complex (Fig. 2.3) onto electrodes using the same mechanism as the naturally occurring iron (III) degradation in their usual habitats (Chang et al. 2006). *Shewanella putrefaciens* was the first iron-respiring bacterium identified that is actively engaged in electron transfer with MFC electrodes in the absence of artificial mediating compounds (Kim et al. 1999). While its exogenous electron transfer mechanisms have been extensively examined, they are still controversial with no unanimous agreement on the exact route. It was previously presumed that electrons within the periplasm proceed across a transmembrane module consisting cytochrome complexes and menaquinone to the external redox site. However, a recent discovery of self-synthesized, electrically-conductive appendages in these species opened up a new dimension to the understanding of extracellular electron transfer (Hernandez and Newman 2001).

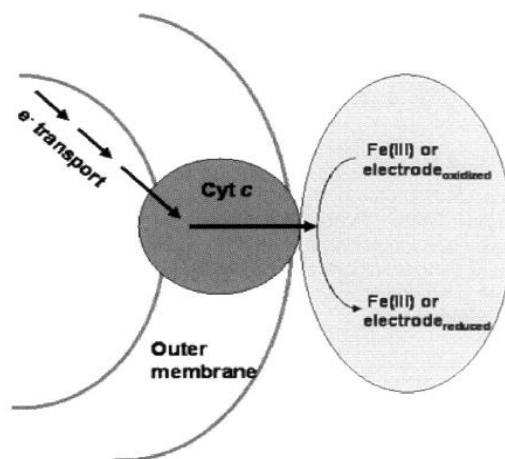


Figure 2.3: Schematic of proposed direct electron transfer upon contact via cytochrome C (Chang et al. 2006).

In the context of the DET mentioned in the last paragraph, physical adhesion of electro-reactive biofilms on MFC anode is essential, restricting electron transfer to the monolayer of cells in direct contact with the electrode. The conductive nanowires observed in *Shewanella oneidensis* MR-1 allow the cells to communicate with metal oxide surfaces which may otherwise be inaccessible by means of direct cell contact. Thus, a ten-fold increase in anode performance was achieved owing to previously impossible electron transfer from beyond the interfacing monolayer (Schroder 2007). This nanowire structure (Fig. 2.4), extends from the transmembrane cytochromes for tens of micrometers with a diameter of 50-150 nm in response to electron acceptor deficiency (Gorby et al. 2006). A similar dependency on this pili-facilitated, electron-exporting mechanism is also present in *Geobacter sulfurreducens*. The observation of the inhibitory effect on Fe (III) reducing ability after disruption of the nanowire encoding *pilA* gene, further emphasized how important the existence of nanowires is to electron communication within and outside the cell (Logan and Regan 2006).

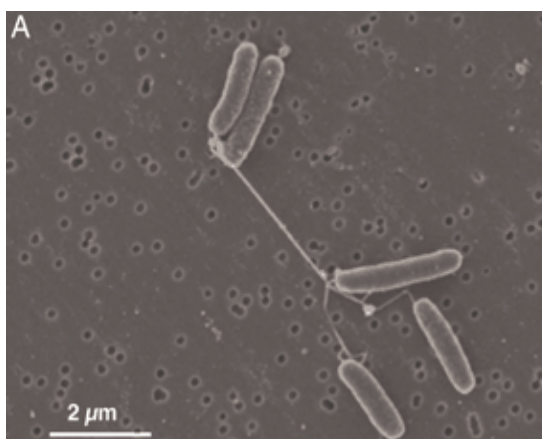


Figure 2.4: SEM image of the pili structure in wild type *Shewanella oneidensis* MR-1 (Gorby et al. 2006).

Alternatively, an indirect mechanism which involves the self-excretion of electron shuttling compounds (mediators) was discovered in some species. The concept was first supported in the study of *Shewanella oneidensis* which reduced Fe (III) oxides at a substantial distance with the aid of flavins. Further investigations revealed phenazine electron shuttles used by *Pseudomonas aeruginosa*. The biosynthesis of electron mediators, though strategically necessary under certain conditions, is energetically costly (Lovley 2006).

In reality, a MFC system that relies on the above electron transfer mechanisms implies diminutive current generation. In many instances, the addition of exogenous mediators is a prerequisite for the operation of MFC systems inoculated with most species (e.g. *Proteus*, *Escherichia coli* and *Bacillus*), if a significant amount of energy is to be harnessed (Lovley 2006). The idea of mediated electron transfer employing artificial electroactive potassium ferricyanide or benzoquinone was proposed by Cohen as early as 1930 (Schroder 2007). An indirect electron transfer mechanism involves the addition of an artificial electron transfer relay which channels electrons between the bacterial redox site and the electrode. In a mediated MFC, these low-molecular-weight mediators capable of undergoing redox cycling are activated by penetrating into the cell inner membrane containing the ETC proteins and intercepting electrons freed from catabolic processes. Once exiting from the cell in its reduced form, the “charged” molecule unloads the electrons onto the electron-withdrawing anode thereby becoming re-oxidized which allows the subsequent recycling process. A general description of these half equations is illustrated below (Bullen et al. 2006).



Ideally, for such reactions to be thermodynamically efficient, a mediator with the standard redox potential (E_0') between the two eventual half reactions is required. Moreover, a suitable mediator should also meet the following physic-chemical properties to ensure a smooth electron transaction between the bacterial redox center and the electrode:

- (i) A high diffusion coefficient into the bacterial periplasm in its oxidized form and out of the cell once reduced. From the above discussion, it is clear that the functionality of electron transfer compounds is heavily reliant on this dynamic cell membrane penetration property.

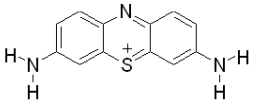
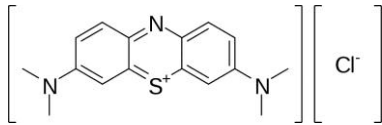
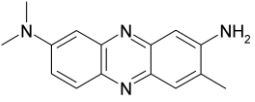
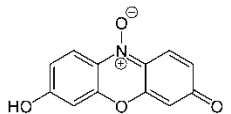
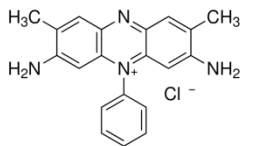
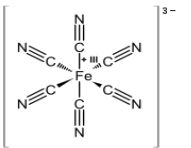
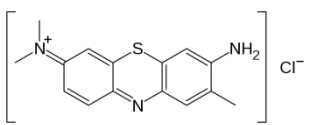
In an electrochemical analysis of thionine and safranine O, Choi *et al.* (2003) prepared a L- α -phosphatidylcholine (PC) wrapped, glassy-carbon electrode mimicking the hydrophobic layer of bacterial cells to investigate the impact of mediator-membrane interaction characteristics on fuel cell performance. In the case of safranine O, the reduced safranine molecule designated to transport electrons out of the lipid layer to the anode accumulated on the inner membrane surface instead. This interference of electron flow inhibited MFC efficiency by delivering a maximum current of only 0.05 mA. Under the same operational conditions, no accumulation on the cell membrane of either oxidized or reduced thionine was detected which contributed to greater, approximately 0.6 mA, current output.

- (ii) A redox potential as negative as possible to obtain a maximum potential difference between anode and cathode while still positive enough from reductive metabolite potential to facilitate efficient electron transfer. The redox potential of a mediator defines the upper limit on the maximum energy per electron that can be delivered (Sund et al. 2007). However, MFC systems applying mediators with optimum E_0' values do not guarantee superior performance and it is rather used as a primary hypothetical selection indicator reflecting the potential performance of the defined system.

- (iii) Be chemically stable in both oxidized and reduced states and not interfere with bacterial metabolic processes. Mediator-induced, adverse metabolic effects on microorganisms have been reported and should be avoided. As demonstrated by Peguin and Soucaille (1995), the addition of methyl viologen as an artificial electron acceptor can decrease the in vivo activity of the hydrogenase in *Cloastridium acetobutylicum* which resulted in a significant increase of the lag phase from 10 to 70 hours.
- (iv) It should display sufficient solubility in the aqueous electrolyte solution for practical purposes.
- (v) Facilitate electron transfer kinetics at the anode

Examples of commonly employed artificial mediators are listed in Table 2.2, as well as their structures and standard redox potentials. The actual working efficiency of a mediator is affected by the entangled biological and chemical complexity of the particular environment it is acting in. It is difficult to fine-tune all aspects of a mediator to achieve the perfect status particularly when its electrochemical reduction and oxidation rates are governed by the anode microbes and electrode respectively. It was concluded in a review paper by Van der Zee and Cervantes (2009) that the observed effectiveness of a mediator in a biological system is mainly influenced by its reduction kinetic and the underlying microbial mediator reduction mechanism. The details of how redox constituents within the cell interact with artificial mediators are still being investigated. And to date, relatively little research has focused on microbial-mediator reduction kinetics.

Table 2.2: Examples of commonly used mediators including their structures, redox potentials and reduction kinetics* by anode inoculum (Katz et al. 2003).

Mediator	Structure	Standard Redox Potential (V vs. NHE)	Reduction Kinetics ($\mu\text{mol/g of cell} \cdot \text{sec}$)
Thionine		+0.064	7.1
Methylene Blue		+0.01	N/A
Neutral Red		-0.33	N/A
Resazurin		-0.051	0.61
Safranine-O		-0.289	0.07
Potassium ferricyanide		-0.36	N/A
Toluidine Blue-O		+0.034	1.47

* Kinetic studies of mediator reduction were carried out by 0.1-0.15 mg dry cell weight ml^{-1} of *Proteus vulgaris* at 30°C with 50 mM mediator concentrations.

2.4 ELECTROCHEMICAL ASPECTS

2.4.1 Architecture

MFC designs vary in complexity; however, many of them are based on the traditional “H” shape dual-chamber MFC. A classic, dual-chamber MFC, as described in Sec 2.1, consists of a segmented anode and cathode compartments connected by either a salt bridge or a proton exchange membrane such as Nafion or Ultrex. An external resistor (R_{ext}) is often applied in conventional dual-chamber reactor experiments while the building components account for an additional resistor (R_{int}). The power output is inversely proportional to the sum of the external and internal resistance squared ($R_{ext}+R_{int}$)². The external resistor can be adjusted, whereas the extended electrode distance to the air-sparging cathode unavoidably amplifies the internal resistance (R_{int}) of the reactor. As a consequence, the maximum power density generated is constrained.

Despite the drawbacks in internal resistance and scale-up, the ease in assembling, sampling and monitoring of this setup provides a convenient tool for refining a specific performance parameter which can potentially result in a new efficient design. For laboratory experiments where high energy output is not the focus, the H-shaped MFCs are widely used in the assessment of the functionality of new building materials, artificial mediator performances, anode microbial-community behaviors and cathode efficiency etc. With its already high, internal resistance, this device is susceptible to systemic changes therefore making any improvement in scale detectable. For example, in a two-compartment system, the replacement of agar salt bridge by PEM contributed to significant increment in electricity output as evidenced in Min et al. (2005) study. Approximately twenty times more power was drawn after the introduction of a PEM as a result of decreasing internal resistance from 19,900 Ω to 1290 Ω .

Many artificial mediator studies are also in favor of this structure. In a study by Rahimnejad (2011), the mediator quality of methylene blue at various concentrations was analyzed in a double-compartment reactor. The system, with a Nafion membrane clamped in the middle of the glass bridge, yielded a maximum current of 232 μA at 300 μM methylene blue concentration. This setup has been implemented in the

research of other important mediators namely neutral red (Park and Zeikus 2000) and thionine (In Ho et al. 2011).

The dual chamber design has been essential to develop a general scientific understanding of MFCs, yet particular considerations are required towards efficient cathode construction if they are to become an economical option for sustainable wastewater treatment. Alternatives to the continuous, energy-draining, cathode aeration have incorporated ferricyanide or permanganate in the cathode as terminal electron acceptors. As demonstrated by Logan (2006), 1.5 to 1.8 times higher energy was recorded with ferricyanide being the cathode electron acceptor instead of dissolved oxygen. Regardless of these compounds dominating the power generation, their operation is inherently costly and lack of durability in practical applications.

Later, the concept of single-chamber system emanated with modified cathode designs attempting to optimize oxygen contact. One of the first successful one-compartment systems was published by Park and Zeikus (2003) in which the cathode was exposed to atmospheric oxygen directly rather than immersed in water thereby obviating the need for uneconomical air feeding and low-oxygen concentration in the electrolyte. A proton exchange, porcelain membrane was sandwiched between a rectangular anode bolted together with a porous air-cathode (Fig. 2.5a) (Du et al. 2007). The anode and the cathode was enhanced with immobilized Mn^{4+} and Fe^{3+} respectively, producing a maximum of 799 mW/m^2 power when supplied with activated sludge as the biological catalyst. Several variations of the single-chamber design have sprouted later on. In a prototype apparatus, Liu et al. (2004) assembled an acrylic cubic container accommodating a Pt-coated, carbon-paper anode and an air-cathode on the opposite sides of the reactor (Fig. 2.5b). The maximum power obtained was 494 mW/m^2 . An advanced version constructed by the same group achieved 80% of chemical oxygen demand (COD) removal while generating electricity. As depicted in Figs. 2.5c and 2.5d, this tubular-shaped reactor integrated eight anode graphite rods surrounding an air-cathode in a concentric arrangement (Liu et al. 2004). The central porous cathode rod was fabricated around by a piece of carbon cloth with a hot pressed PEM interfacing the anode medium. The substrate, domestic wastewater in this case, was injected into the cylinder perpendicularly to the electrode.

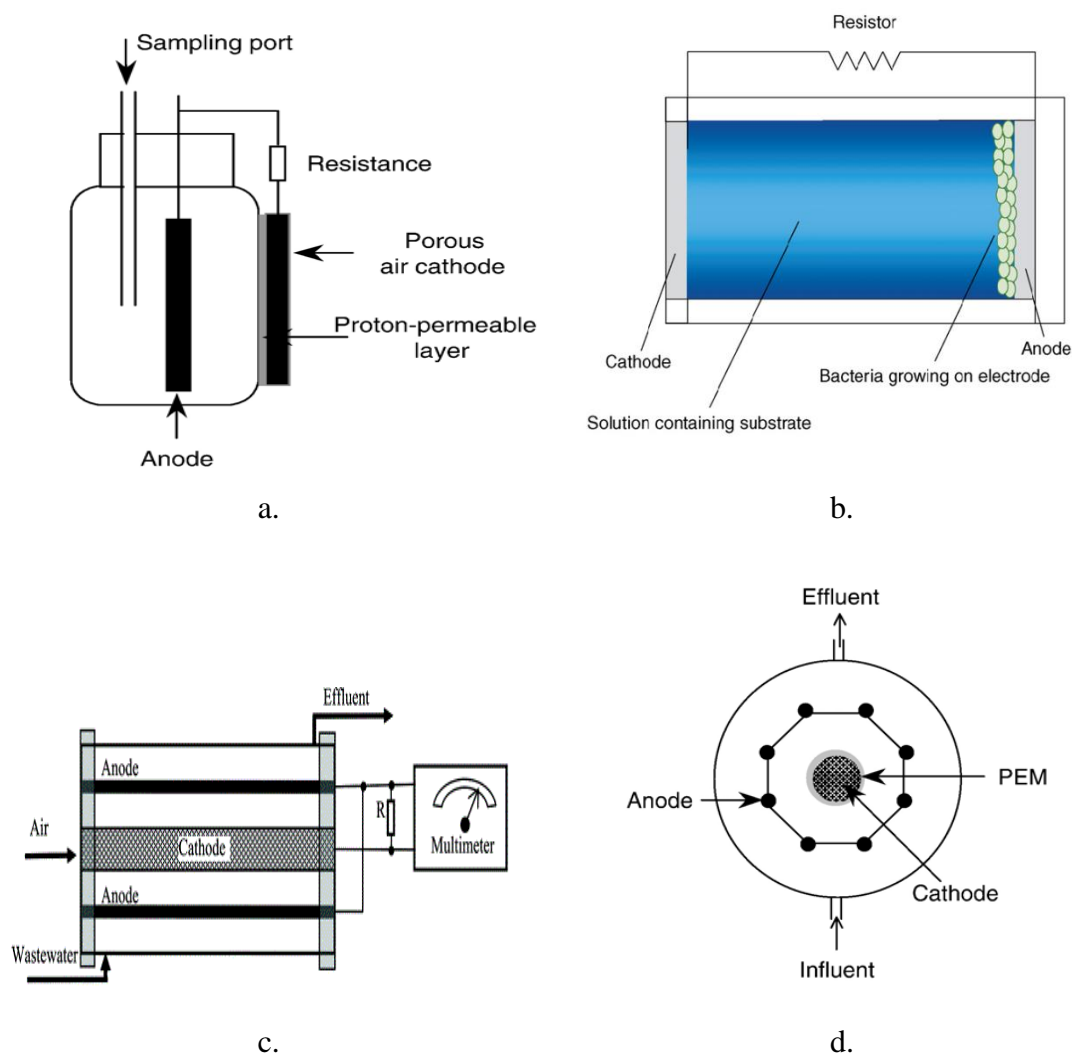


Figure 2.5: Simplified diagrams for various MFC architectures. **a.** a prototype single chamber MFC with air cathode (Du et al. 2007); **b.** a cubic single chamber MFC (Liu et al. 2004) ; **c.** side view of a cylindrical MFC consisting eight graphite anode electrodes surrounding a single cathode in a centric arrangement and **d.** top view of the same cylindrical MFC (Liu et al. 2004)

Furthermore, in the context of scaling up the power yield, stackable MFCs are configured by wiring several reactors in series or in parallel. In an example of a stackable MFC, 6 mini-reactors were connected through a cooper wire with graphite rods embedded into graphite granules in both electrodes. Although a maximum of 59 W/m^3 power was generated, it remained problematic due to voltage reversal in individual cells as pointed out by Logan (2008).

Apart from the continuous attempts in design optimization to increase energy extraction, the high cost of construction materials pose another challenge before industrial application is possible. The carbon-based electrodes frequently selected in MFC studies are versatile in terms of electrical conductivity, biocompatibility and chemical stability in microbial solution. Ranging from basic, carbon cloth and paper to graphite rods and brushes, modifications are constantly evolving to improve MFC performance (Logan et al. 2006). Incorporation of conductive polymers has boosted current density by approximately one order of magnitude in the case of organic polyaniline as demonstrated by Schröder *et al* (2003). Other factors which may limit the efficiency of complementary, cathode-reduction reactions include the availability of cathodic oxidant, proton-transfer kinetics and electrode construction. The cathode building materials are fundamentally the same as the anode except the routine fixation with a platinum (Pt) coating to catalyze oxygen reduction. A 3 to 4 fold higher energetic yield was demonstrated with a Pt-immobilized electrode in comparison to a plain, graphite electrode (Watanabe 2008). Since Pt is costly and potentially toxic to microbes in bio-cathode MFC, its replacement by cost-effective materials including iron complexes, manganese complex or organic compounds like cobalt complexes were successful with negligible performance degradation (Watanabe 2008). A brief summary of typical MFC design components and common building materials is shown in Table 2.3.

Table 2.3: A list of commonly used MFC-building materials.

<i>Components</i>	<i>Materials</i>	<i>References</i>
Anode electrode	Graphite felt	(Aelterman et al. 2008)
	Graphite cloth	(Zhang et al. 2009)
	Graphite foam	(Chaudhuri and Lovley 2003)
	Carbon paper	(Wei et al. 2011)
	Graphite brush	(Wei et al. 2011)
	Stainless steel grid	(Dumas et al. 2008)
Cathode electrode	Graphite cloth	(Logan et al. 2005)
	Carbon paper	(Scott et al. 2008)
	Platinum mesh	(Yu et al. 2007)
	Stainless steel mesh	(Zhang et al. 2010)

Anodic compartment	Packed granular graphite	(Rabaey et al. 2005a)
	Granular activated carbon	(Aelterman et al. 2008)
	Packed bed of Stainless steel balls	(Manohar and Mansfeld 2009)
Proton exchange membrane	Nafion 424	(Logan 2008)
	Ultrex	
	Anion exchange membrane	
	Salt bridge	
Electrode catalysts	Platinum (Pt)	(Sharma et al. 2008)
	Polyaniline	(Scott et al. 2007)
	Manganese complexes	(Watanabe 2008)
	Electron mediators such as Neutral red	(Park and Zeikus 2002)
	and 1,4-naphthoquinone	(Lowy and Tender 2008)

2.4.2 Analysis techniques

Conventional, electrochemical instruments such as resistors, multimeters and voltage meters are generally sufficient for cell voltage and electrode potential measurements. A MFC is wired with a data acquisition system to record the corresponding, cell voltage (V) running through a variable, external load (R_{ext}). The current (I) can be derived from the recorded voltage at known R_{ext} using Ohm's law ($I=VR^{-1}$). The maximum power output of a MFC is estimated from a polarization curve that expresses the cell voltage and power density as a function of the current.

More reliable, direct measurement of the current density can be achieved employing a potentiostat to assign a constant potential. The utilization of a potentiostat allows accurate and independent measurement of either the anode or the cathode behavior which eliminates the problem mentioned earlier about the amplified internal resistance due to the extended electrode spacing (Logan et al. 2006). In addition, a potentiostat can assist in obtaining other specialized performance parameters of the electrochemical system at fixed current values. In MFC experiments, the potentiostat interfaced with a computer system is typically configured with a working electrode, a reference electrode and a counter electrode immersed in the fuel cell's electrolytes for voltammetry studies. The potentiostat ensures the current flow only between the working and counter electrode while

accurate anode potential is applied. Ideally, the distance between the working electrode and the reference electrode is minimized to reduce ohmic potential loss. Cyclic voltammetry studies can be performed to interpret the oxidation-reduction mechanisms within an anode biofilm (Logan et al. 2006). The forward positive scan of a cyclic voltammogram represents the reduction reaction while the reverse negative scan correlates to the oxidation reaction. Furthermore, it can be used to explore the electrochemical reversibility of redox mediators by detecting appreciable oxidation and reduction peaks.

Chronoamperometry is another electrochemical technique which monitors the current as a function of time while the working electrode potential is stepped. In a typical, three-electrode setup, the working-electrode potential is regulated from a resting state where no current is detected to the point where a Faradic current occurs as the result of electron transfer reactions. Upon this potential shift, the current spikes momentarily and then decays exponentially as described by the Cottrell Equation (Eq. 2.4) (Xiong et al. 2012):

$$I = nFA_eC_A\sqrt{\frac{D}{\pi t}} \quad [2.4]$$

n = number of electrons

D = Diffusion coefficient (cm²/second)

F = 96484.6 Coulombs mol⁻¹

t = time (seconds)

A_e = electrode surface area (cm²)

C_A = concentration of electrolyte (mol)

Chronoamperometry is a simple, yet effective technique in obtaining quantitative results in regard to reaction mechanisms, rate constants and the concentration of electroactive species etc. In this account, this research employs the chronoamperometry technique as the primary tool to analyse the operational efficiency of various mediators in an experimental fuel cell apparatus based on current density derived.

Chapter 3: Experimental

3.1 MICROORGANISM ISOLATION AND GROWTH MEDIUM

The pollution concern over ethanol emissions as described in Sec 1.3 was one of the primary incentives of this research. Through the application of the MFC technology, bacterial inoculums transform part of the energy released from ethanol oxidation directly into electrical work via an external circuit. This could result in simultaneous energy production and ethanol emission control. The microorganisms of interest to fulfil such a task thus have to meet the following prerequisites:

- i) They should be ubiquitous in nature and readily obtainable from their dominant habitats in order to the cost of MFC systems.
- ii) They should exhibit inexpensive and vigorous cultivation profiles and be resilient enough to adapt to reasonable environmental variations.
- iii) Most importantly, they should be able to degrade ethanol as the sole carbon source and retain at least portions of microbial vitality at relatively high ethanol concentrations.

Acetic acid bacteria (AAB) are Gram-negative, obligate aerobes that are explicitly known for their acetic acid fermentation from ethanol. A total of 25 genera have thus far been characterized that belong to the *Acetobacteraceae* family (Yakushi and Matsushita 2010). These species occur prevalently in alcoholised or slightly acidic niches such as rhizosphere soil, flowers and fruits (Stasiak and Błażejczak 2009). Aerobic ethanol consuming *Acinetobacter* strains were estimated to constitute more than 0.001% of the entire heterotrophic aerobic population (Juni 1978). Enrichments have been successful using simple mineral media from a wide range of environmental sources, predominantly soil, water and compost samples (Partanen et al. 2010).

3.1.1 Bacteria from soil and compost samples

Mixed ethanol oxidizing consortia were isolated from moist soil and mature compost materials. The soil sample was collected from Parkhouse Garden Supplies, Christchurch, NZ. The garden compost sample of choice was purchased from The

Warehouse Ltd, Christchurch. Soil and compost samples were first sieved (2 mm sieve size) to eliminate the coarse particles and then diluted at 1:10 (w/v) ratios in the pre-sterilized selective medium. After mixing vigorously by stirring on a magnetic stirrer for 10 minutes, all particles were allowed to settle for 30 minutes. Portions of the homogenous soil and compost suspensions were filtered separately using Whatman[®] No.3 filter paper (to further remove particulate matter) before being transferred into the enrichment medium for cultivation. Two, identical, bench-scale incubation systems were assembled in parallel for soil and compost bacteria for cultivation.

3.1.2 Preparation of growth medium and nutrient agar

Synthetic nutrient solutions were prepared following the recipes shown in Table 3.1. The trace elements were added from a suitably concentrated stock solution. Deionized water was used for all aqueous solution in this research unless otherwise stated. An initial pH between 6.5 and 7 was regulated by the addition of phosphate buffer salts into one litre of the enrichment medium to give a final buffer concentration of 1 M. This high buffer composition was proved necessary in later experiments, considering the tendency of dramatic pH drift associated with the acetic acid accumulation ability of AAB. Moreover, the resulting high ionic strength and conductivity of the solution was beneficial for subsequent MFC use, where minimal ionic resistance between the anode and cathode is important. The completed growth medium solution was then sterilized in an autoclave (HS-60, Hanshin Medical, Ltd., Korea) at 121°C for 30 minutes (medium 1). At the beginning of the enrichment process, 99.9% laboratory grade ethanol was added to this medium as the sole carbon source. The initial environmental isolation and the substrate-concentration-preference experiments were conducted utilizing medium 1 (Table 3.1). An enhanced and strain-specific medium was prepared using the recipe illustrated in Table 3.2 (Abbott et al. 1973). It was employed as the preferred medium for all subsequent, growth-optimization experiments.

The nutrient agar solution comprising 1.5 g of agar (Agar Bacteriological, Oxoid Ltd.) and 100 ml of previously prepared growth medium (medium 2) was stirred and heated until clear, followed with sterilization for 15 minutes at 121°C. Ethanol was

injected into the warm agar liquid in a biocabinet to attain a final ethanol concentration of 2% (v/v). This warm agar solution was then poured aseptically into sterile Petri dishes.

Table 3.1: Mineral recipe for the nutrient solution (medium 1).

<i>The composition of the enrichment salt medium is as follow (per litre):</i>		<i>Desired Trace Element solution Composition:</i>	
Chemicals	Concentration	Chemicals	Concentration
NaNO ₃	1 g	ZnSO ₄ ·7H ₂ O	0.07 mg
MgSO ₄ ·7H ₂ O	0.1 g	MnCl ₂ ·4H ₂ O	0.05 mg
CaCl ₂ ·2H ₂ O	0.02 g	H ₃ BO ₃	0.2 mg
FeSO ₄ ·7H ₂ O	0.003g	CoCl ₂ ·6H ₂ O	0.1 mg
Ferric ammonium EDTA	0.003 g	CuCl ₂	0.1 mg
Cycloheximide	0.125 g		
KCl	0.6 g		
KH ₂ PO ₄	4 g		
Na ₂ HPO ₄	4 g		

Table 3.2: Strain-specific mineral recipe for the nutrient solution (medium 2).

<i>The composition of the enrichment salt medium is as follow (per litre):</i>		<i>Desired Trace Element solution Composition:</i>	
Chemicals	Concentration	Chemicals	Concentration
NaNO ₃	1 g	ZnSO ₄ ·7H ₂ O	2 mg
MgSO ₄ ·7H ₂ O	0.2 g	MnCl ₂ ·4H ₂ O	2 mg
CaCl ₂ ·2H ₂ O	0.02 g	H ₃ BO ₃	0.4 mg
FeSO ₄ ·7H ₂ O	0.007 g	CoCl ₂ ·6H ₂ O	0.4 mg
Ferric ammonium EDTA	0.05 g	CuCl ₂	0.4 mg
Cycloheximide	0.125 g	Na ₂ MoO ₄ ·2H ₂ O	0.2 mg
KCl	0.6 g	KI	0.1 mg
KH ₂ PO ₄	4 g		
Na ₂ HPO ₄	4 g		

3.1.3 Cultivation procedures

There are several aspects of concern when designing the cultivation apparatus. Both *Acetobacteraceae* and *Acinetobacter* strains are oxygen-demanding, ethanol oxidizers that require a continuous air supply. However, due to the volatility of ethanol, special care was taken to minimise changes in the ethanol concentration caused by the air flowing through the system. . To minimise this problem, two 250 ml

Erlenmeyer flasks assembled in series (Fig. 3.1), with the first flask functioning as an ethanol reservoir to equilibrate the incoming air with ethanol, so that a minimal amount would be stripped from the second flask containing the culture.

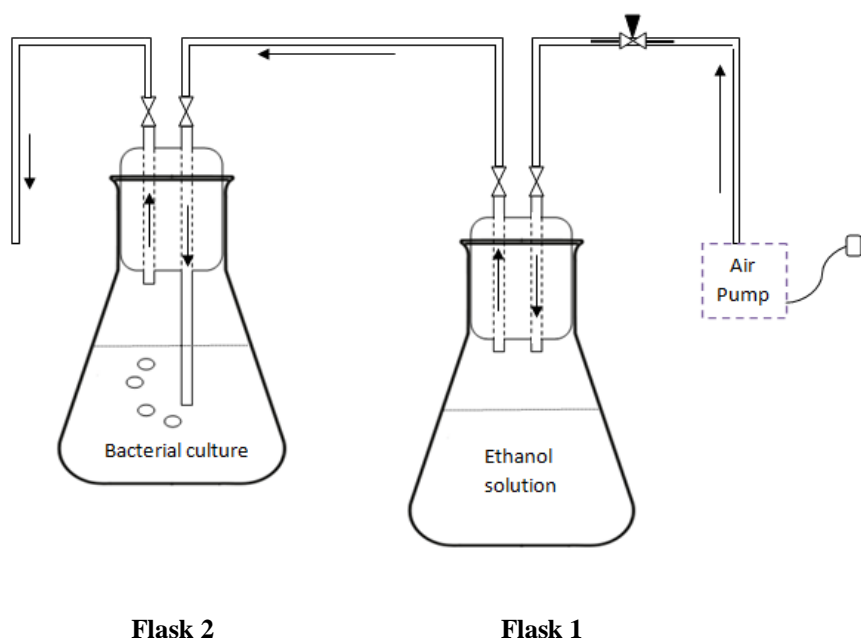


Figure 3.1: Schematic of the bacterial cultivation apparatus.

Bacterial cultures were prepared by inoculating 180 ml of ethanol-containing medium with 20 ml of the previously-filtered, soil and compost microbial suspensions. Protozoa predation is a well-recognized threat to microbial communities inhabiting natural environments, and is particularly relevant in this case due to the use of environmental specimens. Necessary precautions should be taken to support the survival and, furthermore, the fitness of bacterial isolates from these samples. As suggested by Loefer and Matney (1952), 0.025 g of cycloheximide (Sigma-Aldrich, $\geq 93\%$), also referred to as actidione, was dissolved into 200 ml of bacterial inoculum to inhibit or eliminate such a problem. The cultivation reactors were maintained with minimal disturbance in the biocabinet at room temperature (22-25 °C), until a stationary growth phase was observed. The aeration was controlled to between 0.2 and 0.4 vvm (gas volume flow per unit of liquid volume per minute) by a needle valve.

To propagate bacteria on nutrient agar, one loop of the microbial mixture from the cultivation flask was captured and then streaked onto agar plates. They were then

incubated at 30 °C until bacterial colonies appeared, then stored at 4 °C for subsequent cultivation. Frequent subcultures were prepared every month to maintain cell viability. The dominant individual colonies were selected and identified using 16S rRNA analysis by Macrogen Inc. Korea.

3.2 BIOMASS CONCENTRATION ANALYSIS

The biomass concentration increase is the most basic practice in microbial study and routinely followed during the course of bacterial growth in order to quantify the specific yield coefficient and rate of substrate utilisation. In this research, the electron-mediator reduction rate, bacterial-mediator adsorption and MFC current production are all directly influenced by the biomass concentration. There are several, well-established methods to probe the dynamics of biomass production depending on the parameter of interest such as mass, volume, metabolic rates and live cell counts (Pirt 1975).

Spectrophotometric measurements are conventionally used as they are rapid, robust, and suitable for determining the concentration of almost all bacterial cultures. However, neither the exact cell numbers nor the grams of cells are measured directly using this method. If detailed information is required, it is commonly accompanied by dry matter measurement (for mass concentrations) or colony forming unit (CFU) counts. CFU measures the viable cell number present in a culture, assuming that a single colony was derived from one bacterium via binary fission. The dry cell weight method, unlike CFU count, is accurate and acts as a benchmark technique for comparing results. One or all of these techniques were implemented as required during this research.

3.2.1 Optical density test

Sampling from the cultivation flask was withdrawn using a sterile pipette periodically. The optical density was measured in a single beam spectrophotometer (MultiSpec 1500 UV/Vis, Shimadzu[®], Kyoto) at a wave length of 600 nm. Sample dilution factors were chosen such that the absorbance reading fell within the range of 0.1 to 0.6 (Ertl et al. 2000). A growth curve of time vs. actual absorbance, restored by

multiplying the recorded number with its corresponding dilution factor, was plotted and the specific grow rate was calculated from this curve.

3.2.2 Colony forming unit

Colony forming unit counts were determined, involving a series of successive dilutions of the original culture in sterile buffer. At regular time intervals, 0.1 ml of culture was transferred into 0.9 ml of aseptic deionized water for further dilution by up to ten times, based on biomass concentration. 100 µl of aliquots from each dilution level were spread over the surface of nutrient agar plates in duplicate with a sterile, glass-spreading rod. Countable plates with colony numbers of 20-200 were examined after 24 hours incubation at 30°C. The following formula (Eq. 3.1) was used to calculate the CFU per ml of culture:

$$\frac{CFU}{ml} = \frac{\left(\frac{N_{x1} + N_{x2}}{2}\right) \times 10^x}{volume\ spread\ on\ plate} \quad [3.1]$$

N_{x1} = Colony counts at dilution x

N_{x2} = Colony counts on duplicate plate at dilution x

x= Times of dilution

3.2.3 Dry biomass weight

Two slightly different methods were used, method 1 had the advantage of being shorter which was beneficial in order to obtain an instant cell weight at the time selected; whereas method 2 was used when optical density was higher than 1. In the case of utilizing method 2, although time consuming, it was more accurate as it included the non-pellet forming, fluffy material which was observed at high biomass concentrations:

Method 1: For the purpose of tracking the growth of a fresh culture, 10 ml of bacterial solution was removed from the growth flasks at appropriate time intervals for measurement. The sample was evenly distributed into seven pre-weighed dry Eppendorf tubes followed by centrifugation at 13,000 rpm for 5 minutes. The remaining pellets, after the clear supernatant was decanted, were then dried at 105°C

overnight and reweighed once cooled in a desiccator. Duplicate experiments were carried out and the final results were expressed in g/l.

Method 2: This method was applied to quantify the dry cell weight in a selected sample pool used for electron mediator reduction or MFC power generation analysis. 10 ml of bacterial sample was filtered on a piece of dry and pre-weighed Advantec[®] Membrane filter (0.2 µm pore size) with a vacuum pump. A thick bacterial paste was subsequently dehydrated to a constant weight at 80°C before the final weight was recorded (Yu et al. 2001).

3.2.4 Contamination test

Contamination with foreign microorganisms posed a continuous threat to pure cultures in batch cultivation environments. To assess the occurrence of such a problem, samples taken directly from the enrichment flasks were routinely plated out. The consistency of colony morphology on a selected plate was regarded as an important parameter in judging the degree of contamination. However, this method is only approximate and it is difficult to low levels of contamination as assumptions must be made about the uniform distribution of foreign cells in test subjects. With the above reservations, contamination control measures including autoclaving all apparatus components before use and routine UV and 70% ethanol disinfections were performed. For each continuous culture experiment, a total of two purity tests were performed with one after roughly 48 hours and the other at the end of the experiment. All data were invalidated upon detection of foreign colonies on culture plates.

3.2.5 Carbon source utilization

The ethanol degradation rate during the biomass incubation test was measured in an YSI 2700D biochemistry analyser (YSI Incorporated, Ohio). The equipment was calibrated prior to experiment start which had a maximum detection range of 3.2 g/l in liquid samples. A sample consisting of a 1:3 dilution of the microbial suspension was prepared for ethanol concentration determination.

3.2.6 Calculation of specific growth rate

Specific growth rate is a fundamental parameter in modelling microbial growth and determining the fitness of strain under batch conditions. It is defined as the time-dependent increase in microbial population which is commonly represented by the symbol μ with the most common unit in reciprocal hours (h^{-1}). Several consecutive OD_{600} measurements within the region of exponential growth were plotted on a logarithmic scale versus time on a linear scale. A straight line was then fitted to the data. Two data points OD_1 and OD_2 and their equivalent t_1 and t_2 values were chosen from this line for the calculation of specific growth rate. The following equation was used to determine μ and was expressed as h^{-1} .

$$\mu = \frac{\ln \text{OD}_2 - \ln \text{OD}_1}{(t_2 - t_1)} \quad [3.2]$$

3.3 OPTIMIZATION OF GROWTH RATE

Effects of varying cultivation conditions on the bacterial growth behaviour were investigated. Colonies isolated from compost samples were tested for this series of experiments¹. All tests were conducted under the same physical conditions that were presented in prior sections. Once the identity(s) of the dominant strain(s) was (were) revealed, the chemical composition of growth medium was amended to be strain specific.

Experiment 1: In this experiment, preliminary growth profiles of the same bacterial community at different ethanol concentrations were established. Four ethanol concentrations of 0.5%, 1.3%, 2% and 2.6% (v/v) were selected. These systems were operated in parallel and the biomass yields were monitored using the optical density technique described above. The substrate concentration for later biomass cultivation was chosen out of the four in which the fastest growth rate and the highest biomass density were observed. Medium 1 was employed for this group of analyses.

¹ A single bacterial strain was isolated from both soil and compost samples, therefore, only the compost isolate was retained and purified for subsequent cultivation studies.

Experiment 2: To determine if the growth pattern was influenced by different nitrogen sources, a modified, growth medium (medium 2) containing the same ingredients, with the exception of the replacement of NaNO_3 by NH_4Cl was prepared. The optical density, dry cell weight and viable cell count trends of the bacterial growth in the NH_4Cl -containing medium was recorded. The growth curves constructed from these three methods were compared and correlated. A standard curve of OD versus dry biomass was developed based on the data obtained.

Experiment 3: Because aeration is known to be a critical factor in submerged culture environments, the growth patterns at different aeration regimes were recorded. A bubble flow meter was used for the determination of aeration rates. Two parallel cultivation apparatus were prepared and the air sparing rate was set within the range of 0.2-0.4 vvm for the control experiment. An increased aeration rate (0.64-0.68 vvm) was applied for the other culture. All other physical conditions were maintained at the same level as the previous cultivation experiments. The time-dependent increase in optical density was measured in order to derive a growth curve.

Experiment 4: The foaming issue in the culture vessel required intervention which otherwise led to reduced biomass yield due to the biomass stripping effect of foam overflow. A control experiment and Antifoam A (0.6-1% v/v, Sigma-Aldrich) assisted cultivation experiment were analysed by recording the optical density readings at 600 nm.

3.4 CHEMICAL COMPONENTS

In MFC research, redox mediators are frequently added in the anode compartment to promote the electron transfer between the bacteria and the electrode. By incorporating a suitable mediator, the activation losses occurring at the molecular level could be, in theory, compensated (Rabaey et al. 2005b). Among all the requirements defining a good mediator outlined in Sec 2.3.3, two are of paramount concern:

- ❖ Facile transfer across the cell membrane (or to/from the redox sites within the bacteria) of the oxidised and reduced forms of the mediator

- ❖ A thermodynamically-favourable, potential difference between the site in the terminal electron chain and the mediator, plus a favourable, potential difference between the mediator and the terminal electron acceptable at the cathode.

The mediating efficiency of thionine (Sigma-Aldrich), methylene blue (MB) (BDH Laboratory Supplies), resorufin (S.B. Penich & Company) and potassium ferricyanide, in terms of their intracellular accumulation and the correlating current output, were profiled in this set of experiments. These mediators are known to have strong binding affinities towards prokaryotic cells and are often used in biological studies to highlight the organelle of interest (Jockusch et al. 1996). Based on their observations, it was thus reasonable to speculate that this staining property can cause the sorption of the mediator to the microbial membrane over time; consequently, the concentration of mediator that was dynamically involved (at the anode) in the electron transfer process was reduced. In this circumstance, inefficient electron transfer (due to mass transfer limitations) could potentially lead to a diminished current output in an exogenously-mediated MFC. The following experiments were designed to investigate such behaviour.

3.4.1 Biotic reduction of mediators

All mediators chosen for this research were coloured in their oxidized form. The first approach of these sets of experiments, therefore, exploited Beer's law which predicted a linear relationship between the absorbance and the mediator concentration in a solution. A series of standard solutions with known mediator concentrations were prepared. The corresponding absorbance was quantified at the appropriate wavelength in a Shimadzu MultiSpec 1500 to plot a calibration curve of oxidized concentration vs. absorbance for each test subject.

The biotic mediator reduction tests at various concentrations were operated in 25 ml oxygen-limited, glass bottles. An appropriate amount of mediator powder was transferred into the pre-labeled, glass bottle which was then filled with bacterial suspension to final volume of 20 ml. After gentle agitation (using a magnetic stir bar), the homogenous mediator-microbe solution was allowed to stabilize under an argon atmosphere for 10 minutes. It was then sealed immediately for the microbe-mediator interaction reaction. The exact biomass concentration of the bacterial suspension was

determined in g/L by utilizing dry weight method 2. The process of biotic mediator reduction was monitored visually based on the distinct, color change of each mediator.

3.4.2 Intracellular partitioning analysis

At the end of the biologically-driven, reduction process, 2 ml of the sample was subtracted and centrifuged at 13,000 rpm for 5 minutes. The supernatant was diluted, followed by oxygen exposure in a quartz cuvette until complete re-oxidation was achieved (5-10 mins). Absorbance measurements were made relative to a blank (DI water) at the absorbance maxima of the oxidized forms. The mediator concentration remaining in the solution was determined using a previously obtained absorbance vs concentration calibration curve. The mediator partitioning behaviour was presented graphically as the ratio of $\text{Mediator}_{\text{partition}}/\text{Cell mass}$ versus the concentration of $\text{Mediator}_{\text{remain}}$ in aqueous phase. The microbe binding affinity of each participating mediator was assayed following this protocol at various concentrations.

3.5 REACTOR DESIGN

A range of MFC designs are used in literatures. The conventional two-chamber MFC is a widely accepted and inexpensive design for testing concepts and specific parameters. However, the energy conversion of this design is challenged in a number of ways, most significantly by the following inherent features:

- i) Ohmic resistance from the electrode to the outer circuit which limits the flow of electron between the electrodes
- ii) Low ionic conductivity between the two chambers
- iii) Raised internal resistance associated with inappropriate separator materials (e.g. agar bridge)

Although high power generation is not the immediate goal of this research, these factors should be taken into account in the architectural design if meaningful and convincing current is to be generated through appropriate reactor design.

3.5.1 MFC configuration

The experimental fuel cell was constructed from two cylindrical glass containers (purchased from the Glassblowing Workshop, University of Canterbury) in an “H” shape (Fig. 3.2). The connecting glass bridge was clamped in place by two silicone rubber gaskets with a piece of NafionTM Proton Exchange Membrane (PEM) sandwiched in between. The maximum diameter achievable for the bridge was 1.1 cm, and, as a result, the PEM membrane had a contact area of 0.95 cm². The shortened distance of the bridge minimized the internal resistance which, in theory, should increase the power output. Each half cell, including the bridge, had a working capacity of 16 ml. They were covered by two customized polycarbonate stoppers through which the electrodes and (when necessary) gas inlet were placed.

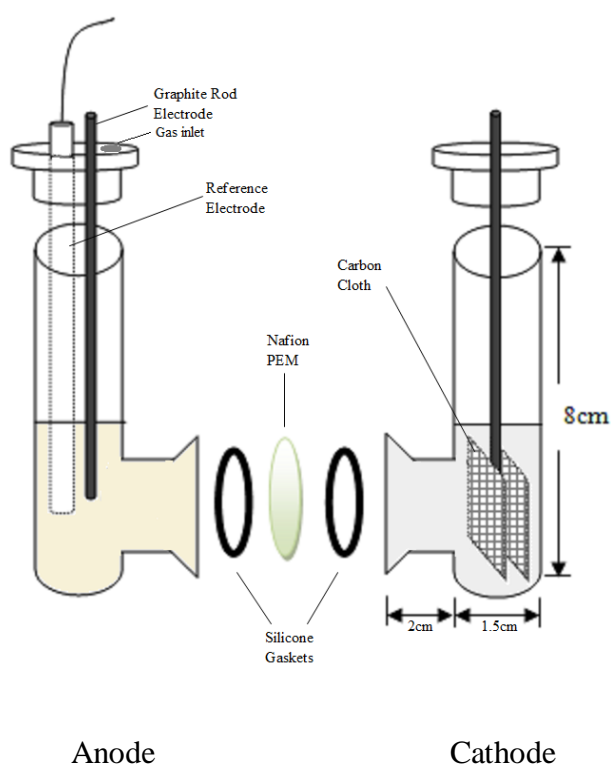


Figure 3.2: Schematic of the MFC design fabricated for this research.

Graphite rods (3x305 mm, SPI Supplies, USA) with a porosity of 16.5% were incorporated as both the anode electrode and the electrode contact material in the cathode chamber. A length of 1 cm of the graphite rod was exposed to anode solution providing an anode working area of 1.03 cm². For the cathode, two pieces of carbon

cloth, 2 cm², were attached to a graphite rod resulting in an overall electrode area of 4 cm² in the cathode cell. For sterilization, the anode and cathode electrodes were submerged in 70% ethanol for 1 hour and rinsed in DI water, dried at 70°C and then stored in phosphate buffer before application (Yuan and Kim 2008).

The NafionTM 117 PEM membrane was pre-treated following the procedure described by Rahimnejad (2011). It was boiled in 3% hydrogen peroxide first for 1 hour to remove organic contaminants before preceded with deionized water soaking and 0.5 M sulfuric acid treatment for 1 hour. Sulfuric acid was used to convert from the Na-form to H-form of the ionomer. It then remained in sterile DI water before use.

3.5.2 Anode and Cathode feed solutions

The MFC anode inoculum was made from appropriate concentrations of redox mediators homogenized in freshly harvested biomass solution. An optical density reading above 1 (refer to App II) indicated a sufficient amount of bacterial cells present to carry out the fuel cell experiments. Dry weight measurement using method 2 was performed simultaneously to determine the cell concentration. It was then followed by dissolving the required amount of electron mediator powder in 10 ml of bacterial sample. The final solution was gently stirred in an oxygen-free environment, created by argon purging, until all chemicals were dissolved.

The cathode vessel was filled with 10 ml of phosphate buffer containing 0.36 g/l KCl, 1.44 g/l KH₂PO₄ and 1.66 g/l Na₂HPO₄. The pH of the catholyte was adjusted within the range of 6.8 to 7.

3.6 ELECTROCHEMICAL ANALYSIS

3.6.1 Electrochemical cell preparation

Prior to starting the experiments, all fuel cell components except the PEM were sterilised with 70% ethanol and then rinsed thoroughly with deionized water. After assembly, the two chambers were continuously bubbled with 100% argon gas (10 ml/min) to ensure anoxic conditions in the empty vessels. The electrolytes were

transferred into the corresponding fuel cell chamber. Under anoxic conditions, the bacteria present in the anode chamber reduced the mediator, as depicted by the gradual fading of the mediator's colour. The rate of this process varied according to the type of the mediator. Once the redox mediator was fully reduced, chronoamperometric investigation was initiated.

3.6.2 Chronoamperometric analysis

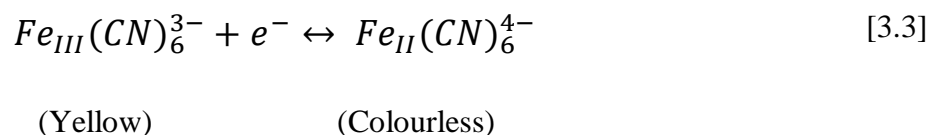
All electrochemical assays were conducted in the MFC at a predefined anode voltage using a Gamry potentiostat (Reference 600, Gamry Instruments, USA) attached to a personal computer. Gentle magnetic stirring in the anode bacterial solution during this procedure helped to increase convection and the current. Argon flow into both compartments was stabilized at 5 ml/min for the entire experimental session. Internal resistance (R_{int}) was checked with the potentiostat at the start of each experiment.

Chronoamperometric measurements were performed in a standard three-electrode mode with the MFC anode as the working electrode and the cathode as the counter electrode and a saturated calomel reference electrode. The calomel reference electrode was positioned as close as possible to the anode working electrode (60 mm) in order to minimize potential loss due to the ionic resistance of the electrolyte. The working electrode potential was poised at 0.3 V more positive to the standard redox potential of the mediator, and the current measured over time. All experimental parameters were the same for each mediator tested.

3.7 MEDIATOR CASE STUDY – POTASSIUM FERRICYANIDE

The ability of Gram-negative microorganism to reduce hydrophilic oxidants such as potassium ferricyanide has been confirmed electrochemically in many previous investigations (Catterall et al. 2001; Ertl et al. 2000). The redox couple of ferri-/ferrocyanide is well characterized and possesses a readily quantitative pigment in its reduced form. As a result, potassium ferricyanide has been repeatedly applied as an electron mediator in a range of fuel cell and amperometric systems (Emde et al. 1989). In these systems, the reduction of ferricyanide ion to ferrocyanide was catalysed by accepting electrons from a membrane-bound dehydrogenase as

represented in Eq. 3.3 (Zahl et al. 2002). Ferrocyanide, the reduced form of ferricyanide, is subsequently reoxidized at a suitable electrode resulting in current generation.



Based on the observations from an earlier set of experiments (Sec 3.6.2), the rate of cellular redox molecule reduction varied significantly and which could have contributed, in part, to the discrepancy in current output. To clarify this, potassium ferricyanide was used as the model redox molecule to probe the microbial reduction event, which confers two major advantages. First, its relative inertness towards atmospheric oxygen increases the accuracy when monitoring trends of reduction photometrically under aerobic conditions. Second, both oxidation and reduction reactions proceed via a single electron transfer process which make the energetic activity interpretation of the biocatalyst more convenient.

3.7.1 Sample preparation

A pure colony was collected aseptically from an agar sample isolated from compost and grown in the flask system on ethanol (Fig. 3.1). Two identical sets were prepared concurrently. The fermentation proceeded at 22 °C while a routine measurement of optical density ($\lambda_{max}=600$ nm) was performed every 8 hours to establish the growth curve. The culture was harvested twice, 100 ml at the midpoint of the exponential phase and the rest at the start of the stationary phase, for ferricyanide reduction tests. The dry mass concentration at each point of collection was measured. Four portions, each with an exact volume of 25 ml, were distributed into four 50 ml sterile conical polypropylene tubes. Accurately weighed potassium ferricyanide powder was homogenized into the bacterial suspension to give the final desired concentration. For each addition, the ferricyanide/cells suspension was incubated for at least 5 minutes before the first measurement of optical density was taken.

3.7.2 Kinetic of ferricyanide reduction

Eight assorted concentrations of ferricyanide were included for the cellular reduction test. They were maintained at room temperature during the process of reduction with minimal disturbance allowed. The decolouration of ferricyanide in each solution was determined by the decrease in absorption at wavelength of 420 nm. At a regular time intervals, 1 ml of the test sample was transferred into an Eppendorf tube for centrifugation. After centrifuging at 13,000 rpm for 3 minutes, the biomass-free supernatant was decanted and diluted till the absorbance was below 0.8 if required. The absorbance was measured with the Multispec1500 UV/Vis spectrophotometer at the maximum absorption wavelength for potassium ferricyanide (420 nm). The measurements continued for a maximum of 8 hours when the dye reduction started to slow down and the difference between each absorbance reading became indistinguishable from instrumental error. The pH of the test solutions was examined every 30 minutes throughout the course of these experiments.

Three, 25-ml samples were removed from the culturing flask when they reached the stationary growth phase and deoxygenated in an anaerobic glove box for 24 hours. In the anaerobic glove box, ferricyanide concentrations of 5 mM, 50 mM and 100 mM were prepared with these oxygen-free solutions for anoxic reduction assays following the same protocol described above. The ferricyanide concentrations remaining in the reaction mixtures were calculated via absorbance by reference to the standard calibration curve. The dye reduction progress curves were plotted as ferricyanide concentration vs. time in order to obtain the gradient from the linear region of the curves. It was then normalized by the biomass dry weight to deliver specific rate constants.

Chapter 4: Microbe Growth analysis

This chapter describes the isolation and cultivation of ethanol oxidizers from environmental samples. Sections 4.1 and 4.2 include the results for the isolation and 16 rRNA identification of the environmentally-selected bacterial strains. In order to identify the optimal incubation conditions for the bacterial strain obtained, the effects of various culture conditions on growth rate are presented in section 4.4.

4.1 ENRICHMENT OF ETHANOL OXIDIZERS

Soil and compost were selected as potential sources for the isolation of ethanol-oxidizing bacterial strains. Two 20-ml suspensions of filtered soil and compost were incubated separately in batch cultures with 2.6% (v/v) of ethanol as the sole external energy source. The growth of each flask was monitored using a spectrophotometer for absorbance determinations every 12 hours at 600 nm (data not shown). Foam accumulation at the liquid surface was observed after 24 hours and continued for the entire course of cultivation. A lag phase of approximately 24 hours was observed and optical density readings plateaued above 1.5 after 136 hours of incubation for both samples investigated. Untypically in this case, no distinct exponential phase was detected, and the initial lag phase was followed by a linear growth phase. To obtain information concerning this linear growth pattern and the identities of the predominant ethanol oxidizing strains, soil and compost batch cultures were propagated for the isolation of single colonies on agar plates.

4.2 AGAR ISOLATION AND STRAIN IDENTIFICATION

After 24 hour of incubation at 30 °C, predominant strains were selected and isolated for detailed identification. It was observed that only one predominant strain (based on colony morphology) has appeared on all the agar samples. Colonies of both soil and compost enrichment cultures were approximately 1 mm in diameter, creamy, and had a circular form with a convex elevation. The colonies possessed a butyrous consistency which pulled out into strands when picked with an inoculating loop for Gram stains. Gram stains were performed on these organisms prior to microscopic examinations. Under the microscope, the majority of the cells were

Gram-negative, non-motile coccoid rods. They were grouped in pairs or short chains; small clumps and tetrads were also observed. A few cells were encapsulated in an extracellular matrix which is typically composed of polysaccharides, polymers of simple sugars. The formation of such a structure under competitive stress was presumably associated with the gluey appearance of the colonies (Esko 2009). It was observed that with repetitive subculturing, this butyrous consistency of the colony disappeared along with the extracellular capsule structures previously observed under the microscope. It was possible that, in the later process, with improved nutrient supply and incubation conditions, the selective pressure that gave rise to the formation of the capsule was lifted, hence the termination in capsule production.

Four pure-culture samples, two from the soil and the compost enrichment respectively, were investigated and identified through 16S rRNA sequencing (Microgen Ltd.). All four isolates belonged to the genus of *Acinetobacter* spp. with one compost isolate specified as *Acinetobacter calcoaceticus*. The *Acinetobacter calcoaceticus* strain was purified on several agar plates for use in subsequent experiments. The identification process was repeated 6 months later with a fresh compost extract and the same organism was retrieved.

It was unexpected that the incubation of crude soil and compost extracts led to the emergence of only one predominant species rather than multiple species. As introduced in Ch. 3, acetic acid bacteria (AAB) are a large group of obligate aerobic Gram-negative bacteria, explicitly known for their ability to produce acetic acid as the major end product of ethanol oxidation. Many species of AAB are able to tolerate ethanol concentrations up to 7% v/v with an optimal growth temperature range of 25-30°C (Gullo and Giudici 2008). They are important microflora broadly distributed in natural habitats, such as flowers, soil and water, which makes them valuable and economical candidates in a range of industrial chemical production (e.g. vinegar and ascorbic acid) (Sharafi et al. 2010). The distribution of AABs in nature coincides with another genus of well recognized ethanol oxidizers, *Acinetobacter* species. Apart from ethanol, these microbes have an extremely broad substrate specificity which includes glucose, hydrocarbons and complex aromatic compounds (Juni 1978). The nutritional properties of *Acinetobacter* spp. and their ubiquitous occurrence in nature allows their successful isolation from soil, compost and water ecosystems through

enrichment procedures using a simple mineral medium maintained at a neutral pH (6.5-7.5). Bearing this in mind, it is important to know why *Acinetobacter calcoaceticus* overgrew ethanol-degrading AAB strains despite their close ecological and physiological similarities.

One obvious explanation is the greater abundance of *Acinetobacter* in the selected habitats than AAB due to its intrinsic ability to grow on a wide range of organic compounds. Its scavenging and remediation properties for numerous pollutants such as biphenyl, chlorinated biphenyl, phenol, benzoate, crude oil, lignin, and phosphate or heavy metals have aroused growing interest in potential biotechnological and environmental applications (Abdel-El-Haleem 2003; Smith et al. 2004). Composting is a controlled biological oxidation process through which biodegradable agricultural, industrial and municipal organic wastes are stabilized. This process involves a complex ecosystem in which the bacterial decomposition and transformation of organic components are dependent on many interacting factors, in particular the physicochemical parameters of the organic materials and the microorganisms. Although the chemical composition of waste materials is diverse and variable, lignin-containing compounds account for a major part of the organic matter found in agricultural residues and municipal packaging (Tuomela et al. 2000). Lignin-degrading microorganisms, such as *Pseudomonas* spp. and *Acinetobacter* spp. are naturally present in waste environments that readily participate in the composting process. A study of Sundberg et al. (2010) addressed the predominance of *Acinetobacter* in the selected composting plants operating on municipal solid wastes. It is further demonstrated by Lin et al. (2012) that *Acinetobacter* is one of the dominant strains exists at the initial and the maturation stages of the composting process. In any soil environment, a periodic fluctuation in resource availability, presumably resulting from events including rainfall or waste disposal, is influential in the growth and survival of bacteria (Eichorst et al. 2007). For this reason, the distribution and population dynamics of a certain microorganism in soil vary in correlation with the physical and chemical properties of the soil (e.g. carbon source, oxygen availability and moisture content). In natural environments where conventional substrates are limited, a few *Acinetobacter* species, including *Acinetobacter calcoaceticus*, are believed to be competent in integrating foreign DNA and carrying out genetic transformation (Palmen et al. 1993). This robust metabolism

characteristic of *Acinetobacter* provides them with a high capacity for adaptation which may explain its metabolic versatility. Furthermore, *Acinetobacter* species display higher survival rates when soil moisture supply remains insufficient, based on the finding of Webster et al. (2000). In contrast, typical AAB strains have a narrower nutritional spectrum, restricted to sugars, sugar alcohols and ethanol. Most of the strains can only thrive on ethanol, acetate, and, in some cases, lactate (Raspor and Goranovič 2008). They lack the metabolic flexibility to switch energy source in accordance with the appropriate physical and chemical conditions within the soil and compost environments. It is then obvious that the competitive advantage of *Acinetobacter* spp., derived from wide substrate spectrum, allows it to outcompete the AAB, leading to its dominant occurrence in the soil and compost samples examined.

An alternative explanation is the growth inhibition of acetic acid bacteria, possibly due to the limited oxygen availability in either the selected environmental samples or the batch culture flasks. AAB are candidates well suited for a variety of biotechnology applications when low biomass accumulation is required (Luttik et al. 1997). The most prominent metabolic feature of AAB is its rapid oxidation of ethanol to acetic acid. The efficient ethanol oxidation capacity of AAB exceeds the capacity for the further oxidation of acetate into carbon dioxide and water. As a consequence, the growth of AAB on ethanol is inevitably accompanied by a vast accumulation of acetic acid making them relatively acid tolerant. This selective advantage may explain the occurrence of AAB at the start of the composting process where the pH falls within the range of 4.5-5.5 (Partanen et al. 2010). The weak lipophilic acetic acid can penetrate into the cytoplasm which causes the dissipation of the transmembrane pH. The resulting acidification of the cytoplasm has to be mitigated by proton translation and consumption by the tricarboxylic acid cycle in the presence of high level of dissolved oxygen (Luttik et al. 1997; Sharafi et al. 2010). Therefore, the degree of acid tolerance of AAB is strongly dependent on oxygen availability. Under oxygen deprivation or other stress conditions, the AAB were proven to exist in a viable but nonculturable state. The difficulty of isolation and cultivation of AAB upon entry into this viable but nonculturable state is one of the reasons why AAB are considered a fastidious microorganisms (Ilabaca et al. 2008).

4.3 GROWTH CURVES AT VARIOUS ETHANOL CONCENTRATIONS

From this point, all experiments involving microbial component were conducted utilizing pure cultures of *Acinetobacter calcoaceticus*. Typical bacterial growth should show four distinct stages representing the lag, exponential, stationary and death phase with respect to time. During the lag phase, bacteria cells are devoted to aligning themselves to the new environment while the total bacterial population remains temporarily unchanged (Robinson et al. 1998). It is then followed with an exponential phase characterized by the continuous doubling of both the number of cells and the rate of population increase through cell division with each consecutive time period. The specific growth rate of an organism can be determined from the slope of this region quoted in terms of the number of divisions per cell per time unit. The horizontal linear region of the growth curve is referred as the stationary phase, commonly indicating the depletion of limiting nutrients or the buildup of inhibitory metabolites or end products (Kolter 1993). If incubation proceeds under nutrient starvation or metabolite poisoning conditions, the viable cell population will decline eventually and the death phase is observed. It should be noted that this phase may be undetectable by the turbidity test as the spectrophotometer cannot differentiate between live and dead cells unless the dead cells lyses.

In these sets of preliminary enrichment tests, growth was terminated once the transition from exponential to the stationary phase was completed, as signaled by the flattening of the absorbance curve. This procedure was adopted because the region of interest for this research was the exponential growth phase from which the specific growth rate could be estimated. The time courses of growth at various ethanol concentrations were plotted using OD₆₀₀ as a measure of cell growth (Fig. 4.1).

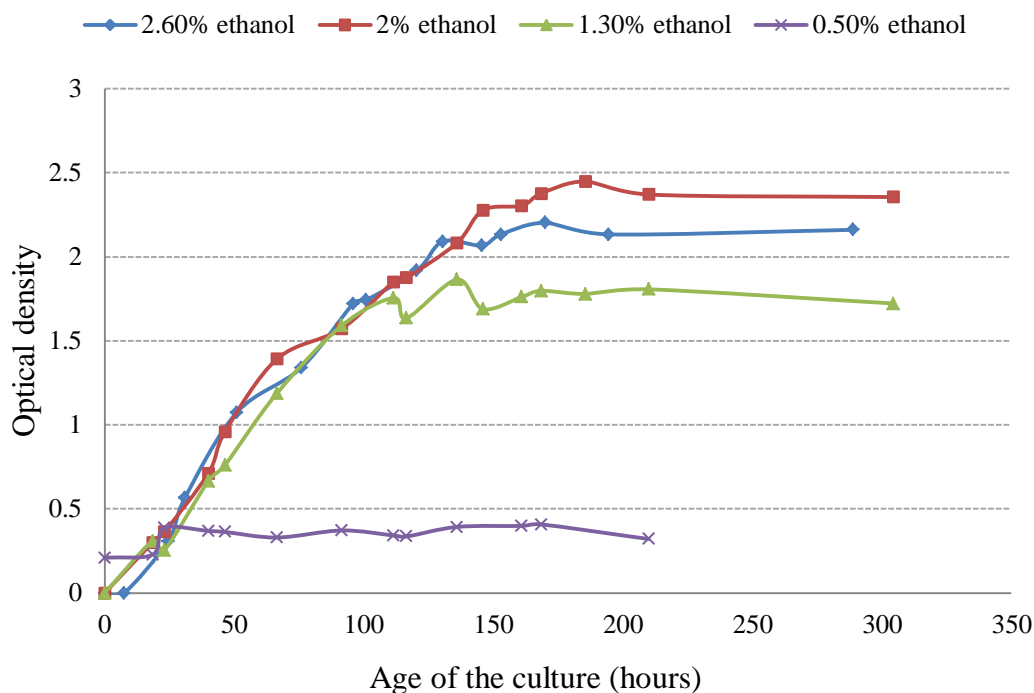


Figure 4.1: A comparison of the optical density versus incubation time plots at various initial ethanol concentrations (in medium 1).

A lag phase under 20 hours was observed for samples containing initial ethanol concentrations of 1.3%, 2% and 2.6%. Unfortunately, this cannot be distinguished from the culture fed with 0.5% ethanol due to insufficient data obtained during the initiation of the growth phase. In this culture, the active multiplication of cells ceased after 40 hours of cultivation as reflected in the stabilization of the optical density (OD) reading at around 0.4. As clarified earlier, the mineral nutrient composition and physical conditions were identical in all culture vessels except for ethanol concentration, it was therefore postulated that the differentiation in growth parameters (maximum growth rate and final biomass density) was ethanol-concentration dependent. The extent of biomass synthesis is directly proportional to the concentration of substrate available; therefore, final biomass density at lower ethanol concentrations should be less than that at high ethanol concentrations. The same argument was assumed to be applicable to the 1.3% ethanol fed sample. However, this correlation did not seem to extend to samples cultivated on 2% and 2.6% ethanol. Whilst containing lower initial substrate concentration, a higher final biomass production, detected as an average turbidity reading of 2.4 at the stationary phase, was achieved in the 2% ethanol culture. This result can be explained by the finding of Abbott (1973) who reported an inhibitory effect of high (>2.6%) ethanol

concentration on the cell growth of *Acinetobacter calcoaceticus*. It was pointed out that the ethanol-induced acetate accumulation is also inhibitory for growth. Choi et al. (1996) later confirmed that this bacterium can tolerate ethanol concentrations up to 16 g/L ($\approx 2\%$ v/v) before a significant reduction in growth rate occurs.

Concerning the rate of growth, the region corresponding to the active reproduction in cultures fed with ethanol concentrations of 1.3%, 2% and 2.6% displayed a similar gradient, implying similarity in the growth kinetics of these cultures. These data suggested that, for the four ethanol concentrations applied, the initial substrate concentration influenced cell growth not by altering growth kinetics but instead by affecting the final biomass production. However, no specific growth rates that fit the exponential growth model can be determined since the cell growth in all cultures proceeded linearly rather than exponentially. Overall, the final biomass concentration of *Acinetobacter calcoaceticus* from this series of experiments were low compared with the yield reported by other authors where absorbance reading above OD 4 was recorded utilizing similar concentrations of ethanol (Abbott et al. 1973). A series of additional attempts to optimize growth of *Acinetobacter calcoaceticus* in terms of demonstrating an exponential growth phase and higher biomass yield will be analyzed in the next section.

4.4 ALTERNATION OF CULTURE CONDITIONS TO OPTIMIZE GROWTH

Additional physiochemical growth parameters that were thought to be responsible for the linear growth were modified for growth optimization attempts. There are many reports in the literature about the favorable physiology and growth of *Acinetobacter calcoaceticus*. The pH optimum when utilizing ethanol as carbon source was between 6.5 and 7.5 as determined in the study of Preez et al. (1981). In this research study, the pH in the enrichment flasks was measured routinely (data not shown) and maintained within the range of 6.5-7. Since the optimal growth rate was obtained within the temperature range of 29 °C to 36 °C as claimed by Preez (1980), two incubation systems were setup in parallel with one at room temperature ($24 \pm 1^\circ\text{C}$) and the other at 33 °C. Based on the results obtained, although not included in the main part of this report (Appendix I) cells grown at different temperatures exhibited no significant variations in terms of growth rates and the final biomass yield. The *Acinetobacter calcoaceticus* specific growth medium (medium 2), as recommended

by Abbott et al. (1973) , was employed for all the following bacterial enrichment analyses. Furthermore, according to Fig. 4.1, the comparison of the biomass production at different ethanol concentrations indicates that 2% (v/v) ethanol concentration is preferred if the goal of high biomass production is to be achieved. Subsequently, the growth optimization experiments were carried out only on an ethanol concentration of 2%.

4.4.1 Nitrogen sources

After the preliminary experiments designed to select the most suitable ethanol concentration for laboratory cultivation, a specified medium designed by Abbott et al. (1973) for the growth of *Acinetobacter calcoaceticus* was prepared. The content of the bacterial nutrient medium was modified and the concentrations of the trace elements magnesium and iron were doubled. Both ammonium and nitrate can serve as the nitrogen source for biosynthesis by *Acinetobacter* spp., with the latter (nitrate medium) being strictly molybdenum dependent (Juni 1978). Therefore, sodium molybdate was added into the nutrient medium which was not included in the preliminary experiments. Sodium nitrate and ammonium chloride were used for this experiment in two separate culture vessels. In order to obtain the same N-content in the two inoculums, 23.5 mmol of sodium nitrate and 64 mmol of ammonium chloride were incorporated in each liter of growth solution. The time courses of the optical density changes from both culture flasks are plotted in Fig 4.2 as bacterial growth proceeded. The growth curves of pure cultures of *A. calcoaceticus* in the presence of different nitrogen sources with identifiable growth regions were obtained. When both cultures were compared, the time periods of the lag phase, the accelerated phase, a brief stationary phase and the onset of death phase were identical for the two inoculums. In both cases, the accelerated cell multiplication phase occurred after 15 hours and reached the maximum density at 53 hours. This observation describes a similar growth pattern between the two systems operating with different nitrogen sources. Such a scenario implied that the growth character of *A. calcoaceticus* was not affected, at least under the given molybdenum concentration, by the source of nitrogen.

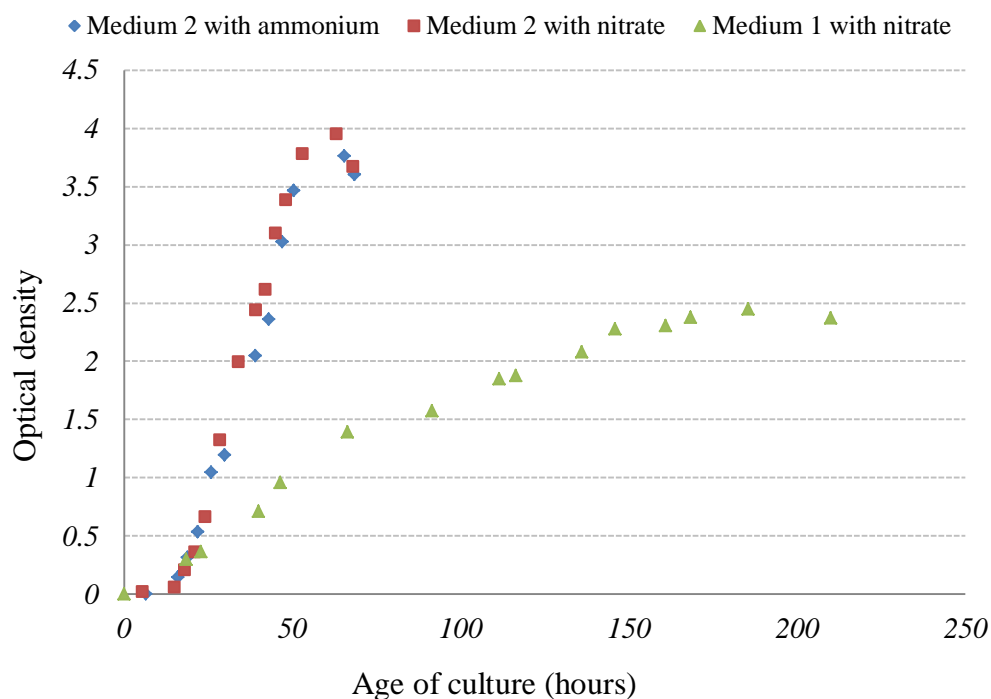


Figure 4.2: Optical density growth data of *A. calcoaceticus* with ammonium chloride or sodium nitrate as the N source in medium 2. ▲ is the growth data from the preliminary test inoculated with 2% ethanol using medium 1.

After overlaying these two growth curves with the one derived from the preliminary experiment containing no molybdenum and significantly less nutrients (Table 3.1), the magnitude of the final biomass concentration increased significantly with a mean stationary phase OD reading above 3.75 (Fig. 4.2). Furthermore, the growth curves resulting from the current experiments shifted to the left, reflecting the shortened time span between the initiation of growth and the stabilization of bacterial population. The maximum biomass concentration and the growth rate are known to be linked to the conservative uptake of nutrients (Kovářová et al. 1997). It is therefore plausible that the increase in the key nutrient concentrations might be responsible for the elevated growth rate and final biomass production. However, the linear ($R^2 = 0.99$) rather than exponential ($R^2 = 0.88$) trend during the accelerated growth phase was retained for the current experiments despite the observation of sharper inclination to the stationary phase.

Bacterial cultures are a collection of viable and dead cells and may also contain cell debris and other metabolic products. Spectrophotometric determination of growth kinetics for microorganisms displays several limitations including the inability to

discriminate dead from viable cells and the interference with metabolic by-products of growth (Pianetti et al. 2005). Absorbance reading is related to not only the number of cells but also the size of the cells and the quantity of metabolic residues in the culture solution. The presence of an external polysaccharide molecule accompanying the growth of *A. calcoaceticus* was noted in Sec. 4.2. In stressed environments, the capsule can expand in response to the need for insulation and protection against nutrient deficiency and predation (Reichert-Schwillinsky et al. 2009). Therefore, theoretically, accumulation of this material on the cell surface or in the growth medium may arise as a potential source of error for relating spectrophotometer analysis to cell number (Biesta-Peters et al. 2010; Lindqvist 2006). Assuming the exponential division of cells was disrupted at an early stage of the experiment, the orderly transition into the stationary phase could result in a morphological change (expansion of capsules in this scenario) when confronted with starvation. At the same time, the total cell numbers, either dead or alive as indistinguishable by spectrophotometry test, may experience a linear or minimal increase which overlaps with the region for the cell size enlargement. For this reason, it is logical to suspect that the linear increment in OD may originate, at least partially, from the quantity increase in this extracellular polysaccharide rather than cell numbers. To investigate in more details, the data reliability for the turbidity test and to ascertain the cell vitality, the classic dry cell weight combined with the viable cell count methods were performed in parallel as data quality control measures.

It should be noted that a reliable quantification by dry cell weight measurement was not possible at the beginning of the cultivation process due to the low number of bacteria. Thus, no results were presented at those sampling points in the dry cell weight analysis. In the case of growth quantification using the plate count method, samples beyond 43 hours of growth were excluded due to the detection of foreign colonies on the counting plates. The contamination was believed to have originated from the plate incubation procedures but not the culture flask, which was confirmed by the purity test. Therefore, the results obtained from the absorbance and dry biomass methods were deemed valid.

In this culture, the biomass production experienced a lag period of less than 16 hours and then accelerated into a growth phase which ended after 50 hours of cultivation. Growth curves plotted from the dry weight measurement and the plate

count test at the linear growth phase were in close conformity with the graph derived from optical density readings. When comparing the trend of growth patterns constructed from the three methods, the graphs shared high degrees of similarity in the growth region (Fig. 4.3). Analyses of variance for the regression model were applied to determine the correlations between the absorbance and dry weight and between the absorbance and colony forming unit (CFU)/ml. A positive correlation between the absorbance data and the plate count values was determined with a high correlation coefficient of 0.996 ($P<0.001$), whereas the correlation between the absorbance and dry weight was 0.986 ($P<0.001$). The viable counts confirmed the presence of mainly viable and reproducible cells during the linear growth phase. Negligible accumulation of dead cells and extracellular polysaccharide materials were present, which would otherwise contribute to the 'dry biomass' growth curve. The lack of difference in the shape and gradient of the three growth curves shown in Fig. 4.3 implies that the linearity of the absorbance growth curve before reaching the stationary phase was associated with the linear increase of viable cell numbers but not, as previously speculated, the expansion in cell size. A standard curve of g/l dry biomass as a function of optical density was developed (refer to Appendix II) for future reference.

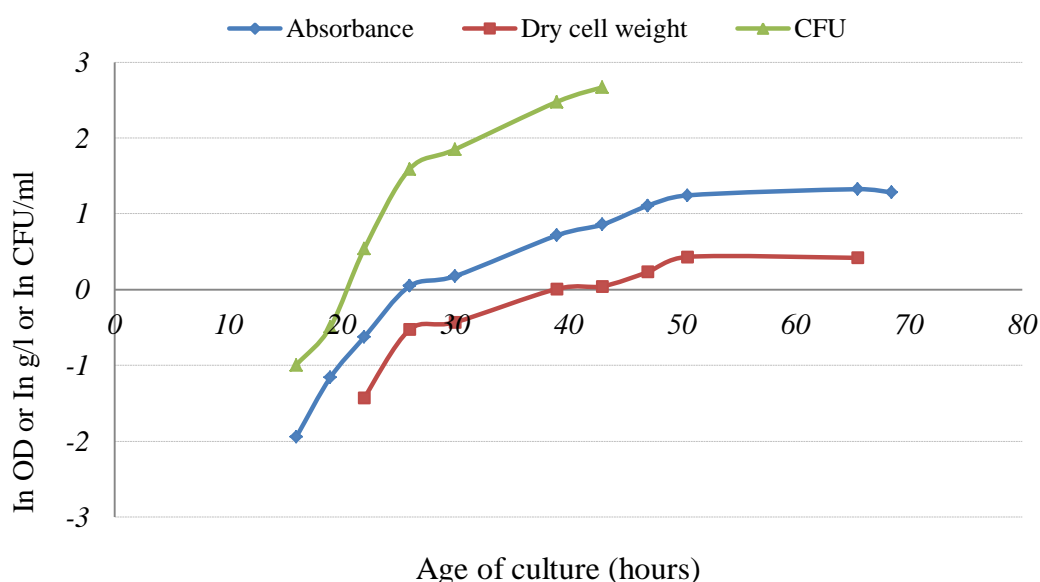


Figure 4.3: Semilogarithmic plot of *A. calcoaceticus* growth data obtained from three growth detection methods: the turbidity reading, the dry biomass and the colony forming unit count (CFU). The three curves shared high degree of similarity proving that the turbidity test was accurate and reliable.

Moreover, the lines in Fig. 4.3 appear to be segmented, each with a short period of exponential growth between 16 and 26 hours, prior to the start of a second phase of exponential growth. Data concerning the initial exponential growth should be interpreted with caution as only four data points were collected. However, the production of an almost identical pattern from the viable cell count method was regarded as strong evidence supporting such an argument. According to Fig. 4.4 (a), with both R^2 values higher than 0.98, it can be confidently concluded that the organisms grew exponentially from 16 to 26 hours.

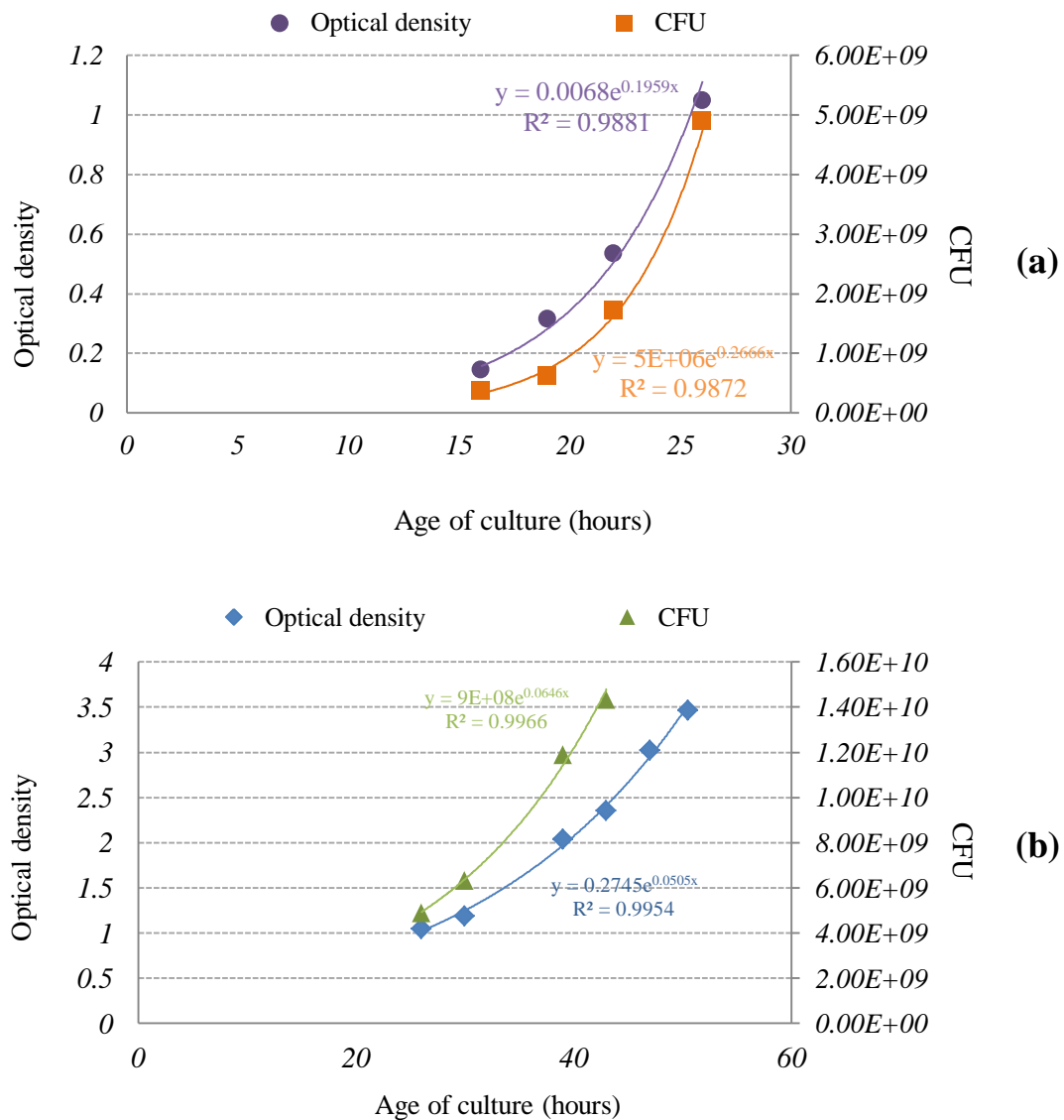


Figure 4.4: *A. calcoaceticus* growth curves showing the exponential relationship between optical density data and CFU count data in the suspected exponential phases. (a) represents the initial exponential phase between 16-26 hours and (b) shows the second exponential growth from 26 hours to 50 hours.

The growth curves derived from the optical density and CFU data demonstrating the second exponential growth phase are shown in Fig 4.4 (b). Both curves showed distinct exponential increases between 26 and 50 hours of incubation as evidenced by the R^2 values higher than 0.99. In similar studies of *A. calcoaceticus* growth, the cessation of exponential growth was typically detected after 25 hours. In the final state of the exponential growth, the dry biomass obtained from these experiments lies in the range of 2 to 6 g/l (Abbott et al. 1973; Choi et al. 1996). For this study, only 0.59 g/l of dry biomass was produced after the exponential phase and later reached a maximum of 1.54 g/l upon completion of the second exponential phase of increase.

The full range growth curves derived from the three methods resemble a diauxic growth pattern (Fig. 4.3); after the interruption of the initial exponential growth, the growth curve resumed in an exponential fashion which proceeded beyond 26 hours until 50 hours. There are several possible reasons that might have provoked this diauxic growth for our batch cultures with the following being most likely:

- i) The active multiplication during the exponential growth has led to the depletion of some essential nutrient substance in the cultivation solution resulting in a slower secondary exponential phase (Kovářová et al. 1997).
- ii) In the case of aerobic organisms, growth at high population densities may become impeded by the decrease in the dissolved oxygen tension (Kovářová et al. 1997).
- iii) Foam accumulation in the growth culture can lead to reduced yields since the foam can carry biomass when escaping out of the culture vessels (Routledge et al. 2011).

Unfortunately, experimental evidence to support the first hypothesis was lacking, but the latter two possibilities were further investigated by increasing aeration rate and adding antifoaming agent respectively.

4.4.2 Oxygen level

For aerobic microorganisms, the concentration of dissolved oxygen is one of the most important prerequisites that allow bacterial growth. As the population density increases, the corresponding increase in oxygen demand should be addressed before growth at high biomass concentration becomes impeded (Preez 1980). At 20 °C, the

solubility of oxygen in fresh water is low, approximately 7.6 mg/l. In submerged culture environments, the fact that the organisms can only access the oxygen dissolved in the culture fluid is often insufficiently appreciated (Gullo and Giudici 2008). With rapid population growth, the rate at which oxygen can dissolve in the solution becomes the limiting factor for the subsequent growth rate of the bacterial consortia. In previous cultivation experiments, the medium was aerated at a rate between 0.2 and 0.4 vvm. Differently than in the previous tests, a fresh cultivation analysis was performed with the aeration rate adjusted to 0.64 vvm to examine the influence of oxygen supply on bacterial production rate and yield. The rate of ethanol evaporation from the culture fluid increased under conditions of higher aeration. Thus, measurements of ethanol concentration in the culture solution were conducted to determine if the amount of substrate was sufficient to support growth. After 50 hours of incubation, 79% of the ethanol was still remained in the solution (refer to App III) indicating the culture is not limited by substrate.

Under the same nutrient environment, an increase in the aeration rate resulted in an extended period of exponential growth. In contrast to the curve constructed from the previous experiment, the current growth curve appears to possess a prolonged initial phase of exponential growth. Before the transit from exponential growth to linear growth at 32 hours, the dry biomass, calculated from the known optical density value using the standard OD versus dry weight curve, was 0.85 g/l, a 44% increase than the previous value of 0.59 g/l. However, as illustrated in Fig. 4.5, the cells in the low aeration experiment had a comparable, or a higher growth rate for the first 26 hours, with the end of the lag phase for the low aeration experiment estimated to be 6 hours less of the current high aeration experiment.

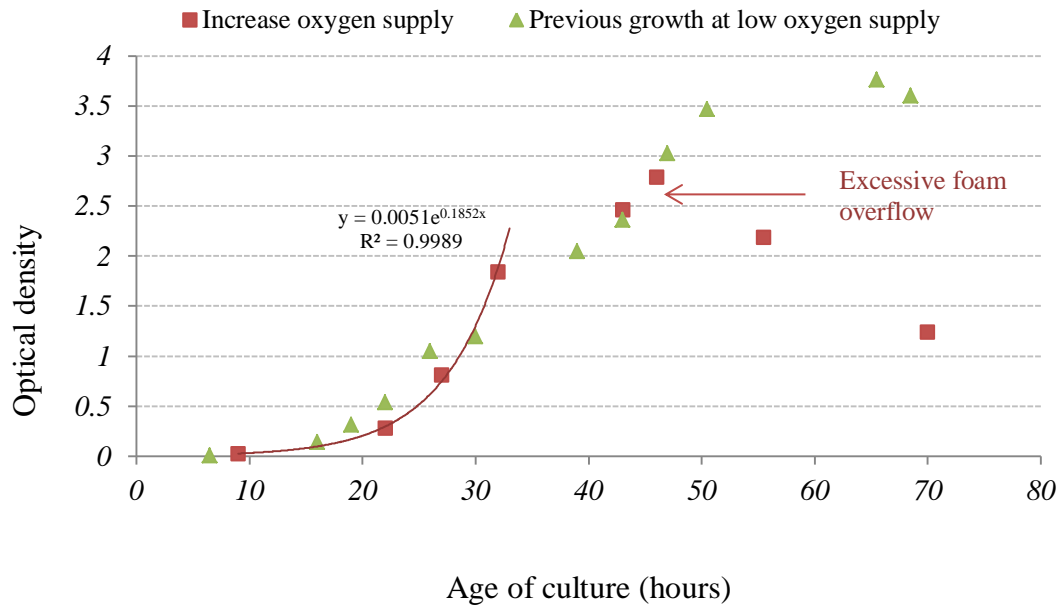


Figure 4.5: Effect of increased aeration rate (from 0.2-0.4 vvm to 0.64 vvm) on bacterial growth. With increased dissolved oxygen concentration, a distinct exponential phase was produced. ▲Refers to the data (red dots) shown in Fig 4.2.

It was possible that this minor disagreement in growth trends, as proved by Casciato et al. (1975), resulted from the difference in initial inoculum size although the same experimental conditions were applied (1975). When Casciato et al. combined the two optical density growth curves of the test bacterium using small and large inoculums, a 6 to 12 hour delay in each growth phase from the small inoculum sample were observed in comparison to the curve derived from the large inoculum. The same characteristic of the growth-phase intervals identified by OD measurements, that is dependence upon inoculum size, was identified by Koutsoumanis and Sofos (2005). They concluded that a large initial inoculum increased the probability of a rapid growth initiation under suboptimal conditions where the growth of smaller inoculum is usually lagged. The growth curve from the present experiment remained below the previous curve, but exhibited a significant incline between 27 and 32 hours of growth. The prominent growth after 27 hours may be attributed to the dissolved oxygen sufficiency in the culture fluid, required to support extended exponential growth and higher yield.

As revealed in earlier results, the same foaming behavior on the surface of the culture fluid was detected in this study after 27 hours of incubation. At 32 hours of cultivation, excessive foam had accumulated around the aeration tube submerged in

the culture medium compared with the foam quantity in the low aeration experiment at a similar time. From 32 to 43 hours, copious foam accumulated which eventually led to a minor leak through the edge of the silicone stopper. Continuous overflow of excessive foam out of the gas outlet tube and the edge of culture flask was observed for the remaining course of cultivation. The growth curve experienced a sudden decline in biomass at 46 hours of incubation. When the substrate concentration was measured at various times during cultivation, it was found the ethanol concentration declined slowly, leaving approximately half of the ethanol (0.96%) present in the culture fluid at the end of the experiment. The bacterial growth was hence not limited by ethanol availability; therefore, foam overflow was possibly responsible for the biomass loss as the foam may have contained a certain amount of cells. It has in turn promoted the following investigation into the effect of foaming on biomass production rate and yield.

4.4.3 Antifoaming agent

In bacterial cultures, deleterious effects such as stripping of metabolic products, nutrients and cells from the system associated with foam formation are potentially destructive to bacterial growth and require intervention (Salleh et al. 2011). The presence of gas bubbles is an essential requirement in foam generation, thus, an unfortunate side effect of vigorous aeration is increased foam production. The previous approach of increasing aeration rate may be beneficial for obtaining an extended exponential growth and a higher biomass yield at the end of the exponential phase while, at the same time, might have alleviated the foaming problem. To prevent excessive accumulation of foam minimizing biomass loss due to foam overflow, antifoaming agents are routinely introduced into the culture medium. Antifoam A purchased from Sigma was injected into a fresh culture sample aseptically (approximately 0.6%- 1% v/v), with the air flow rate maintained at 0.68 vvm. A control experiment was set up in parallel which contained no antifoaming agent and the aeration rate adjusted to 0.66 vvm. It was already tested experimentally that ethanol availability was not a limiting factor for growth, the ethanol concentration changes in the culture fluid was thus not recorded this time.

In this study, the addition of Antifoam A into the culture medium increased the final biomass concentration at the stationary phase compared to the control culture with no antifoam agent (Fig. 4.6). Up to 28 hours of incubation, the sample and control growth curves experienced a temporal alignment which yielded similar logarithmic growth models. This implies that the growth characteristics of the strain tested during the initial phase of exponential increase were not altered by the presence of antifoam. The two plots diverged beyond 28-hours of growth at which point foam formation commenced in the control flask. A further 6-hour of exponential growth was recorded in the antifoam-containing culture. Before obtaining a constant biomass concentration at 53.5 hours, a short period of non-exponential growth was detected. In the exponential phase of growth, organisms are likely to experience dramatic and precipitous changes that would lead inevitably to an exponential rate of consumption of all essential nutrients. In a batch fermentation experiment, it was highly likely that the supply of substrate, nitrogen source or certain essential minerals became insufficient which led to the shift from exponential to non-exponential growth and ultimately the termination of active cell multiplication (Brown and Cooper 1991). Additionally, the estimation of growth-phase based on optical density data is typically dispersed due to different sources of errors. In reality, it was difficult to accurately distinguish, especially when a potentially critical data point was missing between 34 to 47 hours of growth, the exact points at which the culture changes from an exponential to a linear growth or from an exponential to a stationary growth. Therefore, the results of the present study representing the best, although not optimal in comparison of the literature value of 0.7 h^{-1} (Abbott et al. 1973), fit of an exponential growth were used to calculate the specific growth rate (μ) which was 0.23 h^{-1} . As expected, the addition of antifoam was very effective in foam control with hardly any foaming activity noted during the entire course of the experiment. The purity tests were performed at 46.5 hour and a later point of the stationary phase with the absence of foreign cells indicating that the culture was free from contamination.

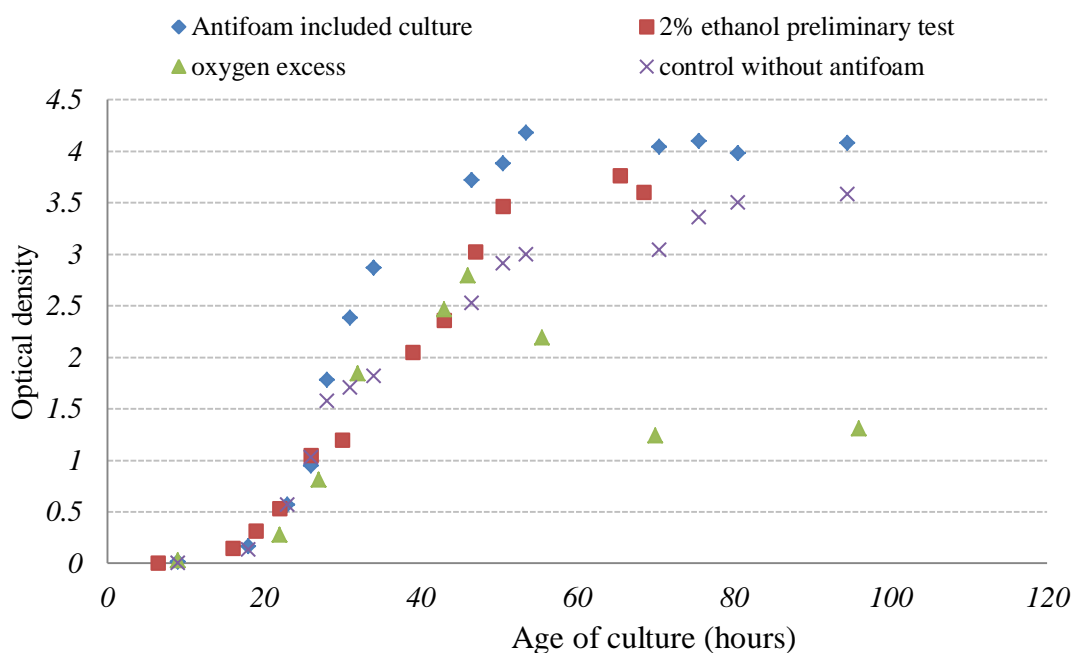


Figure 4.6: Growth behaviour of Antifoam A added culture.

On the other hand, the control test displayed a linear growth behavior, similar to the previous high aeration test, immediately after the detection of foam accumulation. The foam formation intensified overnight and eventually led to an overflow out of the ventilation tube and the opening of the cultivation flask. However, it was not anticipated that, unlike the cells grown at the high aeration rate, no decrease in optical density appeared after foam leakage. Contrarily, the culture seemed to have resumed growth, resulting in a rise in turbidity reading from a mean of 3 to 3.5. The purity assay was attempted afterwards and light contamination was detected, however, no contamination was encountered prior to 46.5 hours of growth according to an earlier purity test. It was pointed out by several authors that foam- overflow -induced loss of process sterility was not uncommon (Routledge et al. 2011; Varley et al. 2004). It is then reasonable to conclude that the recovery of growth as a result of contamination during the later stage of growth was attributable to foam overflow. In conclusion, both the high biomass concentration of *A. calcoaceticus* and the disappearance of foam accumulation emphasized the necessity of the antifoam addition into culture solutions as an effective growth optimization strategy, as least in the case of this study.

4.5 CONCLUDING REMARKS

Concerning the current production in MFC research, bacterial metabolic activity is one of the determining factors influencing the electricity performance of a given MFC (Wang et al. 2010). Cell growth and electron flows are correlated, and the rate of electron generation is proportional to the rate of metabolic synthesis of the biomass inside a fuel cell (Emde et al. 1989; Ledezma et al. 2012). Therefore, in the case of MFC research, a comprehensive understanding of bacterial specific growth (μ) and the biomass production is the key for optimizing operational settings which exploit their potential.

This series of experiments resulted in the isolation of strains of ethanol-degrading bacteria, from soil and compost samples, belonging to the genus of *Acinetobacter*. A pure-culture isolate named *A. calcoaceticus* was identified using 16rRNA sequencing. A sequence of experiments was designed subsequently in order to obtain information in regard to the growth characteristics of this particular strain.

- ❖ A comparison study of the effect of ethanol concentration on the grow rate and yield of *A. calcoaceticus* was initiated. Out of the four ethanol concentrations, 0.5%, 1.3%, 2% and 2.6% (v/v), analyzed, the inoculum fed with 2% ethanol delivered relatively the highest biomass concentration at which ethanol concentration was adapted for all the later cultivation experiments.
- ❖ The identical growth curves as depicted in Fig. 4.2 (N-source) indicated that the growth behavior of *A. calcoaceticus* was not altered by different nitrogen sources. However, in comparison with a preliminary growth pattern, these new curves showed a significant enhancement in both growth rate and concentration when exposed to increased mineral concentrations. In order to assess the viability of the cells in addition to their abundance, the plate count method was performed along with the spectrophotometric and dry biomass methods. The apparent accordance among the data obtained from all three methods suggested that the spectrophotometric method was reliable and accurate in representing the bacterial growth pattern. However, the linear growth of this culture at the supposed exponential region required further investigation.
- ❖ According to many researchers, a dissolved oxygen deficiency in a submerged bacterial culture could inhibit the growth of *A. calcoaceticus*. An increment in

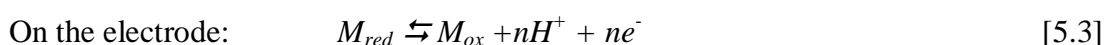
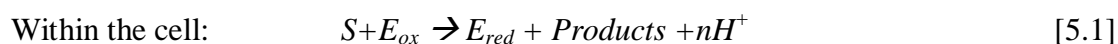
the aeration rate from 0.3 ± 0.1 vvm to 0.64 vvm did accelerate the rate of reproduction to a certain extent which resulted in an exponential growth till 32 hours. However, a sharp decrease of optical density after the occurrence of foam overflow, at 46 hours, prompted the following examination on foam control in relation to biomass production.

- ❖ Cultivation of the organism in the presence of Antifoam A caused a substantial increase in the level of final biomass production, approximately 1.68 g/l, being the maximum biomass concentration for this study, when compared with all previous experimental data (the highest being 1.49 g/l). Most significantly, a distinct region of exponential growth was detected and the maximum specific growth rate of 0.23 h^{-1} was computed.

The systematic analysis of the growth optimization of *A. calcoaceticus* revealed that a combination of factors, such as essential mineral concentration, oxygen availability and foam formation control, are the most significant parameters contributing to the changes in bacterial reproduction rate and yield. While no single factor was sufficient to enhance the growth rate to the optimum level, as evidenced by the defects present in each of the earlier experiments, factors correlate with one another to deliver the best result possible. Other than the reasons discussed above, there is still much to explore about the factors which might have hindered the growth of *A. calcoaceticus*.

Chapter 5: Microbe-mediator interactions and the effect on current responses

There are many existing MFC systems utilizing redox mediators to increase the rate of electron transfer from microorganisms which have no inherent mechanism of direct electron transfer to the anode (Sund et al. 2007). In microbial cells, the aerobic respiration of substrates involves the channeling of electrons through a series of redox enzymes before reaching the terminal electron acceptor, molecular oxygen, where the substrates are ultimately oxidized to CO₂ and H₂O. The replacement of natural electron acceptors by artificial electron mediators can divert the electrons liberated from the respiration process to an electrode, bypassing the oxygen reduction step at the microbe, which results in the current generation of MFCs. During the process of electron transfer between the enzymatic active site in the bacterial cells and the anode, the mediator cycles between its oxidized and reduced forms while the substrate is oxidized to maintain cellular functions. The simplified reaction mechanism of this mediated substrate degradation is illustrated below (Picioareanu et al. 2010):



in which, S represents the substrate, E_{ox} and E_{red} are the oxidized and reduced forms of enzymes; and the oxidized and reduced forms of mediator are shown as M_{ox} and M_{red} . The n stands for the number of protons and electrons involved in the mediation process which is determined upon the mediator compound utilized. During the catalytic reaction, the reactive enzyme reduction is activated when substrate degradation occurs (Eq. 5.1). In Eq. 5.2, the characteristic potential and the structural advantages of the mediator allow its diffusion into the active site and react with the reduced enzyme, leading to the regeneration of the oxidized enzyme. Subsequently, the reduced mediator is converted back to the oxidized form (Eq. 5.3) at the supporting electrode via electrochemical reactions.

This chapter thus focuses primarily on studying the behavior of mediator-microbe interaction and the corresponding effect on the current produced. Thionine, methylene blue, resorufin and potassium ferricyanide have been utilized successfully as electron mediators in many MFCs studies and were therefore selected for this research. In this chapter, the reduction of each of the above compounds by *Acinetobacter calcoaceticus* (Sec 5.1) and the quantity of mediator partitioned into the biomass (Sec 5.2) is reported. More importantly, the use of electrochemistry (chronoamperometry) as a technique to investigate the variation in current responses with different mediator systems at varying concentrations will be revealed and analyzed in Sec 5.3.

5.1 BIOTIC REDUCTION OF MEDIATOR

A suitable mediator must satisfy several criteria, which were discussed in chapter 2, with the first being able to transform into the reduced form upon contact with the microorganisms inoculated in the anode chamber. This section thus investigates the reduction capacity of *Acinetobacter* on the mediators selected for this study, which are thionine, MB, potassium ferricyanide and resorufin.

5.1.1 Thionine

Thionine is a lipophilic redox dye that belongs to the phenothiazine family. This small planar molecule has two $-NH_2$ groups distributed symmetrically on each side as shown in Fig 5.1. As an electron mediator, the oxidized form of thionine shows a distinct violet pigment in aqueous solution and can be readily reduced. It is known to undergo a two-electron reversible process with sound stability and reproducibility (Hu et al. 2012). The reduction reaction proceeds from left to right as indicated in Fig. 5.1 and results in the formation of the colorless leuco-thionine (Yang et al. 1999). The reduced form of thionine is sensitive to atmospheric oxygen which can be oxidized back to thionine upon contact with air. The formal redox potential of thionine is reported to be $E_0 = + 0.064$ V versus a hydrogen electrode (SHE) (Wilkinson et al. 2006).

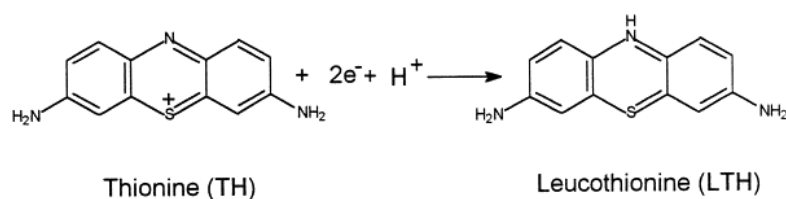


Figure 5.1: The reversible redox reaction of thionine (Yang et al. 1999)

The biological reduction was initiated, as described in chapter 3.4.1, by adding the requisite amount of thionine powder to the freshly harvested bacterial solution of known dry mass weight (0.79 g/l) in test tubes. The changes in the density of the oxidized thionine (i.e. the reduction process) were visually followed for a range of initial concentrations (10 μ M, 20 μ M, 50 μ M, 100 μ M, 200 μ M, 300 μ M, 400 μ M and 500 μ M). A lag phase in the decolorization process was observed for all the samples prepared and the length of this lag period increased as the thionine concentration increased. At concentrations lower than 50 μ M, this lag phase lasted less than 5 minutes. At higher thionine concentrations, it was difficult to distinguish such a phase due to dense color and longer reduction time.

During the process of biotic thionine reduction, a colorless solution appeared first in the lower portion of the test tube and gradually expanded upwards through the entire sample, the reduction time varying according to the thionine concentration. After 20 minutes of incubation, test samples for thionine concentrations from 10 μM to 50 μM were visibly colorless indicating that thionine reduction approached 100% within that time. For samples with 100 μM and 200 μM thionine, a rapid decrease in color was observed after 10 minutes and continued for another 30 minutes. A colorless region was obtained at the lower part of the test vial after approximately 40 minutes in these two samples, with a light purple layer residing on the surface of both solutions. For samples with thionine concentrations beyond 300 μM , complete mediator reduction was not achieved within this timeframe. After 1 hour, it was observed that the color of the sample inoculated with 300 μM thionine changed from dark purple to pale purple-blue. This sample, along with bacterial solutions with 400 μM and 500 μM thionine, were sealed and left undisturbed for further biotic reduction. At the end of the second incubation phase (2 hours), insignificant color change was detected in the 300 μM thionine sample, indicating the reduction process had ended within the initial 1 hour of incubation. The color removal of 400 μM and

500 μM thionine samples stabilized after 2 hours, with visible purple-blue color remaining in both solutions (Fig. 5.2).

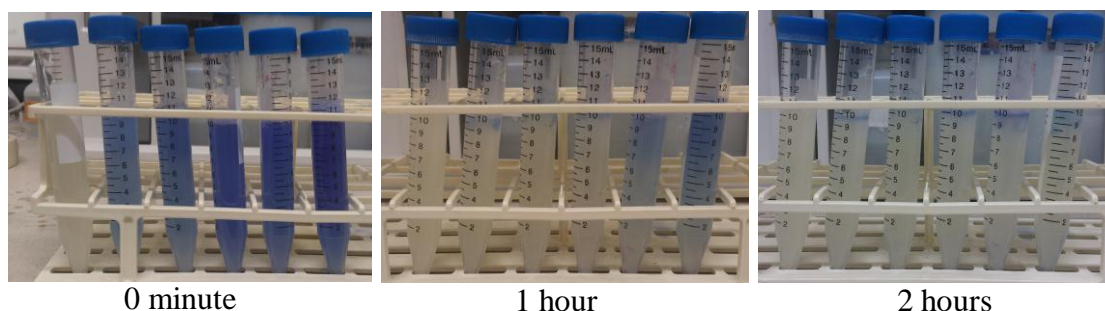


Figure 5.2: The color changes of thionine before and after reduction, the concentrations are control, 100 μM , 200 μM , 300 μM , 500 μM and 600 μM from left to right.

5.1.2 Methylene Blue

Methylene blue (MB) is a water soluble phenothiazine compound which has been exploited for a variety of industrial and scientific applications since its synthesis in 1876 (Impert et al. 2003). In aqueous solution, the oxidized form of MB has an intense blue color which possesses a strong optical absorption at 660 nm. MB has a redox potential of $E_0 = + 0.011$ V versus SHE and can be reduced to the colorless hydrogenated molecule called leuco-methylene blue by a number of chemical and biological agents (Wilkinson et al. 2006). This two-electron transfer reaction, summarized in Fig. 5.3, is reversible upon exposure to an oxidizing agent such as oxygen.

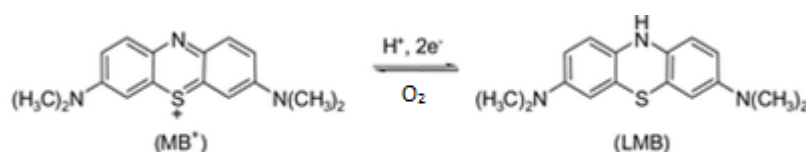


Figure 5.3: The redox reaction of methylene blue

The redox property of this pair enables MB to become the key component of a wide range of optical oxygen sensors. Furthermore, in addition to MB reduction by chemical agents, there are many reports on MB reduction correlating with microbial metabolism. The detection of color change due to MB reduction is a recommended method for the screening of microbial growth in milk (Thornton and Hastings 1930). This phenomenon is attributed to the direct transfer of electrons from bacterial

dehydrogenases during microbial growth which resulted in the formation of the colorless form of MB (Patchett et al. 1988). The direct reduction by intact microorganisms allows the incorporation of redox mediators in many MFC applications to act as a novel mechanism for promoting electron transfer efficiency which, in turn, increases the current output.

In this work, the biological reduction characteristics of methylene blue at concentrations of 50 μ M, 100 μ M, 200 μ M, 300 μ M, 600 μ M, 1 mM and 1.5 mM were investigated. The reaction mixtures were prepared applying the same technique as the thionine tests. It was observed that the decolorization process initiated instantaneously after all MB residues were dissolved, without a lag phase in any concentrations of MB-microorganism samples. For each of the concentrations examined, a colorless zone appeared first at the bottom of the reaction vial and gradually widened to include the rest of the reaction mixture. Compared to thionine, MB reduction was observed to be faster over the whole MB concentration range, despite the lower biomass content used in the MB tests (0.57 g/l compared with 0.79 g/l). At MB concentrations of 50 μ M and 100 μ M, > 95% of the reduction was achieved within the first 15 minutes. The reaction times for the complete reduction of 200 μ M and 300 μ M MB were within 20 minutes, which was significantly shorter than that of thionine. In the case of the 600 μ M MB sample, complete reduction occurred after approximately 40 minutes while reduction of 1 mM and 1.5 mM MB, was achieved in 1 hour. A similar reduction pattern as the thionine tests can be concluded for these data wherein the time required for a complete reduction of the indicator material in each solution increased with the increase in the initial concentration of MB. Despite the alleviated reduction rate of MB, incomplete reduction was also present in samples with mediator concentrations at and higher than 200 μ M, as evidenced by the existence of a persistent band of the oxidized form of MB at the meniscus in each tube after the reduction process ceased (Fig. 5.4). The thickness and the color intensity of this band of oxidized MB increased proportionally to the initial MB concentration. Unfortunately, it was not possible to measure the extent of color removal using a spectrophotometer for these samples due to the oxygen sensitivity issue. Upon contact with molecular oxygen, MB is quickly transformed from its reduced form (colorless) to its oxidized form (blue) which poses great experimental challenge for accurate spectrophotometric measurement as a strict anaerobic condition is required.

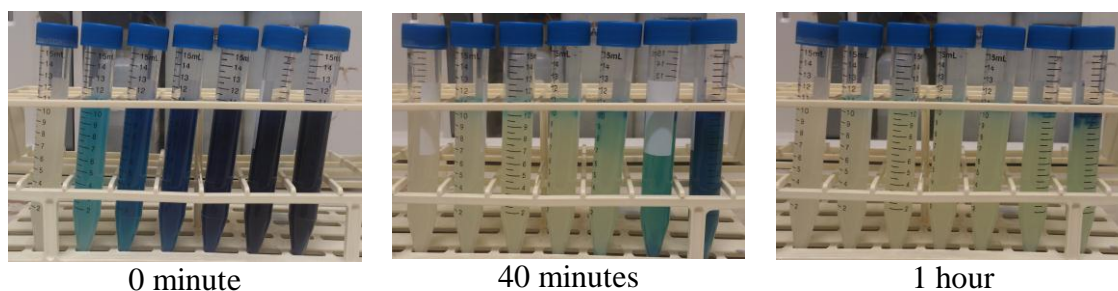


Figure 5.4: The color changes of methylene blue by bacterial suspensions before and after reduction, the concentrations are control, 50 μM , 100 μM , 200 μM , 300 μM , 600 μM , 1 mM and 1.5 mM from left to right.

5.1.3 Potassium Ferricyanide

Potassium ferricyanide is a hydrophilic compound with the formula $\text{K}_3\text{Fe}(\text{CN})_6$. In aqueous solution, this orange-red salt possesses a yellow-green fluorescence which has a widespread use in the photographic industry. Once reduced, potassium ferrocyanide is formed which can be detected by the fading of its yellow-green color into a pale yellow to colorless solution. The ferricyanide/ferrocyanide redox couple has a formal potential (E_o) of +0.36 V which undergoes a one-electron transfer process (Eq. 5.3) (Park and Zeikus 2000).

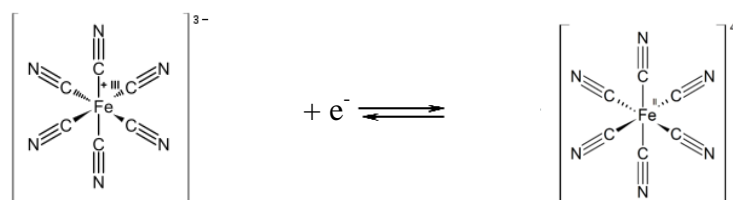


Figure 5.5: The reversible redox reaction of ferricyanide (Park and Zeikus 2000).

Potassium ferricyanide has also been exploited extensively in physiological experiments as a means of increasing the redox potential of a solution (Niranjana et al. 2009). In 1966, the ability of ferricyanide to act as an electron acceptor for the oxidation of glucose and tricarboxylic acid cycle intermediates in a biofuel cell was demonstrated by Hadjipetrou (2005). In recent years, ferricyanide ions have been incorporated in various biological oxygen demand (BOD) sensors and MFC systems to replace oxygen as the terminal electron acceptor during the microbial metabolic processes (Morris et al. 2005; Park and Zeikus 2000).

In the present study, the mediator efficiency and microbial absorption of ferricyanide ion was investigated at ferricyanide concentrations of 100 μ M, 300 μ M, 500 μ M, 700 μ M, 1 mM and 2 mM. The reduction of potassium ferricyanide was followed by monitoring the depletion of the yellow-green color in *Acinetobacter* spp. suspended cultures (1.04 g/l). A time-dependent decrease in the colour of all the ferricyanide-microbe mixtures was observed. Under the same operating conditions applied to the reduction tests of the previous two mediators, the time for complete ferricyanide reduction was longer than thionine and MB at a corresponding concentration. Nonetheless, the same reduction pattern was observed with increasing concentrations of ferricyanide, progressively requiring longer reduction times. Due to the inert nature of the ferricyanide/ferricyanide redox couple under aerobic conditions, spectrophotometric investigations were performed upon the appearance of colorless solutions. For each ferricyanide sample prepared, 1.5 ml of reduced bacteria-mediator suspension was centrifuged (13,000 rpm) for 3 minutes and followed with spectrophotometric analysis of the clear supernatant for the determination of residue ferricyanide. In the 100 μ M and 300 μ M ferricyanide solution, the maximum decolorization was observed (>95%) after incubating for 5 hours, while colorless solutions were obtained after 8 hours in the test vials containing 500 μ M and 700 μ M of ferricyanide with reduction of 92.2% and 85.7% respectively. Meanwhile, the decolorization process in samples including 1 mM and 2 mM ferricyanide was incomplete, although final decolorization of about 85% was detected in these samples when the incubation time was extended to 30 hours. It was noticed that, unlike the final solutions obtained from thionine and MB reduction, the color distribution in the ferricyanide samples was homogenous. This phenomenon may simply be explained by the oxygen sensitivity of the earlier mediators resulting in the presence of a colored layer in the test solutions due to oxygen diffusion at the interface (Wuhrmann et al. 1980).

5.1.4 Resorufin reduction

Resorufin is a phenoxazone dye with a distinct pink colour in its aqueous phase. The UV-visible absorption spectrum of resorufin in aqueous solutions consists of an intense absorption band centered at 572 nm with a weak shoulder band at 535 nm (Bueno et al. 2002). Resorufin can be converted to the colorless dihydroresorufin by

various chemical and biological reducing agents via a reversible two-electron reduction. Re-oxidation of dihydroresorufin can be achieved upon reaction with atmospheric oxygen as illustrated in Fig. 5.6. The formal redox potential of the resorufin/dihydroresorufin redox couple versus SHE is -0.051 V (Tratnyek et al. 2001). Due to its chemical/physical photo-stability, resorufin has been used widely in inverse fluorescence assay to detect H₂O₂ by studying the disappearance of colour upon reduction to the colorless form. Many reports on the use of dihydroresorufin as an oxygen sensitive probe for tracing dissolved oxygen are also available.

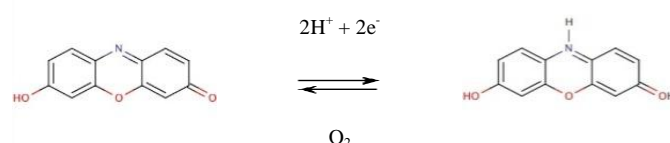


Figure 5.6: The redox reaction of resorufin (Tratnyek and Wolfe 1990).

Five portions of the *Acinetobacter* cultures (0.68 g/l), each containing resorufin concentrations of 25 μ M, 50 μ M, 100 μ M, 150 μ M and 200 μ M, were prepared followed by the study of the characteristics of the biotic dye reduction. At lower resorufin concentrations (20-100 μ M), all reduction processes commenced after an approximately 5 minutes delay. Similar to the reduction tests conducted on thionine and methylene blue, such a lag period cannot be identified in samples with higher resorufin concentrations (150 μ M and 200 μ M). It was observed in all mixtures that a front of the reduced dye progressed gradually up the reaction vial from the bottom. The color intensities in the 25 μ M and 50 μ M inoculated samples decreased dramatically after 5 minutes of contact and resulted in colorless solutions after about 30 minutes. When the initial resorufin concentrations increased to 100 μ M and above, the length of the reduction phase also increased accordingly, indicating a linear relationship between the reduction time and the resorufin concentration. In addition, it was noticed that appreciable amounts of un-reduced mediators remained in these solutions as evidenced by the presence of pink bands at the liquid surface. The thickness of this band was directly proportional to the concentration of resorufin in the inoculum. In the solution including 100 μ M resorufin, the color fading process continued for 60 minutes leaving a pink band at the liquid surface with a similar color regression taking place in the last two samples with the highest resorufin contents. Although a pale pink top layer was still present, the pink color had diminished

completely after about 90 minutes at the bottom of these samples as shown in Fig. 5.7.

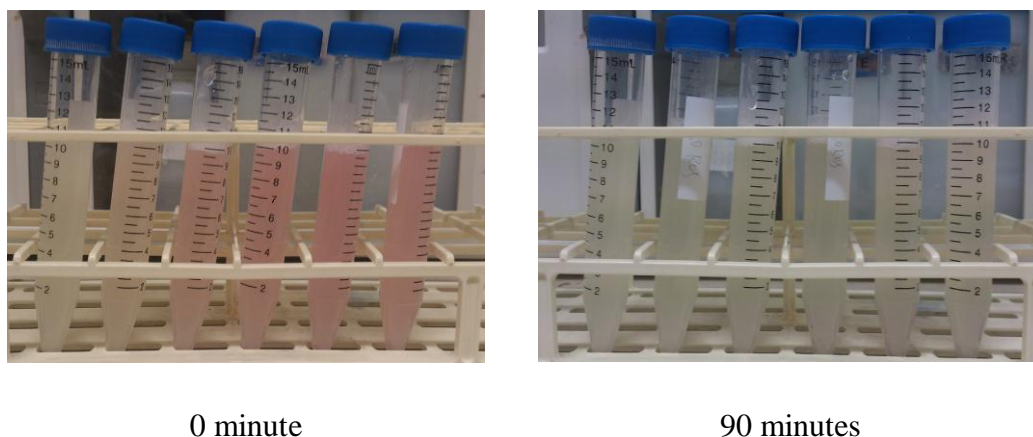


Figure 5.7: The color removal of resorufin at various concentrations by *Acinetobacter* suspensions, the concentrations are control, 25 μM , 50 μM , 100 μM , 150 μM and 200 μM from left to right.

5.1.5 Comparison of biotic reduction rate

In the present work, the biotic reduction of four mediators, thionine, methylene blue, potassium ferricyanide and resorufin, was analyzed separately in *Acinetobacter calcoaceticus* inoculated cultures under similar experimental conditions. Based on the above results, *Acinetobacter calcoaceticus* was capable of reducing all mediators tested in aqueous phase. Clearly, the mediator-microbe reaction capacity varied from case to case as reflected by the difference in the reduction kinetics. In light of the observation of these biotic reduction experiments, at a given mediator concentration, the biotic reduction rate decreased in the order of MB > thionine > resorufin > potassium ferricyanide. A number of influential properties, summarized in Table 5.1, that are potentially significant in the variation of the mediator reduction rate were pointed out in literatures.

Table 5.1: Selected properties of tested mediators and the rate of reduction* (R_{red}), μmol per minute per gram of biomass, at 100 μM .

Mediator and molecular weight (g/mol)	Formal potential (V) vs. SHE	Solubility	R_{red} ($\mu\text{mol}/\text{min}\cdot\text{g}$)
Thionine (287.34)	+0.064	8.7mM (Haugen and Hardwick 1963)	3.2
Methylene blue (319.85)	+0.011	156mM (Shahryari et al. 2010)	11.7
Potassium Ferricyanide (329.24)	+0.36	1432mM (Friend and Smirles 1928)	0.3
Resorufin (213.19)	-0.051	4.7mM (Sigma-Aldrich)	2.5

* R_{red} is the estimated rate of reduction calculated based on the time required for the complete reduction of each mediator.

In a biochemical system, the tendency of electron transfer between redox pairs can be predicted according to their formal redox potentials (E_0). The electrons will transfer from components with more negative redox potential to those with more positive E_0 (Alberts et al. 2002). In this study, the redox potential of the above mediators ranges between -0.051 and +0.064 V which are most likely to accept electrons from the dehydrogenases ($E_0 \approx -0.2$ V) and the quinone ($E_0 \approx +0.05$ V) components of the microbial ETC (Learoyd et al. 1992). It is thus logical to assume that the fastest reduction rate should occur with the mediator possessing a high formal potential in a series of similar compounds (Tratnyek and Wolfe 1990). In this context, potassium ferricyanide with a formal potential of +0.36 V, should hypothetically demonstrate the highest reduction rate. However, the lowest reduction rate was observed when using potassium ferricyanide as the redox mediator. The same disagreement also applies to thionine, which ranked second in the reduction rate chart despite having more positive formal potential than that of MB. Apparently, the contribution of the redox potential to the overall dye reduction is insufficient to account for this disparity especially when comparisons are made between structurally different compounds (Tratnyek and Wolfe 1990).

It has been recognized that the chemical structure of mediators is one of the pertinent factors associated with their reduction rate (Wuhrmann et al. 1980). The intracellular reduction of a mediator by a potential electron donating protein requires the penetration of the mediator molecule from the external medium into the plasma membrane. To a certain extent, this step is governed by the ability of a mediator as defined by its structure, to access this reaction site (Learoyd et al. 1992). In general, mediators with simple structures and lower molecular weights cross the cell membrane and are subsequently reduced by bacterial cells more easily. In addition, Gram-negative bacteria, *Acinetobacter calcoaceticus* in this case, are generally less susceptible to macromolecules, being shielded by the lipophilic outer membrane (Poole 2002). Due to this lipophilic nature of the Gram-negative bacteria membrane, organic molecules possessing certain degrees of lipophilicity are preferred for faster penetration into the internal bacterial cavity. Some studies on microbial dye reduction have shown that compounds with either amine or hydroxyl groups, like those found in thionine, MB and resorufin, are more attracted to the outer membrane, which allows a faster passage into the periplasmic space where reduction takes place (Elisangela et al. 2009). Potassium ferricyanide is a hydrophilic molecule, although highly soluble in aqueous solutions, lower permeability across the plasma membrane was observed. This impeded transport into the reduction site may inhibit the fast reduction of ferricyanide (Pasco et al. 2004). Based on the above discussion, the higher rate of reduction observed in the three structurally similar mediators, thionine, MB and resorufin, implied that the differences in the structure of the mediator are of primary importance in influencing the reaction rate (Tratnyek and Wolfe 1990).

Moreover, several other factors were proposed to contribute to the intracellular reduction of mediator, with two considered to be of particular relevance in determining the rate of reduction in this study.

- i) It has been discussed in several reports that a competitive effect between dissolved oxygen (DO) and the redox mediators may be present, which is responsible for the different patterns of mediator reduction (Roller et al. 1984; Wuhrmann et al. 1980). *Acinetobacter calcoaceticus* is an aerobic Gram-negative bacterium which inherently thrives on the presence of oxygen as its preferred electron acceptor. In this set of experiments, no measure of oxygen control was performed therefore a significant amount of dissolved oxygen was

present. Upon introduction of the mediators, a switching mechanism may be required as the process of electron transfer to the mediator may be suppressed by the available oxygen. It is possible that the initial rate of mediator reduction may remain negligible until oxygen was significantly depleted. The lag phase observed in thionine, MB and resorufin reduction before the initiation of the rapid decolorization phase may be an indication of such a scenario. Although certain amounts of oxygen may still be available outside the cell membrane to accept electrons, after the successful penetration of mediator molecules through the cell membrane, the mediator reduction reaction should remain unaffected if the mediator accepts electrons at an earlier site along the pathway than oxygen (Roller et al. 1984). This may explain why the mediator reduction exhibited the highest rate with MB, thionine and resorufin. The formal potentials of these three mediators, as indicated in Table 5.1, range from -0.05 V to +0.064 V which are close to the formal potential of the succinate/fumarate redox couple (+0.03 V vs. SHE) (Babanova et al. 2011). It is hence presumed that these three compounds are most likely to couple with the succinate/fumarate complex of the electron transport chain where mediator reduction was commenced. These mediator compounds were proposed to act as surrogates for coenzyme Q and enabled the switch in *Acinetobacter calcoaceticus* to anaerobic respiration. In the case of potassium ferricyanide, a much higher redox potential indicates the electron transfer may happen further down the chain of the ETC. While it is unable to across the plasma membrane, the electrons liberated through respiratory activities are believed to be transferred out of the cell membrane via the terminal ETC component known as the NADH dehydrogenase (Dancey and Shapiro 1976). Combined with the slow rate of membrane penetration, constant intense competition with oxygen means the reduction of ferricyanide may be inhibited until oxygen was completely removed (Roller et al. 1984).

- ii) Mediators selected for this study are typical of the many organic redox compounds that have been used as biological stains which are capable of penetrating and adhering to organic membranes. Therefore, investigations of the biotic mediator reduction should consider the fact that the observation of colour removal could provide ambiguous results induced by the mechanism of biological mediator uptake. As stated by Aretxaga et al. (2001), in some cases, physical adsorption alone can account for as much as 70% of colour removal for

a mediator solution upon contact with bacterial suspension. If adsorption by biomass was responsible for a significant part of the colour removal observed, not only adsorption itself is governed by organism-specific variance in the adsorption kinetics but also inhibit the biotic reduction reaction. It is possible that the adsorbed mediator can build up a concentration gradient which inhibits further reduction of oxidized mediator (Roller et al. 1984).

In the present context, it is pertinent to know the extent to which the rate of mediator reduction was dependent on adsorption and the effect of such behaviour in terms of power production within the MFC system. To investigate this assumption, a series of mediator partitioning tests in correlation with current production were performed next.

5.2 BIOMASS MEDIATOR ADSORPTION ANALYSIS

Adsorption of dyes is the foundation of many histology techniques for studying cell biology; cationic dyes such as thionine and MB, in particular, are especially important for staining microorganisms (Giles and McKay 1965b). The aim of the present section is to quantitatively investigate the adsorption of mediator molecules by biomass.

5.2.1 Quantification of mediator adsorption

In order to quantify the amount of mediator partitioned into the cellular membrane, all samples were prepared and maintained under the same experimental conditions as the concentration of each mediator was increased stepwise. The biomass concentration was the same (0.63 g/l) for all test samples apart from thionine solutions which had a biomass concentration of 1.12 g/l. Thionine and MB with 5 μ M, 25 μ M, 50 μ M, 100 μ M, 300 μ M, 500 μ M, 700 μ M and 1 mM concentrations were selected to investigate the behavior of microbial adsorption in response to the concentration changes. As explained previously, resorufin has reached its solubility limit as the concentration exceeded 200 μ M. Notably, due to the inertness of potassium ferrocyanide (reduced form of ferricyanide) in contact with molecular oxygen, potassium ferricyanide cannot be regenerated through oxygen exposure for subsequent measurement of optical density in order to predict the concentration.

Cyclic voltammetry (CV) study provided an alternative means of concentration determination. The results of potassium ferricyanide CV analysis at various initial mediator concentrations were provided kindly by a colleague (Evelyn 2012).

The mediator removal percentage can be calculated as follows:

$$Adsorption\% = \frac{(C_o - C_e)}{C_o} \times 100 \quad [5.4]$$

The adsorption experiments were performed by adding mediators into 10 ml of bacterial suspensions with fixed amounts of biomass to yield the required initial concentration. The amount of mediator adsorbed, which is regarded as the adsorption capacity, q_e ($\mu\text{mol}/\text{gram of cell}$), can be calculated from Eq. 5.5,

$$q_e = \frac{C_o - C_e}{C_b} \quad [5.5]$$

where C_o ($\mu\text{mol}/\text{l}$) is the initial mediator concentration, C_e (refer to Sec 3.4.2) is the final mediator concentration left in solution and C_b (g/l) is the biomass concentration.

5.2.2 Effect of initial mediator concentration on adsorption

The effect of the initial mediator concentration on its adsorption by viable *Acinetobacter* suspensions was evaluated over a concentration range of 5 μM to 700 μM for thionine, MB and resorufin (Fig 5.8). According to the graph, the following are concluded: (1) the initial mediator concentration played a vital role in the uptake of the mediator by the biomass; (2) for the thionine and MB inoculated systems, the percentage of mediator uptake increased with the increase in initial mediator concentration until reaching plateau values close to 90% and 100% at concentrations of 300 μM and 100 μM , respectively; (3) by contrast, of the adsorption in resorufin samples decreased with increasing concentration plateauing just below 60% at an initial resorufin concentration above 100 μM ; (4) MB experienced the highest percentage of adsorption among all mediators tested.

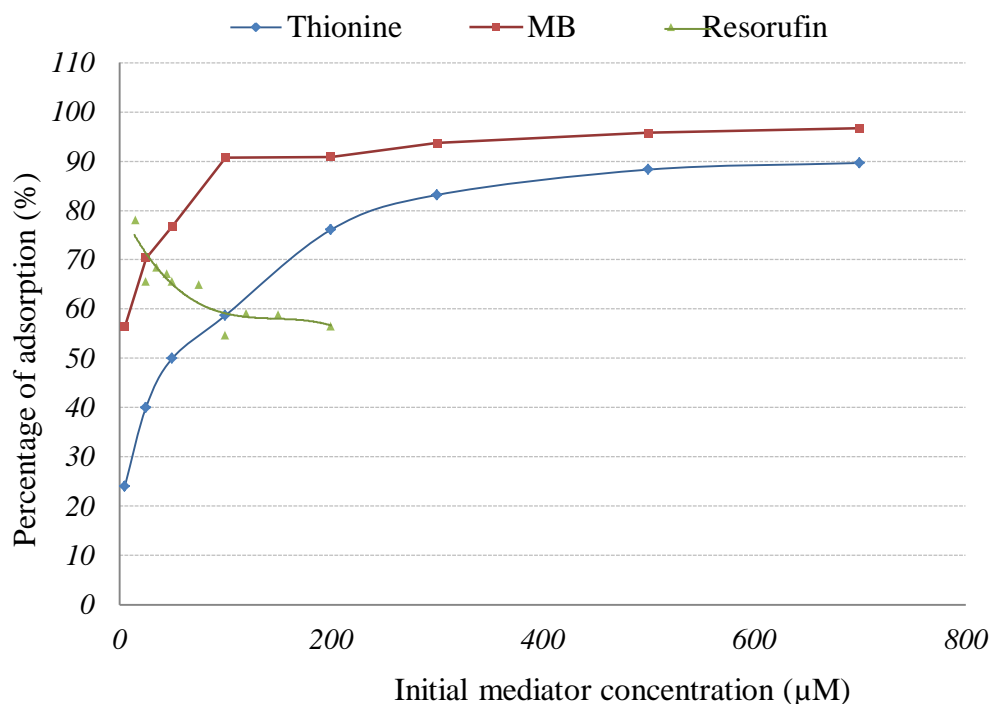


Figure 5.8: The adsorption behavior of thionine, MB and resorufin at a fixed amount of biomass in terms of percentage of mediator adsorbed with respect to the initial mediator concentration.

It is possible that the variation in the adsorption behavior arose from the difference in the interaction between the bioadsorption site and the intrinsic properties of each mediator such as ionic weight, molecular structure and standard redox potential. Thionine has a structure similar to MB which differs only in the presence of $-\text{NH}_2$ groups instead of $-\text{N}(\text{CH}_3)_2$ groups. As demonstrated by Jockusch et al. (1996), this variation in structure may account for the slight deficiency in the binding in comparison to MB. In addition, other factors including the physical and chemical properties of the environment where the adsorption process takes place may also be responsible, the details of which will be discussed later. The higher percentage of adsorption of resorufin at lower initial mediator concentration reported in Fig. 5.8 is likely caused by the large available surface area of the biomass for mediator attachment (Agarry and Aremu 2012). As the adsorption capacity of the biosorbent becomes exhausted, due to the increasing quantity of mediator applied, the adsorption of mediator decreases accordingly. However, assuming the adsorption site becomes crowded, but not saturated, with further increases in mediator concentration, this decline may be compensated for by the reduced effect of mass transfer limitations, leading to a plateau region, as seen in the resorufin curve. However, the same finding

is hard to reconcile with the adsorption trends observed in thionine and MB. The rationalization of the dominant reasons responsible for the ascending adsorption behaviour of thionine and MB will be presented in a later section. It was concluded, based on the CV data provided, that the percentage of bioadsorption for ferricyanide remained relatively constant, around 50%, as a function of increasing the initial mediator concentration to 2 mM.

5.2.3 Adsorption of various mediators

The relationship between the amount of mediator adsorbed per unit of microbe and the amount of mediator preserved in the solution was established (Fig. 5.9). The quantity of adsorbed mediator for each mediator increased with increasing mediator concentration in solution. As pointed out by Cheng et al. (Cheng et al. 2001), this can be rationalized in terms of facilitated multilayer formation of mediator on the surface of biomass, driven by higher concentrations of mediator available in solution.

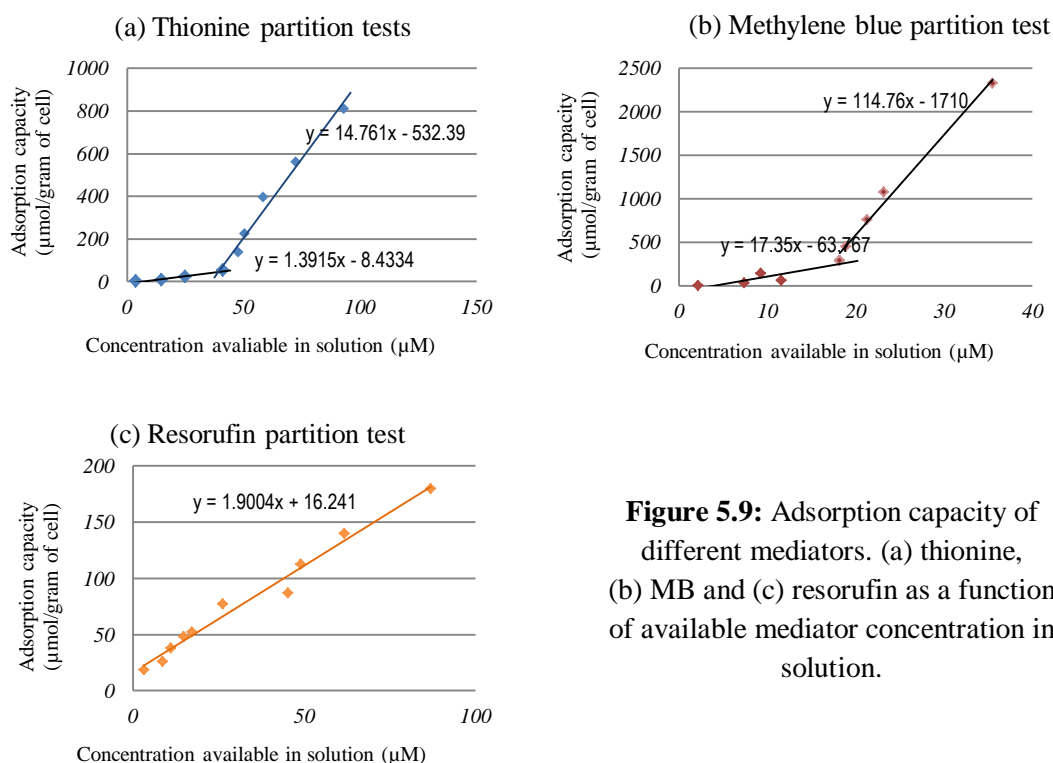


Figure 5.9: Adsorption capacity of different mediators. (a) thionine, (b) MB and (c) resorufin as a function of available mediator concentration in solution.

The adsorption capacity (q_e) of thionine and MB progressed in a similar manner, showing two linear segments against the concentration of mediator remaining in solution. The results indicated dramatic increases in the thionine and MB adsorption per unit of biomass beyond concentrations of 40 μM and 20 μM respectively. As the

concentration of free thionine shifted, from 40 μM to approximately 100 μM , the amount (mg) adsorbed per gram of cells increased 15 fold from 52.4 $\mu\text{mol/g}$ to 809.79 $\mu\text{mol/g}$. As can be seen in Fig. 5.9(b), an 8.1 fold increase in MB adsorption from 288.57 $\mu\text{mol/g}$ to 2324.62 $\mu\text{mol/g}$ was achieved, while the equilibrium concentration in the solution varied by only 20 μM . This superior affinity of MB towards bacterial cells may be attributed to the high polarity of MB molecule which allows higher degree of intercalation with bacterial components residing in the hydrophobic interior of the cells (Jockusch et al. 1996). In the case of resorufin, a linear plot can be fitted to the change in adsorption capacity with the increase in the equilibrium concentration. It was previously reported that the amount of ferricyanide partitioned into the biomass was equivalent (50%) to the concentration of free ferricyanide which remained in solution while keeping the total bacterial content constant. A linear graph, similar to the resorufin adsorption trend, is thus expected for the ferricyanide mediated system according to the CV results, although data were not shown.

In order to analyze the adsorption behavior, the Langmuir and the Freundlich isotherms models were applied to interpret the results. It was found that the classical Langmuir adsorption model cannot be fitted to any of the mediator examined whereas the Freundlich model can only be applied to describe the adsorption characteristics of MB for the initial region of the adsorption before the appearance of the sharp ascending phase. In the case of resorufin, the entire data range fitted well to the Freundlich isotherm. The Freundlich isotherm is normally employed to describe heterogeneous systems which involve the formation of multilayers. It is expressed in the following equation:

$$\log q_e = \log k_f + \frac{1}{n} \log C_e \quad [5.6]$$

where k_f and n are the Freundlich constants and represents the adsorption capacity of the sorbent and the measure of favorability for the adsorption process, respectively (Hameed et al. 2008). The values of these two constants can be calculated from the slope and the intercept of linear plot (Fig. 5.6) of $\log q_e$ as a function of $\log C_e$ and are given in Table 5.2.

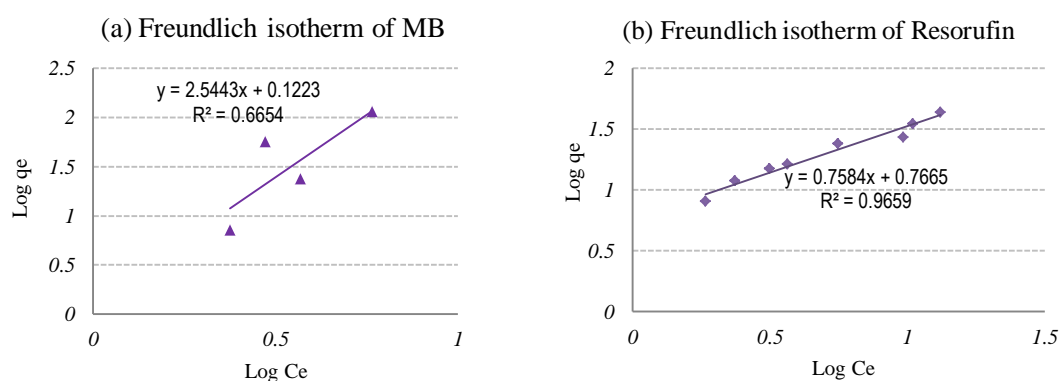


Figure 5.10: Freundlich isotherm of two mediators. (a) presents the Freundlich isotherm of MB at the initial phase (before the sharp ascending region) of the adsorption. Figure (b) demonstrates the Freundlich isotherm of resorufin.

Table 5.2: The Freundlich isotherm constants for MB and resorufin

Compound adsorbed	k_f	n	R^2
MB	0.393	1.33	0.6654
Resorufin	5.84	1.32	0.9659

A favorable adsorption process is identified by values of $n > 1$. In the present study, the adsorption process is favorable for MB and Res as the n value is greater than 1. The linear fit of Res adsorption data to the Freundlich isotherm model with a correlation coefficient $R^2=0.9659$ implies that the surface of the bio-sorbent is heterogeneous and multilayered in character.

5.2.4 Explanations on the adsorption discrepancies

From the above discrepancies observed in the adsorption profiles for different mediators, it is reasonable to conclude that the bio-sorption mechanism for resorufin differs from those of thionine and MB. It is speculated that adhesion onto the biomass may be the dominant, but not the sole, factor causing the reduction of mediator concentrations in solution. The sharp ascending segments detected in the adsorption capacities (Fig. 5.9) for thionine and MB may be a result of the combined effects of biomass adsorption and depletion through precipitation as well as formation of dimers (Fornili et al. 1985; Ghanadzadeh et al. 2008; Lithgow et al. 1986). Both thionine and MB are hydrophobic cationic molecules with flat aromatic structures and their aggregation tendencies at high ($>300 \mu\text{M}$) concentrations have been demonstrated by

many researchers (Ghanadzadeh et al. 2008). In liquid solution, the resulting dimer species from the dipole-dipole interactions between the adjacent monomer units were evidenced by accompanying color changes as indicated by the adsorption peak changes in the absorption spectrum. With increasing concentrations of thionine and MB in solution, a secondary peak emerged in the adsorption spectrum which indicated the presence of dimeric species. The peaks of the thionine monomer and dimer were located at 597 nm and 561 nm, respectively (Lai et al. 1984) while in the case of MB, the adsorption maxima appeared at 664 nm for monomer and 615 nm for dimer (Usacheva et al. 2003). The second peak appeared when thionine concentration increased above 200 μM , as reported by Lai et al (Lai et al. 1984). For thionine, this peak increased gradually as the concentration increased and became the dominant peak when the concentration was higher than 1 mM. The same trend also applied to MB for which the monomeric band diminished with increasing ($> 300 \mu\text{M}$) MB concentration. The addition of Gram-negative bacteria suspension to the MB solution induced far greater dimerization of the mediator, which caused further depression of the monomeric peak than that observed with the Gram-positive bacteria (Usacheva et al. 2003).

Figure 5.11 displays the experimentally observed spectral shifts of thionine and MB samples for this set of experiments. The absorption spectrum of thionine (Fig. 5.11(a)) shifted from its characteristic shape for monomeric species and the absorbance values increased with increasing mediator concentration of 100 μM , 300 μM and 500 μM . The apparent secondary peak occurs at a thionine concentration of approximately 500 μM . At initial MB concentration of 200 μM (purple), certain amount of MB dimer was likely to be present based on the spectral data (Fig. 5.11(b)) as indicated by the appearance of second peak on the lower wavelength side of the 664 nm peak. This secondary peak is becoming apparent when the MB concentration was increased to 300 μM (blue). The appearance of the secondary absorbance peaks at 561 nm and 615 nm can be regarded as the results of dimerization of these two mediators.

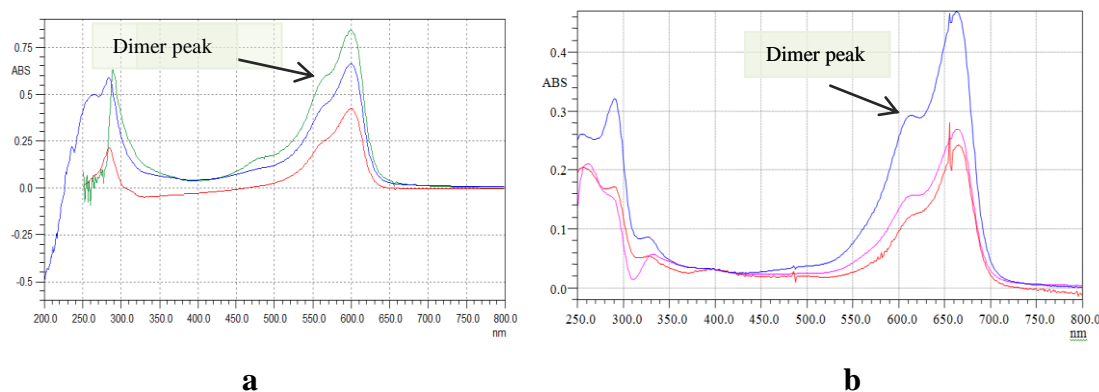


Figure 5.11: The adsorption spectra shift of thionine and MB at different concentrations. a), Thionine with concentrations of 100 μM (red), 300 μM (blue) and 500 μM (green); and b), MB with concentrations of 100 μM (red), 200 μM (purple) and 300 μM (blue) at 5 times dilution.

All phenothiazine dyes are considered effective membrane-destructive agents, capable of binding to the polyphosphates of the bacterial membrane. Once attached to the membrane, they produce molecular damage to lipids and proteins, including membrane-bound enzymes, which will eventually cause cell death. In addition, MB in particular has been demonstrated to be a potent cytotoxin, targeting primarily bacterial cell DNA. At a concentration of 250 μM , MB killed 60% of *E.coli* cells within one hour in experiments conducted by Usacheva *et al.* (2001). In the present study, atypical formation of green-blue fluffy precipitation was detected in samples containing more than 200 μM MB and its quantity grew proportionally with increasing MB concentration (Fig. 5.12).

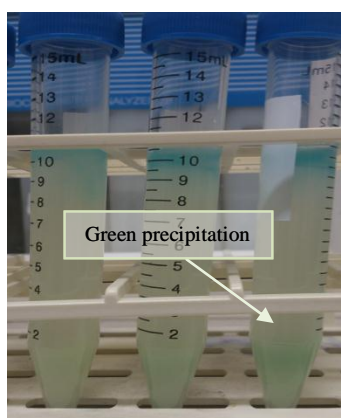


Figure 5.12: Detection of green precipitation in MB-bacteria suspensions.

For the concentrations of MB samples analysed, the formal MB solubility of 156 mM implies these precipitations formed from unknown reactions during the incubation period which did not originate from un-dissolved MB initially injected. Based on the cytotoxic properties of MB, confirmed by Uacheva et al. (2001), it is possible that these precipitations could be attributed to dead bacterial cells with trapped MB which gave rise to the green-blue color.

5.3 THE EFFECT OF MEDIATOR ADSORPTION ON CURRENT RESPONSE

After studying the mediator reaction within the biomass as illustrated in Eqs. 5.1 and 5.2, the examination on the actual performance of each molecule to function as an electron mediator in a MFC system (Eq. 5.3) was performed. In addition, the following discussion considers the hypothetical scenario in which the current response is determined by the mediator concentration (free in solution) involved in the electron transfer process. There is convincing experimental evidence from histochemical studies of dead cells that the cell components within the cytoplasm can be strongly stained by cationic dyes (Giles and McKay 1965a). This mediator entrapment within the enzymatic layer, as pointed out by Bartlett and Pratt (1995), could limit the current output of a fuel cell. In a fuel cell system, the electron current is maintained by continuous oxidation of mediators at the working electrode. Therefore, the current extracted from such a system is a measure of the rate of recovery for electrons from the mediator reoxidation process as simplified in Eq. 5.3. The rate of electrons transfer at the electrode is limited by either the mass transfer of mediator to the surface or kinetics of electron transfer between the mediator and the electrode surface. Both of these processes are dependent on the concentration of reduced mediators within the solution. It is speculated that the sequestered mediators (within the biomass) can no longer contribute to electron transfer, resulting in reduced electron transfer and subsequently affecting the current output.

The quantification of current responses for various mediators was achieved by electrochemical method using a potentiostat. The experiments were initiated after the mediator was fully reduced by the bacterial suspension, as evidenced by the colorless solution. Chronoamperometric measurements were recorded while the working electrode was poised at 0.3 V more positive than the standard redox potential of the mediator under investigation. This large overpotential suggests that the current (i.e.

the rate of oxidation) will be limited by the mass transfer of the reduced mediator to the electrode surface, which in turn is directly proportional to the reduced mediator concentration remaining in the anode solution. The current response recorded using this method is considered to be determined by the free mediator concentration involved in the electron transfer process. It was assumed that the mediator could only be regenerated at the electrode surface giving rise to a current which was used as a direct measure of the rate at which the mediator is oxidized (transfer of electrons from the mediator to the electrode). Although this experimental setup was only a bioelectrochemical device mimicking a conventional MFC system, its simplicity allowed experimentation under well-controlled conditions.

5.3.1 Current response analysis

Chronoamperometric responses for the *Acinetobacter* spp. were determined at a biomass concentration of 0.57 g/l, 100 μ M (total concentration) for the selected mediators (Fig. 5.13). A detailed description of the research method for this section was included in chapter 3.6. On application of the potential (0.3 V positive of the redox potential), the measurable time dependent high current which rapidly decreased within a few seconds was observed. The majority of this current arises from the charging of the electrical double layer and does not represent Faradic electron transfer between the reduced mediator and the electrode. After this process, in all cases, a relatively slow decrease in the current was observed over test periods of 2 to 3 hours. This current is positive and indicates that an oxidation process (mostly likely oxidation of the reduced mediator) is occurring at the electrode. This is partially confirmed by the negligible current observed for an anolyte free of mediator. This also indicates that there is almost no direct electron transfer between the *Acinetobacter* and the electrode, nor direct oxidation of the substrate (ethanol) at the anode. As shown in these curves, during the stable period the highest average current output of 13.2 μ A (mean value at the stable region) was detected for thionine, followed closely by 12.3 μ A for ferricyanide. The two lowest current were extracted from resorufin and MB containing systems which are 5.2 μ A and 2.56 μ A, respectively. The current value of the thionine mediated system was more than two fold higher than the resorufin and MB mediator systems, demonstrating that thionine played a leading role in the mediation of this set of current experiments.

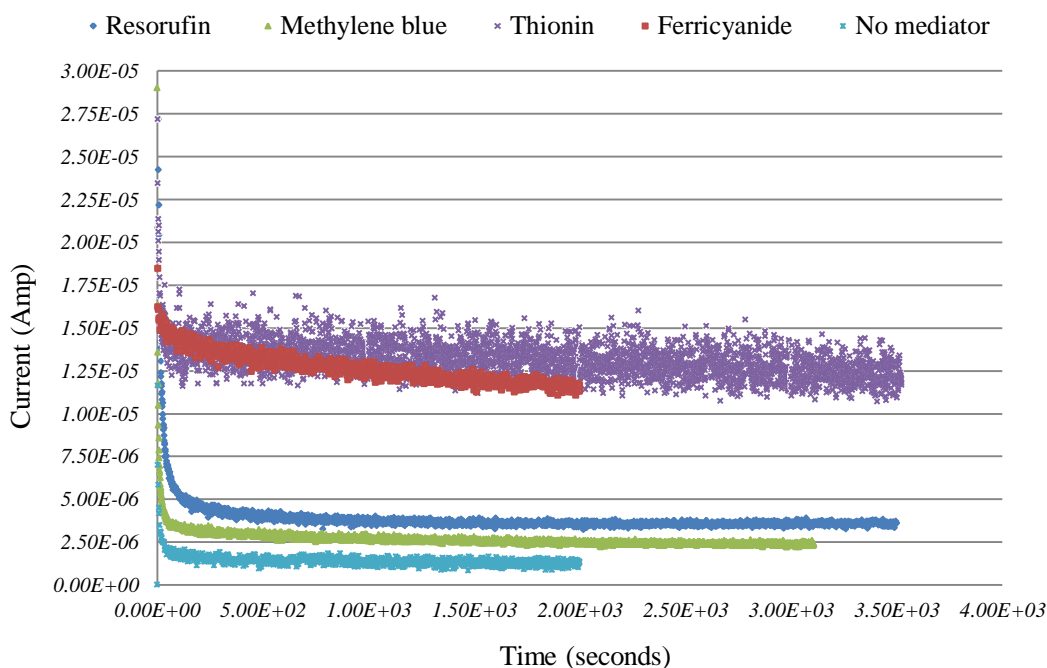


Figure 5.13: The chronoamperometric responses of various mediators at 100 μ M initial concentration. The biomass concentration was 0.57g/l in all mediator-biomass suspensions.

Analogous experiments for the measurements of the changes in current upon the addition of mediator concentrations to 300 μ M with a constant number of microbial cells were performed. Unfortunately, the current measurement of the 300 μ M resorufin mediated system had to be excluded as the predetermined amount of resorufin powder failed to dissolve completely in the bacterial suspension. Thus, the resulting current response cannot be correlated with 300 μ M of resorufin but only the amount dissolved, which was unknown and less than the proposed concentration. The current progression with time for systems mediated by thionine, MB and potassium ferricyanide at an initial concentration of 300 μ M are shown in Fig 5.14. A concentration-induced steady state current increase was observed for all three systems. The average current response with 300 μ M of MB increased to 4.62 μ A, although remaining the lowest of the three. Although tripling the initial thionine concentration, the current increase was only 62.2% and was less than the current response recorded for the potassium ferricyanide mediated system. The highest steady state current, being 35.7 μ A, was achieved when 300 μ M of potassium ferricyanide was present.

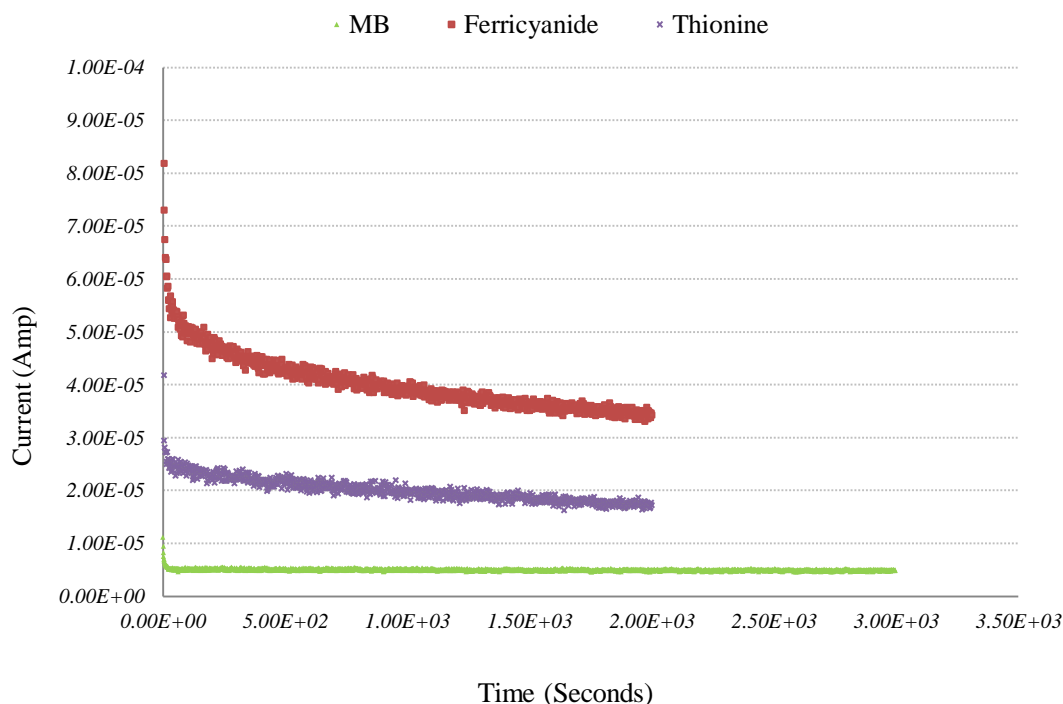


Figure 5.14: The current responses of in samples containing 300 μM of thionine, MB and ferricyanide. The biomass concentration remained the same in all samples which is 0.57 g/l.

The current recorded for this work was a result of the electron transfer between the anode and the reduced mediators. In all cases, MB mediated systems produced the lowest current. These relatively insignificant amounts of current observed were suspected to be an indication of the inability of MB to donate electrons to the electrode or the inhibition of MB diffusion as a result of bacterial entrapment (Ganguli and Dunn 2009).

From the comparison of the current curves shown in Figs. 5.13 and 5.14, it is clear that increasing the initial mediator concentrations increases the current. It is interesting to note that at 100 μM , thionine gave larger currents than ferricyanide, whereas at 300 μM (initial mediator concentration), ferricyanide delivered the highest current of the three. This raises questions as to the predominant factors governing the current response of a mediated fuel cell. Therefore, it is necessary to investigate the changes in current responses with respect to raised initial mediator concentrations above 300 μM and how these current results correlate with the free mediator concentrations in solution.

5.3.2 Free mediator concentration and current response

The anodic currents were measured by further increasing mediator concentrations to 500 μM , 700 μM and 1 mM. In all cases, the potential was applied and current measured once the mediators were colorless (i.e. after microbial reduction). The data reported in Fig. 5.15 shows the relationship between the mean current responses at various initial mediator concentrations for thionine, MB and potassium ferricyanide.

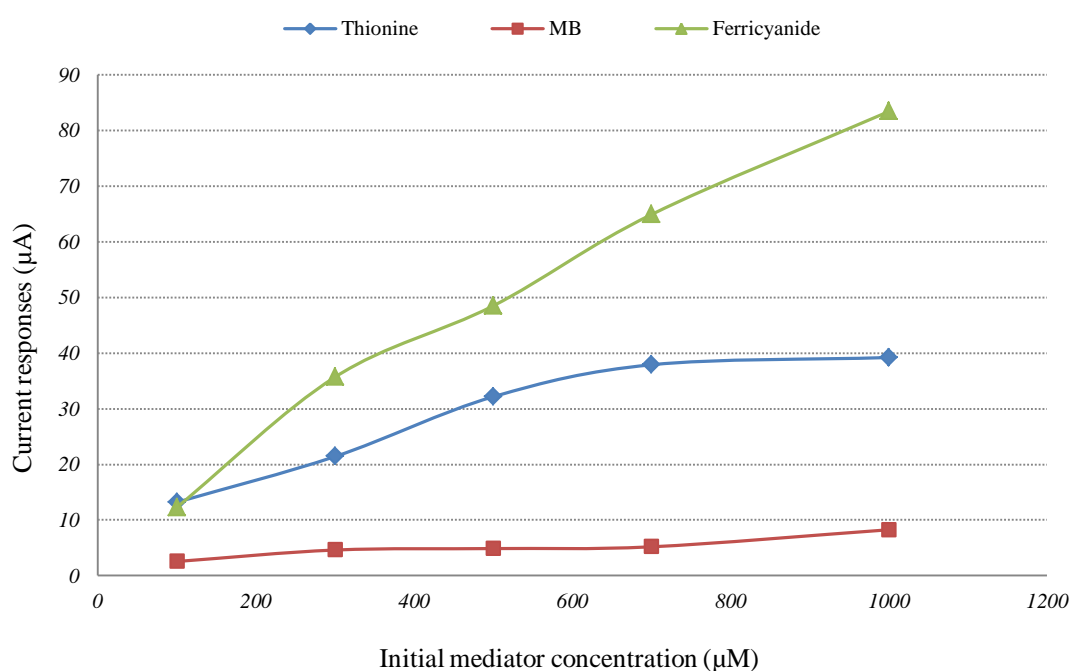


Figure 5.15: The mean current responses as a function of initial mediator concentration in systems containing thionine, MB and ferricyanide as electron mediator.

According to Fig. 5.15, the relationship between the current response and initial potassium ferricyanide concentration was linear over the entire concentration range and applicable to the rotating cylinder electrode equation. No increase in current was observed with increasing concentration for thionine and MB concentrations above 700 μM and 300 μM respectively. Similar responses were observed by many other authors. As reported by Yuan and Kim (2008), in a *Proteus vulgaris* powered MFC system incorporating thionine as the redox mediator, the optimum power density was achieved with 400 μM thionine before declining with increased mediator concentration. The same catalytic characteristics of thionine were described by

Patchett et al. (1988) and Rahimnejad et al. (2011) also, although each reported a different optimal mediator concentration owing to differences in the microbial components and other experimental conditions. According to Rahimnejad et al. (2011), insignificant changes in current was detected for a MB catalyzed fuel cell with concentrations beyond 300 μM , the same value observed in this study. The observation that current was not proportional to concentration for thionine and MB at higher concentrations was considered to be a result of elevated cytotoxicity by these authors. This argument is likely to be true, although not complete. It was discussed earlier that the cytotoxicity of these mediators is one of many causes contributing to reduced amounts of available mediator participating in the electron mediation process, and essentially, it is the quantity of mediator remaining free in solution which controls the rate of diffusion to the electrode and thus the current that can produce. In order to verify this hypothesis for the present system, the rotating cylinder electrode equation was adopted as the first approximation method to estimate the theoretical anodic current developed from chronoamperometry analysis. This equation is particularly suited for the study of the mass transport limited systems with a turbulent flow regime. The equation for calculating the limiting current (ampere) is given as (Fabian et al. 2006):

$$i_L = 0.0791 n F C d_{cyl}^{-0.3} \left(\frac{\mu}{\rho}\right)^{-0.344} D^{0.644} U^{0.7} A \quad [5.7]$$

where i_L is the theoretical current, n is the number of electrons transferred per mediator molecule, F is the Faraday constant, C stands for the reduced mediator concentration (mol/l), d_{cyl} is the electrode outer diameter (cm), μ is the absolute viscosity of solution (g/(cm·s)), ρ is the solution density (g/cm³), D refers to the diffusion coefficient of the mediator, U represents the linear velocity of the rotating electrode (cm/s) and A is the anodic surface area (cm²).

The predicted theoretical currents were derived by applying initial and free reduced mediator (after the mediator is adsorbed by the biomass) concentrations to this rotating cylinder electrode equation for each mediator. The theoretical current values and the experimental data are included in Table 5.3 for comparison.

Table 5.3: The theoretical current of different mediators derived by applying initial and free mediator concentration to the rotating cylinder electrode equation. The experimental current are presented as comparison.

	Initial concentration (μM)	Free mediator concentration (μM)	Predicted current at initial concentration (μA)	Predicted current at free concentration (μA)	Experimental current response (μA)
Thionine	100	66	52.6	34.7	13.2
	300	127	157.8	66.8	21.42
	500	154	263.0	81.0	32.16
	700	183	368.2	96.2	37.9
	1000	192	526.0	101.0	39.2
Methylene blue	100	9	64.0	5.8	2.56
	300	19	192.1	12.2	4.62
	500	21	320.2	13.4	4.88
	700	23	448.3	14.7	5.2
	1500	36	960.5	23.1	8.26
Ferricyanide	100	50	56.1	28.1	12.3
	300	150	168.3	84.2	35.7
	500	250	280.6	140.3	48.5
	700	350	392.8	196.4	64.9
	1000	500	561.2	280.6	87.4
	2000	1000	1122.3	561.2	195.3

Theoretically, referring to Eq. 5.7, the change in current response of the anode compartment employing a single mediator species should be proportional to the mediator concentration if all other physical conditions, e.g. electrode surface area and rotating speed, remain unchanged. It is clear that the experimental data, although systematically lower than the predicted values, can be correlated linearly with the theoretical current values derived from the measurable mediator concentration in solution. It is reasonable that the practical values are lower than the calculated maximum theoretical values due to several irreversible losses during the operation of a MFC system. These irreversible losses may include: a), the energy required, namely activation polarization, to overcome the activation barrier for reactions occurring at the electrode; b), the mass transport losses as a result of the accumulation of reaction products and the depletion of reactants; and c), the ohmic losses due to the electronic flow through the electrolyte. Since the experimental system for this research is limited by mass transfer, the mass transport loss is the main reason accounted for the

current limitation observed. Furthermore, the rotating cylinder equation applied does not completely represent the mass transport behavior in the present system. Hence, the measurable current of the present system ultimately depends upon this complex array of reaction parameter leading to a lower than expected current recorded. From the data presented, higher current responses in systems containing MB than those including thionine should be produced when initial MB concentration is applied. However, owing to the high rate of adsorption onto the biomass and its tendency to form dimers, the measurable MB concentration that is available for electron transfer is one order of magnitude lower than that of thionine. The fact that the catalytic current is determined by the reduced mediator concentration available in the anolyte, but not the initial concentration added, is further confirmed by the above comparison. This observation implies that the mediator sequestered within the biomass or deactivated through aggregation does not contribute to current production. Therefore, the low current of thionine and MB inoculated specimens may be attributed to high percentages of partitioning/dimerization (Ganguli and Dunn 2009; Lai et al. 1984) combined with mediator toxicity to the microbes.

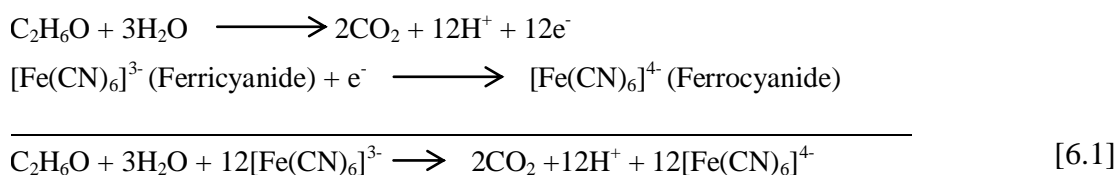
5.4 CONCLUDING REMARKS

The incorporation of a redox mediator, which facilitates the rate of electron transfer from the microorganism to the electrode, is important for the efficient operation of a microbial fuel cell system. The biological reduction of thionine, MB, resorufin and ferricyanide was investigated first in aerobic cultures of *Acinetobacter* spp. oxidizing ethanol. All four mediators were reduced, although to different extents as the concentrations varied, and the rate of reduction (observed by color loss) decreased in the order of MB > thionine > resorufin > potassium ferricyanide. It was noticed that, during the process of biotic reduction, physical adsorption of mediators by cell components accounted for a significant amount of color removal. Consequently, the adsorbed mediators trapped within the intracellular space can no longer participate in electron transfer, representing a significant current limitation in a MFC. The adsorption analysis revealed that as high as 98% of methylene blue was entrapped within the biomass or lost as precipitation when the initial MB concentration was 1.5 mM. In the case of thionine, 81% was adsorbed at an initial concentration of 1 mM. The percentage of adsorption for potassium ferricyanide

remained constant, approximately 50%, as the initial mediator concentration increased, according to the cyclic voltammetry results. The last part of this chapter presented the chronoamperometric results for various mediator systems. The experimental current productions of thionine, MB and ferricyanide mediated systems correlate well with the theoretical current responses derived from free mediator concentrations, suggesting that the current produced depends on the concentration of reduced mediator remaining in solution but not the total mediator initially injected.

Chapter 6: Case study- potassium ferricyanide

Hadjipetrou et al. (1966) was the first to describe the utilization of ferricyanide ion as an electron acceptor in an *E. coli* suspended microbial fuel cell. Like conventional aerobic oxidation, consumption of organic material by microbes can be achieved by the incorporation of ferricyanide ion as an artificial mediator to replace oxygen as the terminal electron acceptor. By accepting electrons liberated from this metabolic process after being shuttled down the ETC, ferricyanide is reduced to ferrocyanide. The overall ferricyanide-mediated reaction with ethanol as substrate is summarized below (Eq. 6.1):



Based on the results presented in the last chapter, potassium ferricyanide was considered as the most suitable mediator for the current experimental setup which fulfills several postulations required for an effective mediation process:

- i) Appropriate formal redox potential for electron shuttling;
- ii) High solubility in aqueous media;
- iii) Stable in both oxidized and reduced forms;
- iv) Relative low rate of sorption onto the biocomponent in a manner which reduces available ferricyanide concentration for electron transport;
- v) Relatively low cytotoxicity to the biocomponent compared with other organic mediators.

Potassium ferricyanide, in contrast to the organic mediators analyzed, resulted in the highest current under the same operational conditions and showed a linear correlation between reduced ferricyanide concentration and current. Furthermore, because of the inherent problems associated with thionine and MB such as short shelf life, instability under strong light, oxygen sensitivity, limited solubility in aqueous

solutions, etc., ferricyanide was selected as the most suitable candidate for the investigation of mediator reduction kinetics. This chapter will investigate specifically the kinetic of microbial ferricyanide reduction under both oxic and anoxic conditions. Furthermore, a study of the ferricyanide toxicity on the *Acinetobacter* species utilized for this research will be performed.

6.1 KINETIC ANALYSIS OF POTASSIUM FERRICYANIDE REDUCTION

The aim of the present study was to elucidate the kinetics for ferricyanide reduction by *Acinetobacter calcoaceticus*. Under ambient conditions, the reduction of ferricyanide by microbial suspension was indicated by the loss of yellow ($\lambda_{max}=420$ nm) color of the bacterial-mediator mixtures. This color loss was indicative of the formation of ferrocyanide, the reduced form of ferricyanide, which is colorless in solution. The decolorization commenced after a lag phase in the active *Acinetobacter* culture and the kinetic investigation was perused by following the decrease in the absorbance value of ferricyanide at 420 nm at regular intervals. By using the calibration data obtained with known concentrations of ferricyanide in solution, the absorbance reading at each time point was converted to the matching ferricyanide concentration. Representative curves of ferricyanide concentration as a function of time are displayed in Fig. 6.1. In all cases, after an initial measurable lag phase, the concentration of ferricyanide decreased linearly with time before the reduction process slowed or ceased completely. The shapes of these curves are characteristic for biotic mediator reduction acquired from batch experiments which are deficient in pH and dissolved oxygen controls (Ertl et al. 2000). According to Fig 6.1, the initial phase of ferricyanide reduction obeys zero order kinetics with respect to time and the slope of this region for each curve gives estimates for the initial rate of ferricyanide reduction ($\mu\text{mol}/(\text{l}\cdot\text{min})$).

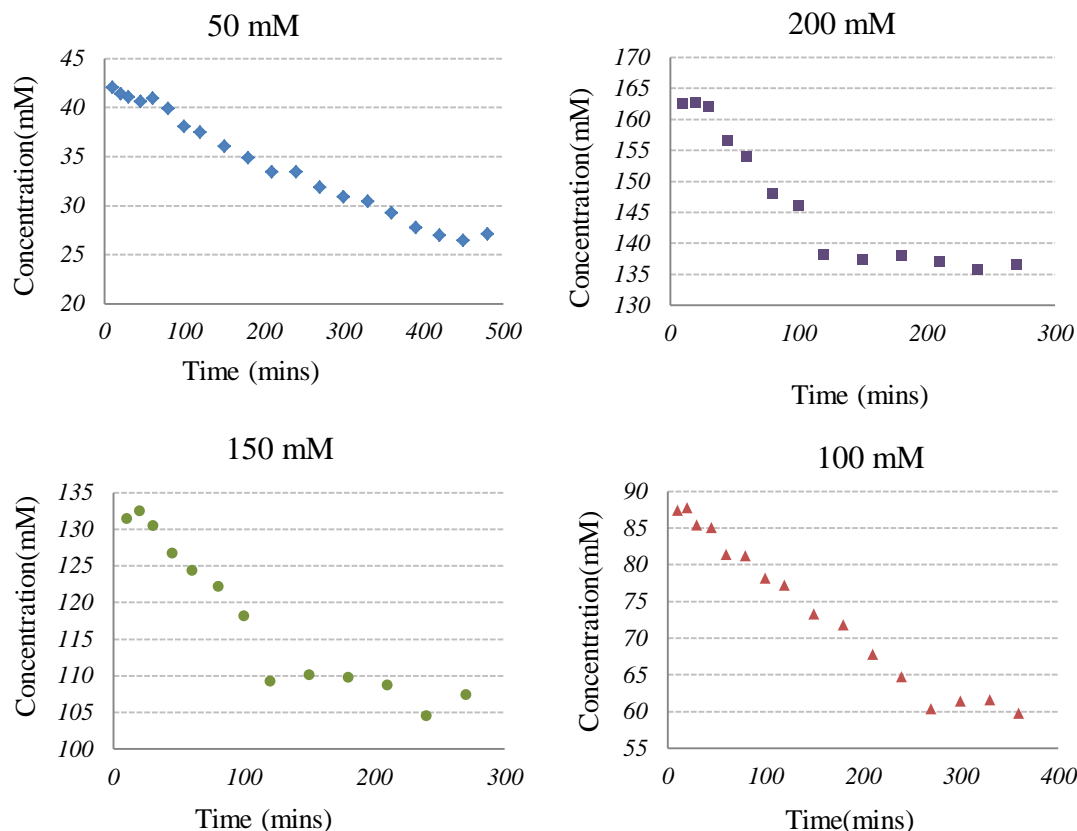


Figure 6.1: Ferricyanide reduction over time by *Acinetobacter* cultures at initial ferricyanide concentration of 50, 100, 150 and 200 mM.

Figure 6.2 shows results of the corresponding specific ferricyanide reduction rates ($\mu\text{mol}/(\text{min}\cdot\text{g})$), normalized by bacterial dry matter) at various initial ferricyanide concentration. As indicated, the rate of ferricyanide reduction by suspensions of actively multiplying *Acinetobacter calcoaceticus* increased linearly with the initial ferricyanide concentration. The specific reduction rate increased from $0.262 \mu\text{mol}/(\text{min}\cdot\text{g})$ to $127.625 \mu\text{mol}/(\text{min}\cdot\text{g})$ when the starting ferricyanide concentration increased from 1 mM to 200 mM. An overlay of results obtained from two parallel experiments at 50 mM initial ferricyanide concentration was observed implying that these kinetic results are reproducible (data not shown).

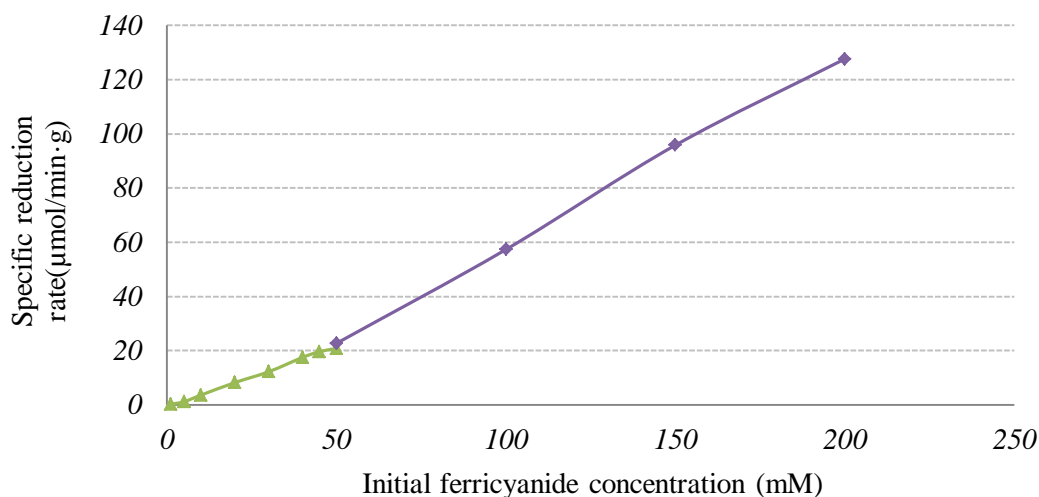


Figure 6.2: Specific reduction rate during the linear region by *Acinetobacter* cultures as a function of initial ferricyanide concentration.

Several literature reports have documented similar results in regard to biotic ferricyanide reduction by *Escherichia coli*. Hadjipetrou et al. (1970) reported an increase of specific reduction rate (from 0.78 to 1.25 $\mu\text{mol}/(\text{min}\cdot\text{g})$) with concentration up to a ferricyanide concentrations of 30 mM. The reduction kinetics stabilized above this concentration before decreasing to a new constant value at 100 mM ferricyanide concentration. Ertl et al. (2000) also demonstrated a plateau region of the specific ferricyanide reduction rate, approximately 105 $\mu\text{mol}/(\text{min}\cdot\text{g})$, after initial ferricyanide concentration has risen above 40 mM. It was argued by these authors that ferricyanide reduction kinetics is dependent on factors such as substrate availability as well as substrate uptake rates and the intrinsic properties of the respiratory enzyme (Ertl et al. 2000). As evidenced experimentally, a maximum value of specific reduction rate for ferricyanide was obtained when high enough ferricyanide concentration was present leading to a complete depletion of substrate (Hadjipetrou et al. 1970). The examination of substrate consumption during the ferricyanide reduction experiments revealed that (details are discussed in a following section) the available ethanol remained was in excess in all samples tested at the end of the initial sharp reduction phase which may explain the disparity of our results in comparison with others based on the conclusions drawn by these authors.

During the experimental process, an interesting observation was recorded that at initial ferricyanide concentrations higher than 50 mM, the test solutions started

turning green after approximately 2 hours of incubation accompanied with sharp pH decrease (Table 6.1).

Table 6.1: pH decrease at various initial ferricyanide concentrations.

Time (hours)	50mM	100mM	150mM	200mM
0	6.46	6.52	6.48	6.56
2	6.32	5.29	4.90	4.07
3.5	6.15	5.22	3.96	3.75
4.5	5.95	4.10	3.89	3.68
6	5.76	3.85	3.68	3.73
7	5.60	3.92	3.80	3.64
24	3.80	3.93	3.69	3.66

It can be seen that the rate of pH decrease varied according to initial ferricyanide concentration. The higher the ferricyanide concentration, the faster the pH decreased to a relatively constant value. The high rates of acidification in these test medium by aerobically grown cultures of *Acinetobacter calcoaceticus* when ferricyanide was reduced showed that the transmembrane ferricyanide reduction is associated with an export of protons. When ferricyanide, which does not become protonated when reduced, was introduced as a final electron acceptor, the protons released thus accumulate to cause acidification of the test suspensions instead of combining with molecular oxygen to form water in conventional aerobic oxidation. The amount of protons accumulated appeared to be proportional to the ferricyanide reduced as confirmed by lower pH value in more ferricyanide reduced samples. This ferricyanide associated proton release was analyzed in a report by Crane et al. (1982). In their study, ferricyanide-stimulated proton extrusion across the cell membrane was quantified through pH measurements of a suspension of yeast cells. It was demonstrated that the amount of proton exported was the same order of magnitude as the rate of ferricyanide reduction. Consequently, when the movement of protons was constrained due to the formation of proton gradient outside the cell membrane, the rate of electron transport was limited and subsequently the rate of ferricyanide reduction declined. The experimental results depicted in Fig. 6.1 showed that inhibition of further ferricyanide reduction appeared at the same time when the effect of proton accumulation starts to emerge (i.e. significant pH drop), approximately 7 and 4.5 hours at 50 mM and 100 mM ferricyanide concentration, and 2 hours when

concentration was raised to 100 mM and 200 mM. This observation is consistent with the concept that proton movement through the membrane is necessary in order to maintain the maximum rate of electron transport and subsequently ferricyanide reduction.

6.2 EFFECT OF OXYGEN ON THE KINETICS OF FERRICYANIDE REDUCTION

Up to now, all the mediator reduction analysis were performed under aerobic conditions with no control of dissolved oxygen level which was considered not appropriate for the reduction of mediators by many researchers (Roller et al. 1984; Wuhrmann et al. 1980). It was discussed earlier that the oxic environment can play an inhibitory effect through competition with mediators for terminal electrons. In order to understand the effect of oxygen on reduction kinetics, this section reveals the experimental findings in regard to ferricyanide reduction under anaerobic conditions.

Figure 6.3 depicts the variation of specific reduction rate throughout the concentration range from 5 mM to 100 mM under anoxic and aerobic conditions for ferricyanide. In this set of experiments, we observed that the rate of reduction with *Acinetobacter calcoaceticus* in anoxic incubations was consistently faster than that obtained in aerobic incubations for all concentration tested. A maximum of 70.3% increase in the specific reduction rate was achieved under anoxic conditions when compared with the sample tested under oxic condition at an initial ferricyanide concentration of 100 mM. The percentage of increase in 5 mM and 50 mM inoculated medium was 63.6% and 69.3%, respectively. It was assumed that the presence of dissolved oxygen induced a similar inhibition effect on ferricyanide reduction regardless of concentration variation. Furthermore, the microbial reduction of ferricyanide favored anoxic conditions. The sensitivity of the reduction to oxygen was concluded by many researchers as a rate competition of the re-oxidation of terminal electron carriers in the ETC between oxygen and ferricyanide. Thermodynamically, oxygen is the preferred electron acceptor as it was the strongest oxidants which results in the highest free energy change owing to high standard redox potential ($E_0 = +0.84\text{V}$) (Rabaey and Verstraete 2005). When dissolved oxygen was available, the reduction of ferricyanide would be suppressed due to the presence of constant competition for electrons imposed by larger thermodynamic driving force when oxygen is available as a terminal electron acceptor. Although this interpretation has

been verified by several authors (Roller et al. 1984; Wuhrmann et al. 1980), it cannot explain why such significant extent of rate increase was observed in our de-aerated samples considering the molar ferricyanide:oxygen ratio is about 20:1, 200:1 and 400:1 (water O₂ saturation at 25 °C is 0.26 mM) in samples each containing 5 mM, 50 mM and 100 mM of ferricyanide. Given the fact that oxygen reduction involves a 4 electron transfer in comparison to 1 electron for ferricyanide, the 70% of rate increase still seemed unlikely if it was exclusively due to competition. It is possible that some physiological problem resulting from the de-aeration procedure rather than to an effect of the presence or not of oxygen in the samples.

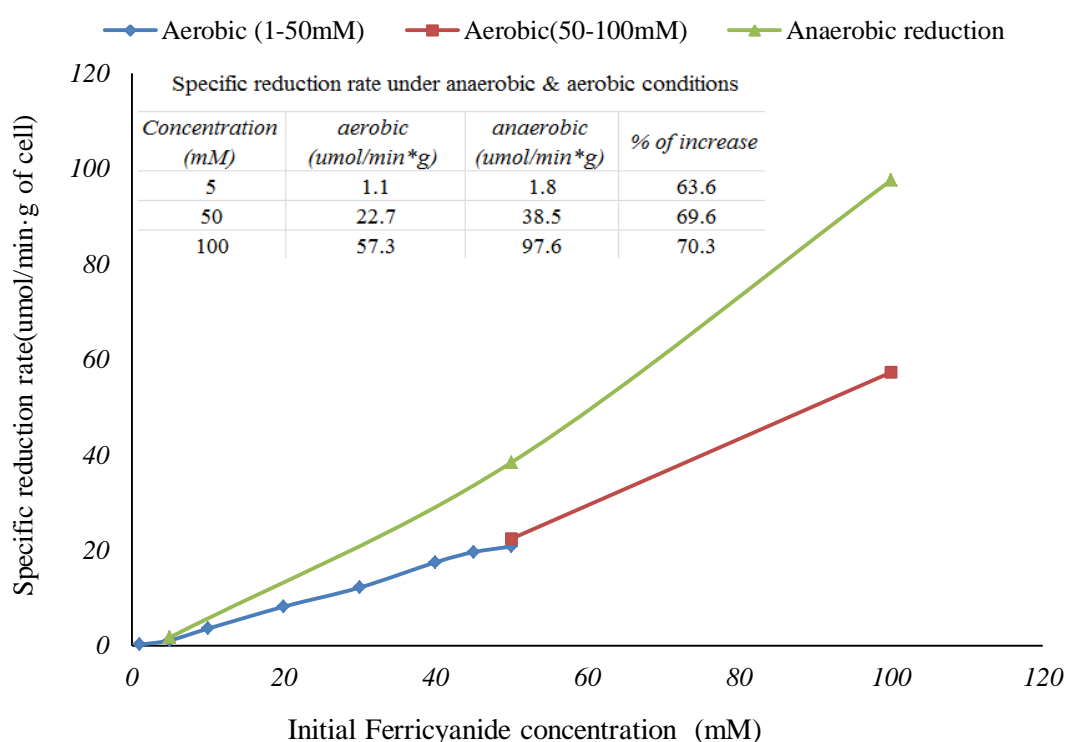


Figure 6.3: Comparison of specific reduction rates of ferricyanide under aerobic and anaerobic conditions. The inset shows the exact values of the specific rate of reduction as well as the percent of increase at selected initial ferricyanide concentrations.

6.3 TOXICITY OF FERRICYANIDE TO *ACINETOBACTER CALCOACETICUS*

Ferricyanide has been used as a terminal electron acceptor to replace oxygen in microbial respiration for a considerable time (Catterall et al. 2010). It has a water solubility of 1432 mM, approximately five magnitudes higher than oxygen, which affords the use of concentrated samples in which the final electron acceptor does not limit respiration rate. It is possible that, in the presence of high ferricyanide

concentration, adverse effects which may disrupt electron transfer within the cell could be induced (Liu et al. 2009). As a result, a toxicity assessment for samples including high ferricyanide concentrations (50-200 mM) is therefore desirable for this study. These toxicity tests were performed at the same time as the kinetic analysis of ferricyanide reduction described in chapter 6.1. The effect of ferricyanide on the biological components was determined by the changes of optical density ($\lambda_{max}=600$ nm) before and after the reduction tests and then compared with a control sample.

Figure 6.4 displays the changes in optical density as a function of time for bacterial suspensions exposed in a range of ferricyanide concentrations (50-200 mM). In the control experiment with only *Acinetobacter* culture, the optical density increased from 1.82 to 2.15 over the 6-hour duration suggesting the microorganisms are viable and capable of further growth. In the sample containing 50 mM ferricyanide, growth inhibition was observed as indicated by the negligible changes in optical density reading after 6 hours of incubation. The presence of ferricyanide at concentrations higher than 50 mM, the general trend of each curve is similar where the optical density decreased over time. The rate of change in optical density increased as the initial ferricyanide concentration increased from 100 mM to 200 mM which implies the cells were becoming more sensitive to the inhibitory effect. The substrate evaluation after 6 hours of incubation revealed that 92-95% of ethanol was still present in all solutions of ferricyanide samples.

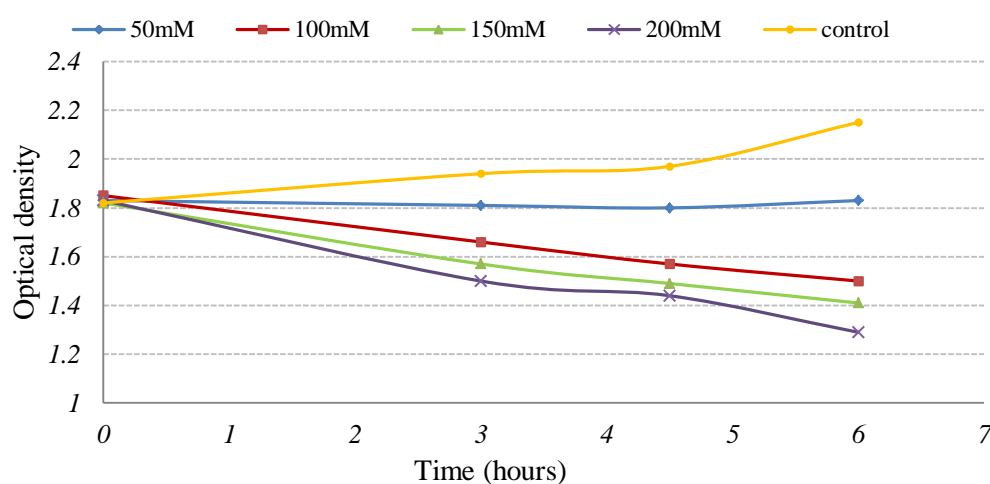


Figure 6.4: Optical density changes over 6 hours in samples containing various ferricyanide concentrations.

According to this observation, it is reasonable to speculate that the inhibition of microbial growth may possibly be introduced by either the inclusion of ferricyanide, as described in chapter 6.1, or the ferricyanide induced pH declines but not lack of substrate. These results are consistent with those reported by Liu et al. (2009) that the growth inhibition on *E. coli* cells started to emerge at ferricyanide concentration of 50mM. With the addition of 100 mM ferricyanide, complete suppression in *E. coli* growth was achieved with obvious damage to the cell structure as detected by nanoscale visualization techniques. Characterization of the cell structure demonstrated that significant portion of the *E. coli* cell wall had disappeared resulting in the lysis of bacteria at 100 mM ferricyanide concentration (Liu et al. 2009).

6.4 CONCLUDING REMARKS

The kinetics of reduction for ferricyanide by viable *Acinetobacter* cultures in the presence of oxygen was investigated at various initial ferricyanide concentrations. According to Fig. 6.2, the specific reduction rate increased as the initial ferricyanide concentration increased from 1 mM to 200 mM. It was observed that ferricyanide reduction was associated with an export of proton as indicated by the obvious pH decreases in samples containing more than 50 mM of ferricyanide. As suggested by Crane et al. (1982), the decrease in the rate of reduction after the initial phase of sharp decline (Fig 6.1) may be attributed to the accumulation of protons which inhibits the electron flow and subsequently ferricyanide reduction. Anaerobic ferricyanide reduction was initiated in order to analyses the effect of oxygen on the rate of ferricyanide reduction. In the absence of oxygen, the specific rate of reduction in samples inoculated with 5 mM to 100 mM ferricyanide was increased by 63.6-70.3%. A combination effect of anaerobic condition and physiological state of changes at molecular level may be used to explain such a significant increase in the rate of reduction. Moreover, although ferricyanide is generally considered nontoxic to microorganisms, it is desirable to evaluate the potential adverse effect on microbes at high concentrations. The experimental findings from this study are in agreement with those reported by Liu et al. (2009) that the inhibitory effect on cell growth starts to emerge at 50 mM ferricyanide concentration. With further increase in ferricyanide concentration to 100 mM, cell death due to destruction of cell wall was observed.

Chapter 7: Conclusion and future work

7.1 SUMMARY OF THIS RESEARCH

MFC is a promising technology which provides an alternative route of sustainable electricity production via the direct conversion of chemical energy stored in renewable biomass to electricity. In this study, a biological fuel cell powered by the metabolism of ethanol by *Acinetobacter calcoaceticus* was assembled. This MFC was developed with the advantage of a small reactor volume, using a proton exchange membrane as a barrier between the anode and cathode part of the fuel cell.

In chapter 4, the isolation and investigation of the microbial consortia were explored. This series of experiments resulted in the isolation of strains of ethanol degrading bacteria, from crude soil and compost samples, belonging to the genus of *Acinetobacter*. A pure-culture isolate named *A. calcoaceticus* was identified using 16S rRNA sequencing. Subsequently, the effect of ethanol concentration, oxygen content, nitrogen sources and antifoaming control on the growth of this particular strain was evaluated. The optimum growth conditions within the scope of those used in this study for biomass production were obtained with a μ_{\max} of 0.231 h^{-1} in an antifoam included and aerated (0.68 vvm) culture flask containing 2% ethanol.

The performance of MFCs is dependent on the efficiency of several consecutive-step reactions, typically, the oxidation of organic substrate, anodic electron transport from bacteria to electrode and finally the electron flow through the circuit. It is generally accepted that the electron transfer from the anode microbial cells to the anode is the principle limitation in increasing the power production of a MFC (Ganguli and Dunn 2009). To improve the efficiency of electron transfer, research efforts have focused on finding suitable artificial mediators, and several effective mediators such as thionine, MB, resorufin and potassium ferricyanide were identified. In chapter 5, the microbe-mediator interactions and the effect of biological mediator adsorption on current responses were analyzed and interpreted. It was demonstrated in this section that *Acinetobacter calcoaceticus* is capable of reducing all mediators (thionine, MB, resorufin and potassium ferricyanide) selected at different rate. The variation in the rate of mediator reduction was possibly associated with the structure,

intracellular site of reduction and the biological adsorption of mediator. In this context, the subsequent investigation on biological adsorption of mediators revealed that MB experienced the highest percentage of adsorption which approached 98% when the initial mediator concentration was raised to 700 μM . The lowest percentage of adsorption was observed for potassium ferricyanide. Based on literature findings and spectrophotometric results, the percentage of biomass adsorption was possibly enhanced by the high aggregation potential and cellular toxicity of thionine and MB. The last part of this chapter presented the chronoamperometric results for various mediator systems which is one of the main findings of the present work. The experimental current productions of thionine, MB and ferricyanide mediated systems correlate well with the theoretical current responses derived from free mediator concentrations, suggesting that the current produced depends on the concentration of reduced mediator remaining in solution but not the total mediator initially injected. Similar to the results concluded by Ganguli and Dunn (2009), the sequestered mediator within biomass was shown not to participate in electron transfer which resulted in significant power density limitation.

According to the results presented in Chapter 5, potassium ferricyanide was considered as the most suitable mediator for this experimental setup which was selected for a detailed study of mediator-microbe reaction. In chapter 6, the kinetic analysis of biotic potassium ferricyanide reduction revealed that the initial ferricyanide concentration had great influence on reduction rate. It was observed that as the initial ferricyanide concentration increased from 1 mM to 200 mM, the specific reduction rate increased accordingly. Further investigations on anaerobic ferricyanide reduction permitted the understanding of the effect of oxygen on reduction rate through comparison of specific reduction rate between aerobic and anaerobic reduction. For the range of ferricyanide concentrations prepared (5-100 mM), the reduced competition stress with oxygen combined with the prevailing physicochemical properties under anaerobic conditions may be responsible for the 63.6 -70.3% increase in the specific reduction rate. At last, the toxic effect of ferricyanide to *Acinetobacter calcoaceticus* was evaluated by monitoring the biomass density changes of the potassium ferricyanide included samples. The experimental findings from this study is in agreement with those reported by Liu et al. (2009) that the inhibitory effect on cell growth starts to emerge at 50 mM ferricyanide concentration.

7.2 RECOMMENDATIONS FOR FUTURE RESEARCH

In light of the present findings, more avenues of research and debate arise from this work. In principle, the operation of a MFC relies on the microbial activities of the biocatalysts and the rate of microbial respiration is closely correlated with the rate of mediator reduction. Therefore, an important consideration on finding more strains of ethanol oxidizers and further improvement of the microbial growth will be a reasonable initial step. The utilization of redox mediators have greatly elevated the current production in MFC as demonstrated in Fig. 5.13. In such cases, the redox mediators replaced oxygen and functioned as an alternative electron acceptor. While the mediators were being reduced, the organic substrate is oxidized to carbon dioxide. In current study, the knowledge on substrate availability during the process of mediator reduction is lacking. It is therefore necessary to develop analytical methods in order to monitor and evaluate the effect of substrate concentration on mediator reduction and furthermore MFC current production.

Results in this work demonstrated that biomass adsorption of redox mediators posed a great challenge on improving MFC performance. In consequence, subsequent attention should be focused on designing more accurate mediator adsorption quantification and control techniques.

References

- (2011). "Report on Carcinogens." In: *National Toxicology Program*.
- (2012). "National Pollutant Inventory." In: *Australian Government Department of Sustainability, Environment, Water, Population and Communities*.
- A.Silvestre-Albero, J.Silvestre-Alberol, A.Sepúlveda-Escribano, and F.Rodríguez-Reinoso. (2009). "Ethanol removal using activated carbon: Effect of porous structure and surface chemistry." *Microporous and Mesoporous Materials*, 120, 62-68.
- Abbott, B. J. (1973). "Ethanol Inhibition of a Bacterium (*Acinetobacter calcoaceticus*) in Chemostat Culture." *Journal of General Microbiology*, 75, 383-389.
- Abbott, B. J., Laskin, A. I., and McCOY, C. J. (1973). "Growth of *Acinetobacter calcoaceticus* on Ethanol." *Applied Microbiology* 25(5), 787-792.
- Abdel-El-Haleem, D. (2003). "Acinetobacter: environmental and biotechnological applications." *African Journal of Biotechnology* 2(4), 71-74.
- Aelterman, P., Versichele, M., Marzorati, M., Boon, N., and Verstraete, W. (2008). "Loading rate and external resistance control the electricity generation of microbial fuel cells with different three-dimensional anodes." *Bioresource Technology*, 99(18), 8895-8902.
- Agarry, S. E., and Aremu, M. O. (2012). "Batch Equilibrium and Kinetic Studies of Simultaneous Adsorption and Biodegradation of Phenol by Pineapple Peels Immobilized *Pseudomonas aeruginosa* NCIB 950." *British Biotechnology Journal*, 2(1), 26-48.
- Alberts, B., Johnson, A., Lewis, J., Raff, M., Roberts, K., and Walter, P. (2002). "Electron-Transport Chains and Their Proton Pumps." In: *Molecular Biology of the Cell*, Garland Science, New York.
- Aretxaga, A., Romero, S., Sarrà, M., and Vicent, T. (2001). "Adsorption Step in the Biological Degradation of a Textile Dye." *Biotechnology Progress*, 17(4), 664-668.
- Atkinson, R. (2000). "Atmospheric chemistry of VOCs and NOx." *Atmospheric Environment*, 34, 2063-2101.
- Atkinson, R., and Arey, J. (2003). "Atmospheric degradation of volatile organic compounds." *Chemical Reviews-Columbus*, 103(12), 4605-4638.
- B.Ozturk, and D.Yilmaz. (2006). "Absorptive Removal of Volatile Organic Compounds from Flue Gas Streams." *Process Safety and Environmental Protection*, 84(B5), 391-398.
- Babanova, S., Hubenova, Y., and Mitov, M. (2011). "Influence of artificial mediators on yeast-based fuel cell performance." *Journal of Bioscience and Bioengineering*, 112(4), 379-387.

- Bartlett, P. N., and Pratt, K. F. E. (1995). "A study of the kinetics of the reaction between ferrocene monocarboxylic acid and glucose oxidase using the rotating-disc electrode." *Journal of Electroanalytical Chemistry*, 397(1–2), 53-60.
- Biesta-Peters, E. G., Reij, M. W., Joosten, H., Gorris, L. G. M., and Zwietering, M. H. (2010). "Comparison of Two Optical-Density-Based Methods and a Plate Count Method for Estimation of Growth Parameters of *Bacillus cereus*." *Applied and Environmental Microbiology*, 76(5), 1399-1405.
- Brown, W. A., and Cooper, D. G. (1991). "Self-Cycling Fermentation Applied to *Acinetobacter calcoaceticus* RAG-1." *Applied and Environmental Microbiology*, 57(10), 2901-2906.
- Bueno, C., Villegas, M. L., Bertolotti, S. G., Previtali, C. M., Neumann, M. G., and Encinas, M. V. (2002). "The Excited-State Interaction of Resazurin and Resorufin with Amines in Aqueous Solutions. Photophysics and Photochemical Reaction." *Photochemistry and Photobiology*, 76(4), 385-390.
- Bullen, R. A., Arnot, T. C., Lakeman, J. B., and Walsh, F. C. (2006). "Biofuel cells and their development." *Biosensors and Bioelectronics*, 21(11), 2015-2045.
- Campbell, N. A., and Reece, J. B. (2002). *Biology* 6th ed Ed., Benjamin Cummings, San Francisco.
- Casciato, D. A., Stewart, P. R., and Rosenblatt, J. E. (1975). "Growth Curves of Anaerobic Bacteria in Solid Media." *Applied Microbiology*, 29(5), 610-614.
- Catterall, K., Morris, K., Gladman, C., Zhao, H., Pasco, N., and John, R. (2001). "The use of microorganisms with broad range substrate utilisation for the ferricyanide-mediated rapid determination of biochemical oxygen demand." *Talanta*, 55(6), 1187-1194.
- Catterall, K., Robertson, D., Teasdale, P. R., Welsh, D. T., and John, R. (2010). "Evaluating use of ferricyanide-mediated respiration bioassays to quantify stimulatory and inhibitory effects on *Escherichia coli* populations." *Talanta*, 80(5), 1980-1985.
- Chang, I. S., Moon, H., Bretschger, O., Jang, J. K., Park, H. I., Nealson, K. H., and Kim, B. H. (2006). "Electronchemically Active Bacteria (EAB) and Mediator-Less Microbial Fuel Cells." *Journal of Microbiology and Biotechnology*, 16(2), 163-177.
- Chaudhuri, S. K., and Lovley, D. R. (2003). "Electricity generation by direct oxidation of glucose in mediatorless microbial fuel cells." *Nat Biotech*, 21(10), 1229-1232.
- Cheng, F., Yue-lin, L., and Xing-yao, Z. (2001). "The electrochemical properties of thionine adsorbed monolayer on gold electrode." *Wuhan Univ. J. Nat. Sci.*, 6(4), 846-850.
- Choi, J.-W., Choi, H.-G., and Lee, W.-H. (1996). "Effects of ethanol and phosphate on emulsan production by *Acinetobacter calcoaceticus* RAG-1." *Journal of Biotechnology*, 45, 217-225.
- Choi, Y., Kim, N., Kim, S., and Jung, S. (2003). "Dynamic Behaviors of Redox Mediators within the Hydrophobic Layers as an Important Factor for Effective Microbial Fuel Cell Operation." *Bulletin of the Korean Chemical Society*, 24(4), 437-440.

- Chung, Y.-C., Lin, Y.-Y., and Tseng, C.-P. (2005). "Removal of high concentration of NH_3 and coexistent H_2S by biological activated carbon (BAC) biotrickling filter." *Bioresource technology*, 96(16), 1812-1820.
- Crane, F. L., Roberts, H., Linnane, A. W., and Löw, H. (1982). "Transmembrane ferricyanide reduction by cells of the yeast *Saccharomyces cerevisiae*." *J Bioenerg Biomembr*, 14(3), 191-205.
- Dancey, G. F., and Shapiro, B. M. (1976). "The NADH Dehydrogenase of the Respiratory Chain of *Escherichia coli*." *The Journal of Biological Chemistry*, 251(19), 5921-5928.
- Davis, F., and Higson, S. P. J. (2007). "Biofuel cells—Recent advances and applications." *Biosensors and Bioelectronics*, 22(7), 1224-1235.
- Du, Z., Li, H., and Gu, T. (2007). "A state of the art review on microbial fuel cells: A promising technology for wastewater treatment and bioenergy." *Biotechnology Advances*, 25(5), 464-482.
- Dumas, C., Basseguy, R., and Bergel, A. (2008). "Electrochemical activity of *Geobacter sulfurreducens* biofilms on stainless steel anodes." *Electrochimica Acta*, 53(16), 5235-5241.
- Eccleston, C. H., March, F., and Cohen, T. (2012). "Sustainability and energy policy." In: *Inside Energy: Developing and Managing an ISO 50001 Energy Management System*, C. H. Eccleston, F. March, and T. Cohen, eds., Taylor & Francis Group, United States of America, 289.
- Eichorst, S. A., Breznak, J. A., and Schmidt, T. M. (2007). "Isolation and Characterization of Soil Bacteria That Define *Terriglobus* gen. nov., in the Phylum Acidobacteria." *Applied and Environmental Microbiology*, 73(8), 2708-2717.
- Elisangela, F., Andrea, Z., Fabio, D. G., de Menezes Cristiano, R., Regina, D. L., and Artur, C.-P. (2009). "Biodegradation of textile azo dyes by a facultative *Staphylococcus arlettae* strain VN-11 using a sequential microaerophilic/aerobic process." *International Biodeterioration & Biodegradation*, 63(3), 280-288.
- Emde, R., Swain, A., and Schink, B. (1989). "Anaerobic oxidation of glycerol by *Escherichia coli* in an amperometric poised-potential culture system." *Applied Microbiology and Biotechnology*, 32(2), 170-175.
- Ertl, P., Unterladstaetter, B., Bayer, K., and Mikkelsen, S. R. (2000). "Ferricyanide Reduction by *Escherichia coli*: Kinetics, Mechanism, and Application to the Optimization of Recombinant Fermentations." *Analytical Chemistry*, 72(20), 4949-4956.
- Esko, J. D. (2009). "Bacterial Polysaccharides." In: *Essentials of Glycobiology*, A. Varki, R. D. Cummings, J. D. Esko, H. H. Freeze, P. Stanley, C. R. Bertozzi, G. W. Hart, and M. E. Etzler, eds., Cold Spring Harbor Laboratory Press, New York.
- Fabian, C., Ridd, M. J., and Sheehan, M. (2006). "Rotating cylinder electrode study of the effect of activated polyacrylamide on surface roughness of electrodeposited copper." *Hydrometallurgy*, 84(3-4), 256-263.

- Fornili, S. L., Sgroi, G., and Palumbo, L. (1985). "Effects of Solvent on Stacking Interactions." *J. Chem. Soc., Faraday Trans*, 81(1), 255-258.
- Franks, A. E., and Nevin, K. P. (2010). "Microbial Fuel Cells, A Current Review." *Energies*, 3(5), 899-919.
- Friend, J. A. N., and Smirles, W. N. (1928). "CCXCI.-The solubility of potassium ferricyanide in water between 0° and 100°." *Journal of the Chemical Society (Resumed)*, 0(0), 2242-2245.
- Ganguli, R., and Dunn, B. S. (2009). "Kinetics of Anode Reactions for a Yeast-Catalysed Microbial Fuel Cell." *Fuel Cells*, 9(1), 44-52.
- Gavrilescu, M. (2009). "Environmental Biotechnology: Achievements, Opportunities and Challenges." *Dynamic Biochemistry, Process Biotechnology and Molecular Biology*, 4(1), 1-36.
- Ghanadzadeh, A., Zeini, A., Kashef, A., and Moghadam, M. (2008). "Concentration effect on the absorption spectra of oxazine1 and methylene blue in aqueous and alcoholic solutions." *Journal of Molecular Liquids* 138, 100-106.
- Giles, C. H., and McKay, R. B. (1965). "Adsorption of cationic (basic) dyes by fixed yeast cells." *Journal of Bacteriology*, 89, 390-397.
- Gorby, Y. A., Yanina, S., McLean, J. S., Rosso, K. M., Moyle, D., Dohnalkova, A., Beveridge, T. J., Chang, I. S., Kim, B. H., Kim, K. S., Culley, D. E., Reed, S. B., Romine, M. F., Saffarini, D. A., Hill, E. A., Shi, L., Elias, D. A., Kennedy, D. W., Pinchuk, G., Watanabe, K., Ishii, S. i., Logan, B., Nealson, K. H., and Fredrickson, J. K. (2006). "Electrically conductive bacterial nanowires produced by *Shewanella oneidensis* strain MR-1 and other microorganisms." *Proceedings of the National Academy of Sciences*, 103(30), 11358-11363.
- Govind, R., Fang, J., and Melarkode, R. "Biofiltration of Ethanol Emissions from Bakery Operations."
- Guenther, A., Hewitt, C. N., Erickson, D., Fall, R., Geron, C., Graedel, T., Harley, P., Klinger, L., Lerdau, M., and McKay, W. (1995). "A global model of natural volatile organic compound emissions." *Journal of geophysical research*, 100(D5), 8873-8892.
- Gullo, M., and Giudici, P. (2008). "Acetic acid bacteria in traditional balsamic vinegar: Phenotypic traits relevant for starter cultures selection." *International Journal of Food Microbiology*, 125, 46-53
- Hadjipetrou, L., Lilly, M. D., and Kourounakis, P. (1970). "Effect of ferricyanide on *Escherichia coli*." *Antonie van Leeuwenhoek*, 36(1), 531-540.
- Hadjipetrou, L. P., T.Gray-Young, and Lilly, M. D. (1966). "Effect of Ferricyanide on Energy Production by *Escherichia coli*." *Journal of General Microbiology*, 45, 479-488.
- Hafner, S. D., Montes, F., Rotz, C. A., and Mitloehner, F. (2010). "Ethanol emission from loose corn silage and exposed silage particles." *Atmospheric Environment*(44), 4172-4180.

- Hameed, B. H., Mahmoud, D. K., and Ahmad, A. L. (2008). "Equilibrium modeling and kinetic studies on the adsorption of basic dye by a low-cost adsorbent: Coconut (*Cocos nucifera*) bunch waste." *Journal of Hazardous Materials*, 158(1), 65-72.
- Haugen, G. R., and Hardwick, E. R. (1963). "IONIC ASSOCIATION IN AQUEOUS SOLUTIONS OF THIONINE." *The Journal of Physical Chemistry*, 67(4), 725-731.
- Hernandez, M. E., and Newman, D. K. (2001). "Extracellular electron transfer." *Cellular and Molecular Life Sciences*, 58(11), 1562-1571.
- Hu, B., Quhe, R., Chen, C., Zhuge, F., Zhu, X., Peng, S., Chen, X., Pan, L., Wu, Y., Zheng, W., Yan, Q., Lu, J., and Li, R.-W. (2012). "Electrically controlled electron transfer and resistance switching in reduced graphene oxide noncovalently functionalized with thionine." *Journal of Materials Chemistry*, 22(32), 16422-16430.
- Ilabaca, C., Navarrete, P., Mardones, P., Romero, J., and Mas, A. (2008). "Application of culture culture-independent molecular biology based methods to evaluate acetic acid bacteria diversity during vinegar processing." *International Journal of Food Microbiology*, 126(1-2), 245-249.
- Impert, O., Katafias, A., Kita, P., Mills, A., Pietkiewicz-Graczyk, A., and Wrzeszcz, G. (2003). "Kinetics and mechanism of a fast leuco-Methylene Blue oxidation by copper(ii)-halide species in acidic aqueous media." *Dalton Transactions*(3), 348-353.
- In Ho, P., Gnana Kumar, G., Kim, A. R., Kim, P., and Suk Nahm, K. (2011). "Microbial electricity generation of diversified carbonaceous electrodes under variable mediators." *Bioelectrochemistry*, 80(2), 99-104.
- Jacobson, M. Z. (2007). "Effect of Ethanol (E85) versus Gasoline Vehicles on Cancer and Mortality in the United States." *Environmental Science and Technology*, 41(11), 4150-4157.
- Jockusch, S., Lee, D., Turro, N. J., and Leonard, E. F. (1996). "Photo-induced inactivation of viruses: Adsorption of methylene blue, thionine, and thiopyronine on Q β bacteriophage." *Proceedings of the National Academy of Sciences*, 93, 7446-7451
- Juni, E. (1978). "Genetics and Physiology of *Acinetobacter*." *Annual Review of Microbiology*, 32(1), 349-371.
- Katz, E., N.Shipway, A., and Willner, I. (2003). "Biochemical fuel cells." In: *Handbook of Fuel Cells-Fundamentals Technology and Applications*, W. Vielstich, H. A. Gasteiger, and A. Lamm, eds., John Wiley & Sons, Ltd, Jerusalem.
- Kim, B. H., Chang, I. S., and Gadd, G. M. (2007a). "Challenges in microbial fuel cell development and operation." *Appl Microbiol Biotechnol*, 76(3), 485-494.
- Kim, B. H., Kim, H. J., Hyun, M. S., and Park, D. H. (1999). "Direct electrode reaction of Fe (III)-reducing bacterium, *Shewanella putrefaciens*. ." *Journal of Microbiology and Biotechnology*, 9, 127-131.
- Kim, H. J., Park, H. S., Hyun, M. S., Chang, I. S., Kim, M., and Kim, B. H. (2002). "A mediator-less microbial fuel cell using a metal reducing bacterium, *Shewanella putrefaciens*." *Enzyme and Microbial Technology*, 30(2), 145-152.

- Kim, I. S., Chae, K.-J., Choi, M.-J., and Verstraete, W. (2008). "Microbial Fuel Cells: Recent Advances, Bacterial Communities and Application Beyond Electricity Generation." *Environmental Engineering Research*, 13(2), 51-65.
- Kim, J. R., Jung, S. H., Regan, J. M., and Logan, B. E. (2007b). "Electricity generation and microbial community analysis of alcohol powered microbial fuel cells." *Bioresource Technology*, 98(13), 2568-2577.
- Kirstine, W., and Galbally, I. (2004). "A simple model for estimating emissions of volatile organic compounds from grass and cut grass in urban airsheds and its application to two Australian cities." *Journal of the Air & Waste Management Association*, 54(10), 1299-1311.
- Kolter, R. (1993). "The stationary phase of the bacterial life cycle." *Annual Review of Microbiology*, 47, 855-874.
- Koutsoumanis, K. P., and Sofos, J. N. (2005). "Effect of inoculum size on the combined temperature, pH and aw limits for growth of *Listeria monocytogenes*." *International Journal of Food Microbiology*, 104, 83-91.
- Kovárová, K., Käch, A., Zehnder, A. J., and Egli, T. (1997). "Cultivation of *Escherichia coli* with mixtures of 3-phenylpropionic acid and glucose: steady-state growth kinetics." *Applied and Environmental Microbiology*, 63(7), 2619-2624.
- Lai, W. C., Dixit, N. S., and Mackay, R. A. (1984). "Formation of H Aggregates of Thionine Dye in Water." *Journal of Physical Chemistry*, 88, 5364-5368.
- Learoyd, S. A., Kroll, R. G., and Thurston, C. F. (1992). "An investigation of dye reduction by food-borne bacteria." *Journal of Applied Microbiology*, 72(6), 479-485.
- Ledezma, P., Greenman, J., and Ieropoulos, I. (2012). "Maximising electricity production by controlling the biofilm specific growth rate in microbial fuel cells." *Bioresource Technology*, 118(0), 615-618.
- Levin, M., and Stevenson, C. G. (2012). "Regulation of Cell Behavior and Tissue Patterning by Bioelectrical Signals: Challenges and Opportunities for Biomedical Engineering." *Annual Review of Biomedical Engineering*, 14(1), 295-323.
- Lin, C., Sheu, D.-S., Lin, T.-C., Kao, C.-M., and Grassp, D. (2012). "Thermophilic Biodegradation of Diesel Oil in Food Waste Composting Processes Without Bioaugmentation." *Environmental Engineering Science*, 29(2), 117-123.
- Lindqvist, R. (2006). "Estimation of *Staphylococcus aureus* Growth Parameters from Turbidity Data: Characterization of Strain Variation and Comparison of Methods." *Applied and Environmental Microbiology*, 72(7), 4862-4870.
- Lithgow, A. M., Romero, L., Sanchez, I. C., Souto, F. A., and Vega, C. A. (1986). "Interception of the Electron-transport Chain in Bacteria with Hydrophilic Redox Mediators.
- Liu, C., Sun, T., Zhai, Y., and Dong, S. (2009). "Evaluation of ferricyanide effects on microorganisms with multi-methods." *Talanta*, 78(2), 613-617.

- Liu, H., Ramnarayanan, R., and Logan, B. E. (2004). "Production of Electricity during Wastewater Treatment Using a Single Chamber Microbial Fuel Cell." *Environmental Science & Technology*, 38(7), 2281-2285.
- Loefer, J. B., and Matney, T. S. (1952). "Growth Inhibition of Free-Living Protozoa by Actidione." *Physiological Zoology*, 25(3), 272-276.
- Logan, B. E. (2007). *Microbial Fuel Cells*, John Wiley & Sons Inc., New Jersey.
- Logan, B. E. (2008). "Architecture." In: *Microbial Fuel Cells*, John Wiley & Sons, Inc., 85-110.
- Logan, B. E. (2009). "Exoelectrogenic bacteria that power microbial fuel cells." *Nat Rev Micro*, 7(5), 375-381.
- Logan, B. E., Hamelers, B., Rozendal, R., Schröder, U., Keller, J., Freguia, S., Aelterman, P., Verstraete, W., and Rabaey, K. (2006). "Microbial Fuel Cells: Methodology and Technology†." *Environmental Science & Technology*, 40(17), 5181-5192.
- Logan, B. E., Murano, C., Scott, K., Gray, N. D., and Head, I. M. (2005). "Electricity generation from cysteine in a microbial fuel cell." *Water Research*, 39(5), 942-952.
- Logan, B. E., and Regan, J. M. (2006). "Microbial Fuel Cells—Challenges and Applications." *Environmental Science & Technology*, 40(17), 5172-5180.
- Lovley, D. R. (2006). "Bug juice: harvesting electricity with microorganisms." *Nat Rev Micro*, 4(7), 497-508.
- Lowy, D. A., and Tender, L. M. (2008). "Harvesting energy from the marine sediment–water interface: III. Kinetic activity of quinone- and antimony-based anode materials." *Journal of Power Sources*, 185(1), 70-75.
- Luttik, M., Van Spanning, R., Schipper, D., Van Dijken, J. P., and Pronk, J. T. (1997). "The Low Biomass Yields of the Acetic Acid Bacterium *Acetobacter pasteurianus* Are Due to a Low Stoichiometry of Respiration-Coupled Proton Translocation." *Applied and Environmental Microbiology*, 63(9), 3345-3351.
- Maltoni, C., Ciliberti, A., Cotti, G., Conti, B., and Belpoggi, F. (1989). "Benzene, an experimental multipotential carcinogen: results of the long-term bioassays performed at the Bologna Institute of Oncology." *Environmental health perspectives*, 82, 109.
- Manohar, A. K., and Mansfeld, F. (2009). "The internal resistance of a microbial fuel cell and its dependence on cell design and operating conditions." *Electrochimica Acta*, 54(6), 1664-1670.
- Mohan, S. V., Mohanakrishna, G., and Sarma, P. N. (2008). "Effect of Anodic Metabolic Function on Bioelectricity Generation and Substrate Degradation in Single Chambered Microbial Fuel Cell." *Environmental Science & Technology*, 42(21), 8088-8094.
- Morris, K., Zhao, H., and John, R. (2005). "Ferricyanide-Mediated Microbial Reactions for Environmental Monitoring." *Australian Journal of Chemistry*, 58(4), 237-245.

- Niessen, J., Schröder, U., and Scholz, F. (2004). "Exploiting complex carbohydrates for microbial electricity generation – a bacterial fuel cell operating on starch." *Electrochemistry Communications*, 6(9), 955-958.
- Niranjana, E., Kumara Swamy, B. E., Raghavendra Naik, R., Sherigara, B. S., and Jayadevappa, H. (2009). "Electrochemical investigations of potassium ferricyanide and dopamine by sodium dodecyl sulphate modified carbon paste electrode: A cyclic voltammetric study." *Journal of Electroanalytical Chemistry*, 631(1–2), 1-9.
- Observatory, M. L. (2013). "CO₂ Now." (April 19, 2013).
- Oh, S. E., and Logan, B. E. (2006). "Proton exchange membrane and electrode surface areas as factors that affect power generation in microbial fuel cells." *Appl Microbiol Biotechnol*, 70(2), 162-169.
- Palmen, R., Vosman, B., Buijsman, P., Breek, C. K. D., and Hellingwerf, K. J. (1993). "Physiological characterization of natural transformation in *Acinetobacter calcoaceticus*." *Journal of General Microbiology*, 139(2), 295-305.
- Park, D. H., and Zeikus, J. G. (2000). "Electricity Generation in Microbial Fuel Cells Using Neutral Red as an Electronophore." *Applied and Environmental Microbiology*, 66(4), 1292-1297.
- Park, D. P., and Zeikus, J. Z. (2002). "Impact of electrode composition on electricity generation in a single-compartment fuel cell using *Shewanella putrefaciens*." *Applied Microbiology and Biotechnology*, 59(1), 58-61.
- Partanen, P., Hultman, J., Paulin, L., Auvinen, P., and Romantschuk, M. (2010). "Bacterial diversity at different stages of the composting process." *BMC Microbiology*, 10(1), 94.
- Pasco, N., Baronian, K., Jeffries, C., Webber, J., and Hay, J. (2004). "MICREDOX®—development of a ferricyanide-mediated rapid biochemical oxygen demand method using an immobilised *Proteus vulgaris* biocomponent." *Biosensors and Bioelectronics*, 20(3), 524-532.
- Passant, N. R., Richardson, S. J., Swannell, R. P. J., Gibson, N., Woodfield, M. J., van der Lugt, J. P., Wolsink, J. H., and Hesselink, P. G. M. (1993). "Emissions of volatile organic compounds (VOCs) from the food and drink industries of the European community." *Atmospheric Environment. Part A. General Topics*, 27(16), 2555-2566.
- Patchett, R. A., Kelly, A. F., and Kroll, R. G. (1988). "Use of a microbial fuel cell for the rapid enumeration of bacteria." *Applied Microbiology and Biotechnology*, 28(1), 26-31.
- Peguín, S., and Soucaille, P. (1995). "Modulation of Carbon and Electron Flow in *Clostridium acetobutylicum* by Iron Limitation and Methyl Viologen Addition." *Applied and Environmental Microbiology*, 61(1), 403-405.
- Pianetti, A., Falcioni, T., Bruscolini, F., Sabatini, L., Sisti, E., and Papa, S. (2005). "Determination of the Viability of *Aeromonas hydrophila* in Different Types of Water by Flow Cytometry, and Comparison with Classical Methods." *Applied and Environmental Microbiology*, 71(12), 7948-7954.

- Piciooreanu, C., Katuri, K., Loosdrecht, M. M., Head, I., and Scott, K. (2010). "Modelling microbial fuel cells with suspended cells and added electron transfer mediator." *J Appl Electrochem*, 40(1), 151-162.
- Pirt, S. J., ed. (1975). *Principles of Microbe and Cell Cultivation*, Blackwell Scientific, Oxford.
- Poole, K. (2002). "Outer Membranes and Efflux: The Path to Multidrug Resistance in Gram-Negative Bacteria." *Current Pharmaceutical Biotechnology*, 3(2), 77-98.
- Potter, M. C. (1911). "Electrical Effects Accompanying the Decomposition of Organic Compounds." *Proceedings of the Royal Society of London. Series B, Containing Papers of a Biological Character*, 84(571), 260-276.
- Preez, J. C. D. (1980). "Growth kinetics of *Acinetobacter calcoaceticus* with special reference to acetate and ethanol as carbon sources " Ph.D thesis, University of the Orange Free State, Bloemfontein, South Africa.
- Preez, J. C. D., Toerien, D. F., and Lategan, P. M. (1981). "Growth Parameters of *Acinetobacter calcoaceticus* on Acetate an Ethanol." *European Journal of Applied Microbiology and Biotechnology*, 13(45-53).
- Rabaey, K., Clauwaert, P., Aelterman, P., and Verstraete, W. (2005a). "Tubular Microbial Fuel Cells for Efficient Electricity Generation." *Environmental Science & Technology*, 39(20), 8077-8082.
- Rabaey, K., Lissens, G., Siciliano, S. D., and Verstraete, W. (2003). "A microbial fuel cell capable of converting glucose to electricity at high rate and efficiency." *Biotechnology Letters*, 25(18), 1531-1535.
- Rabaey, K., Lissens, G., and Verstraete, W. (2005b). "Microbial fuel cells: performances and perspectives." In: *Biofuels for Fuel Cells: Renewable Energy from Biomass Fermentation*, P. Lens, P. Westermann, M. Haberbauer, and A. Moreno, eds., IWA Publishing, London 23.
- Rabaey, K., and Verstraete, W. (2005). "Microbial fuel cells: novel biotechnology for energy generation." *Trends in Biotechnology*, 23(6), 291-298.
- Rahimnejad, M., Najafpour, G. D., Ghoreyshi, A. A., Shakeri, M., and Zare, H. (2011). "Methylene blue as electron promoters in microbial fuel cell." *International Journal of Hydrogen Energy*, 36(20), 13335-13341.
- Ralebitso-Senior, T. K., Senior, E., Di Felice, R., and Jarvis, K. (2012). "Waste gas biofiltration: advances and limitations of current approaches in microbiology." *Environmental Science & Technology*.
- Ramirez, A. A., Jones, J. P., and Heitz, M. (2007). "Biotrickling filtration of air contaminated with ethanol." *Journal of Chemical Technology and Biotechnology*, 82, 149-157.
- Raspor, P., and Goranovič, D. (2008). "Biotechnological Applications of Acetic Acid Bacteria." *Critical Reviews in Biotechnology*, 28(2), 101-124.

- Reichert-Schwillinsky, F., Pin, C., Dzieciol, M., Wagner, M., and Heim, I. (2009). "Stress- and Growth Rate-Related Differences between Plate Count and Real-Time PCR Data during Growth of *Listeria monocytogenes*." *Applied and Environmental Microbiology* 75(7), 2132-2138.
- Risholm-Sundman, M., Lundgren, M., Vestin, E., and Herder, P. (1998). "Emissions of acetic acid and other volatile organic compounds from different species of solid wood." *Holz als Roh-und Werkstoff*, 56(2), 125-129.
- Robinson, T. P., Ocio, M. J., Kaloti, A., and Mackey, B. M. (1998). "The effect of the growth environment on the lag phase of *Listeria monocytogenes*." *International Journal of Food Microbiology*, 44(1-2), 83-92.
- Roller, S. D., Bennetto, H. P., Delaney, G. M., Mason, J. R., Stirling, J. L., and Thurston, C. F. (1984). "Electron-transfer Coupling in Microbial Fuel Cells: 1. Comparison of Redox-mediator Reduction Rates and Respiratory Rates of Bacteria." *Journal of Chemical Technology and Biotechnology*, 34(B), 3-12.
- Routledge, S. J., Hewitt, C. J., Bora, N., and Bill, R. M. (2011). "Antifoam addition to shake flask cultures of recombinant *Pichia pastoris* increases yield." *Microbial Cell Factories*, 10:17.
- Rozendal, R. A., Hamelers, H. V. M., Rabaey, K., Keller, J., and Buisman, C. J. N. (2008). "Towards practical implementation of bioelectrochemical wastewater treatment." *Trends in biotechnology*, 26(8), 450-459.
- Salleh, S. M., Noh, N. A. M., and Yahya, A. R. M. (2011). "Improving Biosurfactant Recovery from *Pseudomonas aeruginosa* Fermentation." In: *Progress in Molecular and Environmental Bioengineering - From Analysis and Modeling to Technology Applications* A. Carpi, ed., 646.
- Schaetzle, O., Barriere, F., and Baronian, K. (2008). "Bacteria and yeasts as catalysts in microbial fuel cells: electron transfer from micro-organisms to electrodes for green electricity." *Energy & Environmental Science*, 1(6), 607-620.
- Schroder, U. (2007). "Anodic electron transfer mechanisms in microbial fuel cells and their energy efficiency." *Physical Chemistry Chemical Physics*, 9(21), 2619-2629.
- Schröder, U., Nießen, J., and Scholz, F. (2003). "A Generation of Microbial Fuel Cells with Current Outputs Boosted by More Than One Order of Magnitude." *Angewandte Chemie International Edition*, 42(25), 2880-2883.
- Scott, K., Cotlarciuc, I., Head, I. M., Katuri, K. P., Hall, D., Lakeman, J. B., and Browning, D. (2008). "Fuel cell power generation from marine sediments, investigation of cathode materials " *Journal of Chemical Technology and Biotechnology*, 83(9), 1244-1254.
- Scott, K., Rimbu, G. A., Katuri, K. P., Prasad, K. K., and Head, I. M. (2007). "Application of Modified Carbon Anodes in Microbial Fuel Cells." *Process Safety and Environmental Protection*, 85(5), 481-488.

- Shahryari, Z., Goharrizi, A. S., and Azadi, M. (2010). "Experimental study of methylene blue adsorption from aqueous solutions onto carbon nano tubes." *International Journal of Water Resources and Environmental Engineering*, 2(2), 016-028
- Sharafi, S., I, R., and K, B.-M. (2010). "Isolation, characterization and optimization of indigenous acetic acid bacteria and evaluation of their preservation methods." *Iranian Journal of Microbiology*, 2(1), 38-45
- Sharma, T., Mohana Reddy, A. L., Chandra, T. S., and Ramaprabhu, S. (2008). "Development of carbon nanotubes and nanofluids based microbial fuel cell." *International Journal of Hydrogen Energy*, 33(22), 6749-6754.
- Sigma-Aldrich. "Resorufin sodium salt." (18/10, 2012).
- Smith, M. G., Etages, S. G. D., and Snyder, M. (2004). "Microbioal Synergy via an Ethanol-Triggered Pathway." *Molecular and Cellular Biology*, 24(9), 3874-3884.
- Stasiak, L., and Błażej, S. (2009). "Acetic Acid Bacteria - Perspectives of Application in Biotechnology - A Review." *Polish Journal of Food and Nutrition Sciences*, 59(1), 17-23.
- Sund, C., McMasters, S., Crittenden, S., Harrell, L., and Sumner, J. (2007). "Effect of electron mediators on current generation and fermentation in a microbial fuel cell." *Applied Microbiology and Biotechnology*, 76(3), 561-568.
- Sundberg, C., Franke-Whittle, I. H., Kauppi, S., Romantschuk, D. Y. M., Insam, H., and Jönsson, H. (2010). "Characterisation of source-separated household waste intended for composting." *Bioresource Technology*, 102(3), 2859-2867.
- Taylor, P., Olivier Lavagne d'Ortigue, Trudeau, N., and Francoeur, M. (2008). "Energy Efficiency Indicators for Public Electricity Production from Fossil Fuels." I. E. Agency, ed., Communication and Information office, France, 23.
- Tender, L. M., Gray, S. A., Groveman, E., Lowy, D. A., Kauffman, P., Melhado, J., Tyce, R. C., Flynn, D., Petrecca, R., and Dobarro, J. (2008). "The first demonstration of a microbial fuel cell as a viable power supply: Powering a meteorological buoy." *Journal of Power Sources*, 179(2), 571-575.
- Thornton, H. R., and Hastings, E. G. (1930). "Studies on Oxidation-Reduction in Milk: The Methylene Blue Reduction Test." *Journal of Dairy Science*, 13(3), 221-245.
- Thurston, C.F., Bennetto, H. P., Delaney, G. M., Mason, J. R., Roller, S. D., and Stirling, J. L. (1985). "Glucose Metabolism in a Microbial Fuel Cell. Stoichiometry of Product Formation in a Thionine-mediated *Proteus vulgaris* Fuel Cell and its Relation to Coulombic Yields." *Journal of General Microbiology*, 131(6), 1393-1401.
- Tratnyek, P. G., Reilkoff, T. E., Lemon, A. W., Scherer, M. M., Balko, B. A., Feik, L. M., and Henegar, B. D. (2001). "Visualizing Redox Chemistry: Probing Environmental Oxidation-Reduction Reactions with Indicator Dyes." *The Chemical Educator*, 6(3), 172-179.

- Tratnyek, P. G., and Wolfe, N. L. (1990). "Characterization of the reducing properties of the anaerobic sediment slurries using redox indicators." *Environmental Toxicology and Chemistry* 9, 289-295.
- Tuomela, M., Vikman, M., Hatakka, A., and Itävaara, M. (2000). "Biodegradation of lignin in a compost environment: a review." *Bioresource Technology*, 72(2), 169-183.
- Usacheva, M. N., Teichert, M. C., and Biel, M. A. (2001). "Comparison of the methylene blue and toluidine blue photobactericidal efficacy against gram-positive and gram-negative microorganisms." *Lasers Surg Med*, 29(2), 165-173.
- Usacheva, M. N., Teichert, M. C., and Biel, M. A. (2003). "The role of the methylene blue and toluidine blue monomers and dimers in the photoinactivation of bacteria." *Journal of Photochemistry and Photobiology B: Biology*, 71(1-3), 87-98.
- Van der Zee, F. P., and Cervantes, F. J. (2009). "Impact and application of electron shuttles on the redox (bio)transformation of contaminants: A review." *Biotechnology Advances*, 27(3), 256-277.
- Varley, J., Brown, A. K., Boyd, J. W. R., Dodd, P. W., and Gallagher, S. (2004). "Dynamic multi-point measurement of foam behaviour for a continuous fermentation over a range of key process variables." *Biochemical Engineering Journal*, 20(1), 61-72.
- Wang, C.-T., Chen, W.-J., and Huang, R.-Y. (2010). "Influence of growth curve phase on electricity performance of microbial fuel cell by *Escherichia coli*." *International Journal of Hydrogen Energy*, 35(13), 7217-7223.
- Watanabe, K. (2008). "Recent Developments in Microbial Fuel Cell Technologies for Sustainable Bioenergy." *Journal of Bioscience and Bioengineering*, 106(6), 528-536.
- Webster, C., Towner, K. J., and Humphreys, H. (2000). "Survival of *Acinetobacter* on Three Clinically Related Inanimate Surfaces." *Infection Control and Hospital Epidemiology*, 21(4), 246.
- Wei, J., Liang, P., and Huang, X. (2011). "Recent progress in electrodes for microbial fuel cells." *Bioresource Technology*, 102(20), 9335-9344.
- Wilkinson, S., Klar, J., and Applegarth, S. (2006). "Optimizing Biofuel Cell Performance Using a Targeted Mixed Mediator Combination." *Electroanalysis*, 18(19-20), 2001-2007.
- Wuhrmann, K., Mechsner, K., and Kappeler, T. (1980). "Investigation on Rate - Determining Factors in the Microbial Reduction of Azo Dyes." *European Journal of Applied Microbiology and Biotechnology*, 9, 325-338.
- Xiong, L., Aldous, L., Henstridge, M. C., and Compton, R. G. (2012). "Investigation of the optimal transient times for chronoamperometric analysis of diffusion coefficients and concentrations in non-aqueous solvents and ionic liquids." *Analytical Methods*, 4, 371-376.
- Yakushi, T., and Matsushita, K. (2010). "Alcohol dehydrogenase of acetic acid bacteria: structure, mode of action, and applications in biotechnology." *Applied Microbiology and Biotechnology*, 86(5), 1257-1265.

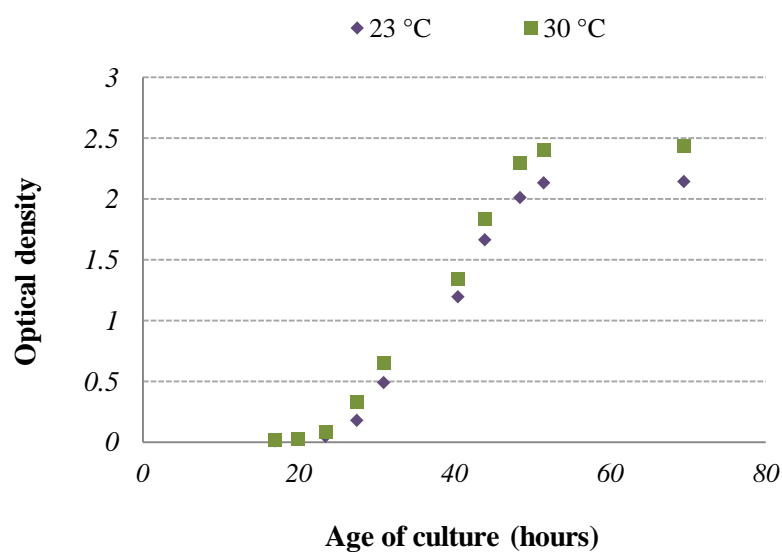
- Yang, R., Ruan, C., Dai, W., Deng, J., and Kong, J. (1999). "Electropolymerization of thionine in neutral aqueous media and H₂O₂ biosensor based on poly(thionine)." *Electrochimica Acta*, 44(10), 1585-1596.
- Yu, E. H., Cheng, S., Scott, K., and Logan, B. (2007). "Microbial fuel cell performance with non-Pt cathode catalysts." *Journal of Power Sources*, 171(2), 275-281.
- Yu, J., Wang, X., and Yue, P. L. (2001). "Optimal Decolorization and Kinetic Modeling of Synthetic Dyes by Pseudomonas Strains." *Water Research*, 35(15), 3579-3586.
- Yuan, Y., and Kim, S. (2008). "Improved Performance of a Microbial Fuel Cell with Polypyrrole/Carbon Black Composite Coated Carbon Paper Anodes." *Bulletin of the Korean Chemical Society*, 29(7), 1344-1348.
- Zahl, A., van Eldik, R., and Swaddle, T. W. (2002). "Cation-Independent Electron Transfer between Ferricyanide and Ferrocyanide Ions in Aqueous Solution." *Inorganic Chemistry*, 41(4), 757-764.
- Zhang, F., Saito, T., Cheng, S., Hickner, M. A., and Logan, B. E. (2010). "Microbial Fuel Cell Cathodes With Poly(dimethylsiloxane) Diffusion Layers Constructed around Stainless Steel Mesh Current Collectors." *Environmental Science & Technology*, 44(4), 1490-1495.
- Zhang, X., Cheng, S., Wang, X., Huang, X., and Logan, B. E. (2009). "Separator Characteristics for Increasing Performance of Microbial Fuel Cells." *Environmental Science & Technology*, 43(21), 8456-8461.
- Zverlov, V., Berezina, O., Velikodvorskaya, G., and Schwarz, W. (2006). "Bacterial acetone and butanol production by industrial fermentation in the Soviet Union: use of hydrolyzed agricultural waste for biorefinery." *Applied microbiology and biotechnology*, 71(5), 587-597.

Appendices

APPENDIX I: EFFECT OF TEMPERATURE ON THE GROWTH OF *A. CALCOACETICUS*

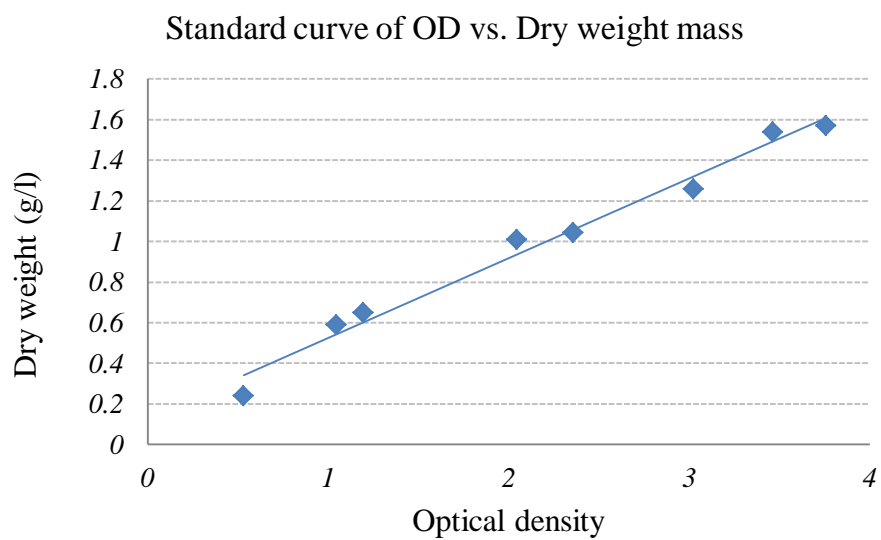
Both growth samples inoculated with *A. calcoaceticus* were set up using medium 2 with aeration rates at around 0.56 to 0.6 vvm. One was incubated at 33 °C and the other at 23 °C.

Sample Incubated at 23 °C		Sample Incubated at 33°C	
Time (hr)	Optical density	Time (hr)	Optical density
17	0.009	17	0.0199
20	0.022	20	0.033
23.5	0.044	23.5	0.085
27.5	0.178	27.5	0.33
31	0.488	31	0.654
40.5	1.194	40.5	1.35
44	1.662	44	1.836
48.5	2.01	48.5	2.3
51.5	2.134	51.5	2.406
69.5	2.142	69.5	2.436



APPENDIX II: OPTICAL DENSITY VS. DRY WEIGHT MASS

Optical density	Dry weight mass(g/l)
0.534	0.24
1.047	0.59
1.194	0.65
2.045	1.01
2.358	1.045
3.024	1.26
3.465	1.54
3.76	1.57



APPENDIX III: ETHANOL CONSUMPTION OF *A. CALCOACETICUS* DURING BATCH CULTURE.

Hour	Ethanol concentration (g/l)
0	13.85
5.5	13.45
10.5	13.3
19	13
23	12.9
28.5	12.55
39	11.7
45	11.35
53	10.9